

**RADIOSENSITIVITY ENHANCEMENT OF HUMAN GLIOBLASTOMA
MULTIFORME BY A HERPES SIMPLEX VIRUS VECTOR**

by

Constantinos G. Hadjipanayis, M.D.

BA, University of Delaware, 1994

MD, Jefferson Medical College of Thomas Jefferson University, 1998

Submitted to the Graduate Faculty of

The School of Medicine, Biochemistry and Molecular Genetics Graduate Program,

in partial fulfillment

of the requirements for the degree of

Doctor of Philosophy

University of Pittsburgh

2005

We have read this dissertation entitled, “Radiosensitivity enhancement of human glioblastoma multiforme by a herpes simplex virus vector” by Constantinos G. Hadjipanayis, M.D., and recommend that it be accepted towards partial fulfillment of the requirements for the degree of Doctor of Philosophy.

UNIVERSITY OF PITTSBURGH
FACULTY OF ARTS AND SCIENCES

This dissertation was presented

by

Constantinos G. Hadjipanayis, M.D.

It was defended on

June 14, 2005

and approved by

Stephen G. Grant, Ph.D.
Dept. of Environmental and Occupational Health

Saleem Khan, Ph.D.
Dept. of Molecular Genetics and Biochemistry

Paul R. Kinchington, Ph.D.
Depts. of Ophthalmology and Molecular Genetics and Biochemistry

Robert Scwabassi, M.D., Ph.D.
Dept. of Neurological Surgery

Neal A. DeLuca, Ph.D.
Dissertation Director
Dept. of Molecular Genetics and Biochemistry

A modified version of the data presented in Chapter 3 appeared in “Inhibition of DNA repair by a herpes simplex virus vector enhances the radiosensitivity of human glioblastoma cells,” Costas G. Hadjipanayis and Neal A. DeLuca, *Cancer Research*, 2005, volume 65 (12), pages 5310-5316, copyright © 2005, American Association of Cancer Research. All rights reserved.

RADIOSENSITIVITY ENHANCEMENT OF HUMAN GLIOBLASTOMA MULTIFORME BY A HERPES SIMPLEX VIRUS VECTOR

Constantinos G. Hadjipanayis, MD, PhD

University of Pittsburgh, 2005

Ionizing radiation (IR) is the primary adjuvant treatment for glioblastoma multiforme (GBM), the most aggressive primary brain tumor in adults. Enhancement of the effects of IR may increase patient survival and quality of life in patients with GBM. The repair of DNA double strand breaks (DSBs) produced by IR proceeds along two pathways, nonhomologous end-joining (NHEJ) and homologous repair (HR). The herpes simplex virus (HSV) immediate-early protein, ICP0, has been shown to induce the degradation of the catalytic subunit of DNA-dependent protein kinase (DNA-PK_{cs}). DNA-PK_{cs} is the primary component of NHEJ, the major DNA DSB repair pathway in mammalian cells. A replication-defective HSV-1 vector, d106, which solely expresses the immediate-early (IE) protein, ICP0, was used to determine the effect of ICP0 on GBM cell survival and DNA repair after IR treatment. Preinfection of two radioresistant GBM cell lines by d106 resulted in decreased cell survival and proliferation, protein degradation of DNA-PK_{cs}, inhibition of DNA DSB repair, and enhanced apoptosis following IR. Optimal intracerebral delivery of the HSV-1 mutant, d106, was established by convection-enhanced delivery (CED) in a mouse model. Translation of the effects of ICP0 in combination with IR was performed with CED of d106 in a mouse glioma model. CED of d106 in combination with whole-brain irradiation significantly increased animal survival.

TABLE OF CONTENTS

ACKNOWLEDGEMENTS	x
1. INTRODUCTION	1
1.1. Overview	1
1.2. Glioblastoma Multiforme	3
1.2.1. Astrocyte Differentiation and Glioma Formation	3
1.2.2. GBM Incidence, Classification, and Molecular Genetics	4
1.2.2.1. Growth Factor Signaling Pathways, Mouse Modeling, and GBM	6
1.2.2.2. Deregulation of Cell Cycle Arrest Pathways and GBM	7
1.2.3. GBM Clinical Features, Prognosis, and Histopathology	8
1.2.4. GBM and Surgical Resection	9
1.2.5. GBM and Ionizing Radiation	10
1.2.6. GBM and Chemotherapy	11
1.2.6.1. GBM and Chemoradiation	13
1.2.6.2. Convection-Enhanced Delivery	13
1.2.7. Gene Therapy for GBM	14
1.3. Ionizing Radiation	15
1.3.1. Types and Quantity of Ionizing Radiation	15
1.3.2. Absorption and Action of Ionizing Radiation	16
1.3.3. DNA Double-Strand Breaks and Cell Response	17
1.3.4. DNA Double-Strand Break Repair	19
1.3.4.1. NHEJ and DNA DSBs	20
1.4. Herpes Simplex Virus	21
1.4.1. Clinical HSV Infection and Treatment	21
1.4.2. HSV Structure and Genome	23
1.4.3. HSV Life Cycle	24
1.4.3.1. HSV Cell Entry	24
1.4.3.2. HSV Pathogenesis	25
1.4.3.3. HSV Gene Expression	26
1.4.3.4. HSV Immediate-Early Proteins	27
1.4.3.5. HSV DNA Replication and Recombination	31
1.4.3.6. HSV Infection, ND10 Domains, and DNA Damage Response	33
1.4.3.7. HSV Assembly and Release	35
1.4.4. ICP0	35
1.4.4.1. ICP0 Conquest of Host Cell Metabolism	36
1.4.4.2. ICP0 Degradation of DNA-PK _{CS}	38
1.4.5. HSV-1 and NHEJ	38
1.4.6. HSV-1 Replication-Defective Mutants	38
1.4.6.1. d106 and d109	39
1.4.7. HSV-1 Replication-Conditional (Oncolytic) Viruses	41
1.4.7.1. Oncolytic HSV-1 and Ionizing Radiation	43
2. STATEMENT OF THE PROBLEM	44

3. INHIBITION OF DNA REPAIR BY A HERPES SIMPLEX VIRUS VECTOR ENHANCES THE RADIOSENSITIVITY OF HUMAN GLIOBLASTOMA CELLS	47
3.1. Abstract.....	47
3.2. Introduction.....	48
3.3. Material and Methods.....	49
3.3.1. Cells and Viruses.....	50
3.3.2. HSV-1/Adenovirus Infection, IR, and Cell Survival/Proliferation.....	50
3.3.3. Western Blot Analysis of DNA-PK _{cs} and Cleaved Caspase-3	51
3.3.4. Apoptosis	52
3.3.5. Indirect Immunofluorescence for γ H2AX and ICP0.....	53
3.3.6. Statistical Analysis	53
3.4. Results	54
3.4.1. Effect of ICP0 and IR on Human GBM Cell Survival and Proliferation: MTT Assay	54
3.4.1.1. Adenovirus Expression of ICP0	57
3.4.2. Effect of ICP0 and IR on Human GBM Cell Survival: Clonogenic Survival Assay	57
3.4.3. Apoptosis as a Mode of GBM Cell Death with ICP0 Production and IR	58
3.4.4. ICP0 Degradation of DNA-PK _{cs} in Human GBM Cells	60
3.4.5. Persistent DNA DSBs with ICP0 Production and IR in Human GBM Cells	61
3.5. Discussion.....	63
4. INTRACEREBRAL CONVECTION-ENHANCED DELIVERY OF A HERPES SIMPLEX VIRUS VECTOR IN A MOUSE MODEL	66
4.1. Abstract.....	66
4.2. Introduction.....	67
4.3. Material and Methods.....	68
4.3.1. Animals and HSV-1 Vector	68
4.3.2. CED Apparatus	68
4.3.3. HSV-1 CED and Heparin or Dextran Sulfate Co-infusion.....	69
4.3.4. Persistent HSV-1 Transgene Expression and In vivo Toxicity.....	70
4.3.5. Histologic Analysis	70
4.4. Results	72
4.4.1. HSV-1 Cell Infection, Spatial Distribution, Reflux, and Transduction After CED.....	72
4.4.2. HSV-1 CED and Heparin or Dextran Sulfate Co-infusion.....	73
4.4.3. Intracerebral Toxicity of d106 After CED.....	75
4.5. Discussion.....	77
5. A HERPES SIMPLEX VIRUS VECTOR ENHANCES THE RADIOSENSITIVITY OF MOUSE INTRACRANIAL HUMAN GLIOBLASTOMA XENOGRAFTS AFTER CONVECTION-ENHANCED DELIVERY	79
5.1. Abstract.....	79
5.2. Introduction.....	81
5.3. Material and Methods.....	83
5.3.1. Animals, Cells, and HSV-1 Vector	83
5.3.2. CED Apparatus	84
5.3.3. Tumor Inoculation, HSV-1 Convection Procedure, and Irradiation	84
5.3.4. Intracerebral HSV-1 CED or Stereotactic Injection Alone	86

5.3.5.	Animal Observation.....	86
5.3.6.	Histologic Analysis	87
5.3.7.	Statistical Analysis	88
5.4.	Results	88
5.4.1.	HSV-1 Stereotactic Injection vs. CED	88
5.4.2.	HSV-1 Xenograft Infection and Cell Transduction	89
5.4.3.	Antitumor Effect of d106 and IR	92
5.5.	Discussion.....	94
6.	SUMMARY AND DISCUSSION.....	97
6.1.	Summary of Results	97
6.2.	Role of ICP0 in Cellular DNA Repair.....	100
6.3.	Therapy of Human GBM with d106	102
6.4.	Future Studies	103
	BIBLIOGRAPHY	106

LIST OF TABLES

Table 1. Summary of treatment group results including number of animals, protocol, median survival, and percent survival at 80 days.	85
Table 2. Summary of U87-MG xenograft infection rate and treatment response in animals that underwent d106 CED and whole-brain irradiation that were randomly sacrificed.	93

LIST OF FIGURES

Figure 1. GBM cell signaling.....	6
Figure 2. Production of DNA DSBs, cellular response, and repair.....	19
Figure 3. Structures of the isogenic HSV-1 mutants, d106 and d109.....	41
Figure 4. Effect of HSV mutant viruses and escalating doses of ionizing radiation (IR) on U87-MG and T98 cell proliferation and survival using the MTT assay.....	56
Figure 5. Effect of empty adenovirus (AdS.11D) and ICP0-producing adenovirus [AdS.11E4(ICP0)] on U87-MG cell proliferation and viability after IR.....	57
Figure 6. Clonogenic survival performed on U87-MG cells after d106 infection and IR treatment plotted on a logarithmic scale.....	58
Figure 7. Apoptosis as a mode of GBM cell death with ICP0 production and IR.....	59
Figure 8. Effect of HSV mutant viruses on DNA-PK _{CS} protein levels in U87-MG and T98 cells.....	61
Figure 9. Indirect immunofluorescence for γ H2AX and ICP0 in U87-MG and T98 cells.....	62
Figure 10. Convection-enhanced delivery (CED) mouse model.....	69
Figure 11. Photomicrographs of mouse brain sections 48 hours after CED of d106.....	73
Figure 12. Photomicrographs of mouse brain sections stained with GFP 4, 6, and 21 days after d106 CED.....	73
Figure 13. Photomicrographs of mice brain sections after heparin or dextran sulfate co-infusion with d106.....	74
Figure 14. Intracerebral toxicity of d106 after CED.....	76
Figure 15. Photomicrographs of BALB/c mice brain sections after immunohistochemistry staining for GFP. A comparison of intracerebral manual stereotactic injection and CED.....	89
Figure 16. Photomicrographs of athymic nude mice brain sections containing U87 MG xenografts after stereotactic intracerebral CED of d106.....	91
Figure 17. Kaplan-Meier survival curves of athymic nude mice after intracranial implantation of U87-MG cells and treatment by stereotactic CED of d106 or HBSS and irradiation (0 and 10 Gy).....	93
Figure 18. Photomicrographs of brain sections revealing antitumor efficacy of stereotactic CED of d106 in combination with ionizing radiation (10 Gy) in athymic nude mice implanted with U87 MG xenografts.....	94

ACKNOWLEDGEMENTS

Completing graduate training while in a neurological surgery residency has been the most challenging academic endeavor I have taken part in. My graduate training would not have been possible without the unquestionable support and guidance by my wife, Lorraine, who has been there for me at all times. I would like to thank my two children, Panikos and Athena, for their love and support during my graduate training. I would like to thank my parents who have been models to me in regards to their hard work ethic. I would like to thank Dr. Clayton Wiley and Dr. Steve Phillips for their counseling and assistance entering the interdisciplinary biomedical graduate program as a neurosurgical resident in training. I would like to thank Dr. Wendy Fellows-Mayle for all her help with the animal work presented in my dissertation. I would also like to thank all the members of my thesis committee for their valuable insight and unquestionable support. I especially would like to thank my research mentor, Dr. Neal DeLuca, who has been the driving force behind my dissertation work and the ultimate guide through a difficult path in becoming a physician-scientist. He has been a role model to me in regards to his scientific approach, integrity, and knowledge. I look forward to working with him in the near future. Finally, I would like to thank all the neurosurgery residents in my residency program, the faculty, and my department chair, Dr. L. Dade Lunsford, who supported my graduate training endeavor at all times during my neurosurgery residency and let me pursue my career goal of becoming a physician-scientist.

1. INTRODUCTION

1.1. Overview

Glioblastoma multiforme (GBM) is the most common primary brain tumor in adults. The incidence of GBM is dwarfed by the incidence of patients with lung, colon, or breast cancer, but GBM may be the most devastating and therapy resistant of all malignancies. Despite over four decades of advances in microneurosurgery, ionizing radiation (IR) therapy, radiology imaging, and the introduction of novel chemotherapeutic agents, the prognosis is poor (65, 184, 191, 234, 264, 268, 333) (237, 292). The median life expectancy of patients with GBM is 12 months; only 5% of patients or fewer will be alive five years after diagnosis (25, 331). Systemic metastases can occur with GBM but are relatively rare. The tumors are extremely aggressive in a locally invasive fashion. After treatment, the majority of tumors recur within two centimeters of their original tumor margin (145). On magnetic resonance (MR) imaging, infiltrating tumor cells extend beyond the area of contrast enhancement (165). The goal of surgical resection is to remove the contrast-enhancing portion of the tumor due to the potential morbidity from removing adjacent normal neural tissue (140, 166). All resections of GBMs leave behind nonenhancing infiltrative tumor cells that reside away from the primary tumor mass. These tumor cells are responsible for recurrence and the ultimate demise of patients with GBM.

Radiation therapy remains the sole agent that increases the survival of patients with GBM (191, 330, 331). IR exerts its lethal effects on cells primarily by inducing DNA double-strand breaks (DSBs). Both adult primary (de novo) and secondary GBMs are remarkably resistant to

IR treatment. The limited efficacy of radiation treatment is believed to arise from the poor apoptotic response to IR by the tumor cells and the hypoxic environment present within tumors (84, 164, 167, 353, 356).

Herpes simplex virus 1 (HSV-1) is a large, neurotropic DNA virus that has been studied for use in the therapy of human GBM. A large number of HSV-1 genes have been shown to be non-essential and can be deleted from the genome to provide additional room for potential gene insertions. A number of different genetically engineered viruses have been constructed with deletions or mutations in one or more HSV genes (e.g. $\gamma_{134.5}$, U_L39 [ribonucleotide reductase], thymidine kinase [tk], and UTPase) in an effort to decrease toxicity of HSV to the central nervous system (CNS) and provide a condition for viral replication only in replicating cells that can provide cellular homologues (49, 51, 152, 208, 222). Several phase I clinical trials have been completed for use of the conditionally-replicative HSV mutants G207 and 1716, on patients with recurrent malignant gliomas failing IR treatment (134, 206, 252, 271). All clinical studies performed have shown little overall efficacy, and delivery of HSV-1 to the brain by stereotactic injection has been a limiting factor.

New therapeutic strategies need to be developed for improved long-term management of GBM. Multi-modal treatment approaches are required which attack the molecular and biological features of malignant gliomas. Enhancement of the effects of IR treatment, by inhibition of DNA repair, may allow for better tumor control. Since these tumors rarely metastasize away from the nervous system and the majority recur in a local fashion, local tumor control must be achieved to significantly extend the survival of patients with GBM. Convection-enhanced delivery (CED) is an approach developed to overcome the obstacles associated with current CNS agent delivery (26, 230) and is increasingly used to distribute therapeutic agents for treatment of

malignant gliomas. Currently, multiple clinical trials involve CED for the treatment of recurrent GBM (182, 326, 336, 338).

The study presented here identifies the HSV-1 immediate-early (IE) protein, ICP0, as an inhibitor of DNA repair that enhances the radiosensitivity of experimental human glioblastoma multiforme. Optimal intracerebral delivery of the ICP0-producing virus, d106, was developed in a mouse model by CED. Translation of the in vitro effects of ICP0 was performed by CED of d106 in a mouse glioma model in combination with IR.

1.2. Glioblastoma Multiforme

1.2.1. Astrocyte Differentiation and Glioma Formation

The mammalian CNS is composed of two main cell populations: neurons and glia. Glial cells are further divided into three subpopulations with distinctive morphologies and functions: (1) astrocytes, (2) oligodendrocytes, and (3) microglia. Astrocytes are the most abundant glia type in the CNS, and they fulfill various important functions, including supporting and protecting neurons, inducing neurogenesis, regulating synapse formation and transmission, and initiating immune responses (63).

Multipotent, self-renewing neuroepithelial stem cells give rise to glial cells in response to both extracellular and intracellular stimuli (63). Extracellular stimuli include growth factors and cytokines, such as epidermal growth factor (EGF), fibroblast growth factor (FGF), platelet-derived growth factor (PDGF), ciliary neurotrophic factor/leukemia inhibitory factor (CNTF/LIF), bone morphogenetic protein, interleukin-6 (IL-6), and sonic hedgehog (SHH). EGF, FGF, and PDGF act as mitogens to confer neural progenitors the self-renewal capacity during multilineage differentiation (170, 323). EGF signaling also induces astroglial

differentiation. Epidermal growth factor receptor (EGFR) overexpression in neural progenitors has been shown to lead to an increase in the number of astrocytes while loss of EGFR expression in mice delays astrocyte differentiation and decreases astrocyte numbers (174).

Gliomas are a group of CNS neoplasms with distinct histologic characteristics, comprising almost 60% of total human CNS malignancies. Gliomas are classified into two major groups: astrocytomas and oligodendrogliomas. Glioblastoma multiforme (GBM) is a tumor derived from astrocytes and is classified in the group of gliomas known as the diffuse (infiltrating) astrocytomas. The diffuse astrocytomas are classified into three malignancy grades: grade 2 (astrocytoma), grade 3 (anaplastic astrocytoma), and grade 4 (GBM). GBM is the most common diffuse astrocytoma, representing 82% of these cases diagnosed in the United States. Among all neuroepithelial tumors, GBM is the most common and represents nearly half of all cases.

1.2.2. GBM Incidence, Classification, and Molecular Genetics

GBM is the most common primary brain tumor, accounting for more than 60% of all primary brain tumors. Approximately 10,000-15,000 new cases of GBM are diagnosed in the United States yearly (64, 315). The incidence of GBM is 7.7 cases/100,000 person-years. GBM may manifest at any age, but preferentially affects adults, with a peak incidence between 45 and 70 years.

GBM can be divided into at least two subgroups based on the genetic makeup of the tumor. Primary GBM arises de novo clinically and most often occurs in elderly patients. It is characterized genetically by over-expression (80% of cases) or amplification (40% of cases) of the epidermal growth factor receptor gene (EGFR), which encodes a tyrosine kinase involved in cell replication (Fig. 1) (107, 137, 185, 199, 327, 334). Notably, p53 mutation almost never

occurs in primary GBMs with EGFR amplification (272). Approximately 10% of primary GBMs have amplification of MDM2 (murine double minute 2), a transcriptional target of p53 (199). Other genetic alterations include retinoblastoma (Rb) gene mutations on chromosome 13, loss of p15 (CDKN2B) and p16 (CDKN2A) on chromosome 9, and mutation or deletion of PTEN (phosphatase and tensin homology) on chromosome 10 (Fig.1). Close association of EGFR amplification and p15/p16 deletions, occurring primarily in elderly patients with primary GBM without a p53 mutation, may contribute to the worst prognosis of elderly GBM patients. The pattern of genetic alterations in primary pediatric GBM is distinct from that of adult GBM. Amplification of EGFR or MDM2 proto-oncogenes and p15/p16 deletions occur randomly and nonsequentially in pediatric GBM (177). Instead, p53 alterations have been found in approximately 50% of cases (31, 314). Overexpression of p53 in primary pediatric GBM is strongly associated with adverse outcome, independent of clinical prognostic factors and histologic findings (263).

Secondary GBM arises in a younger population through progression from a lower-grade glioma (World Health Organization (WHO) grade II and III) and accounts for approximately one third of GBM tumors (250). Numerous genetic alterations accumulate and become linked together sequentially to parallel malignant progression. Secondary GBM is characterized by mutation and inactivation of the p53 gene and overexpression of PDGF ligands and receptors (Fig. 1). These steps occur early in secondary GBM tumorigenesis. The subsequent loss of chromosomes 1, 9p, 13q, and 19q are considered to be major events in tumor progression. Transition from anaplastic astrocytoma (WHO grade III) to secondary glioblastoma (WHO grade IV) requires the loss of chromosome 10q (PTEN deletion).

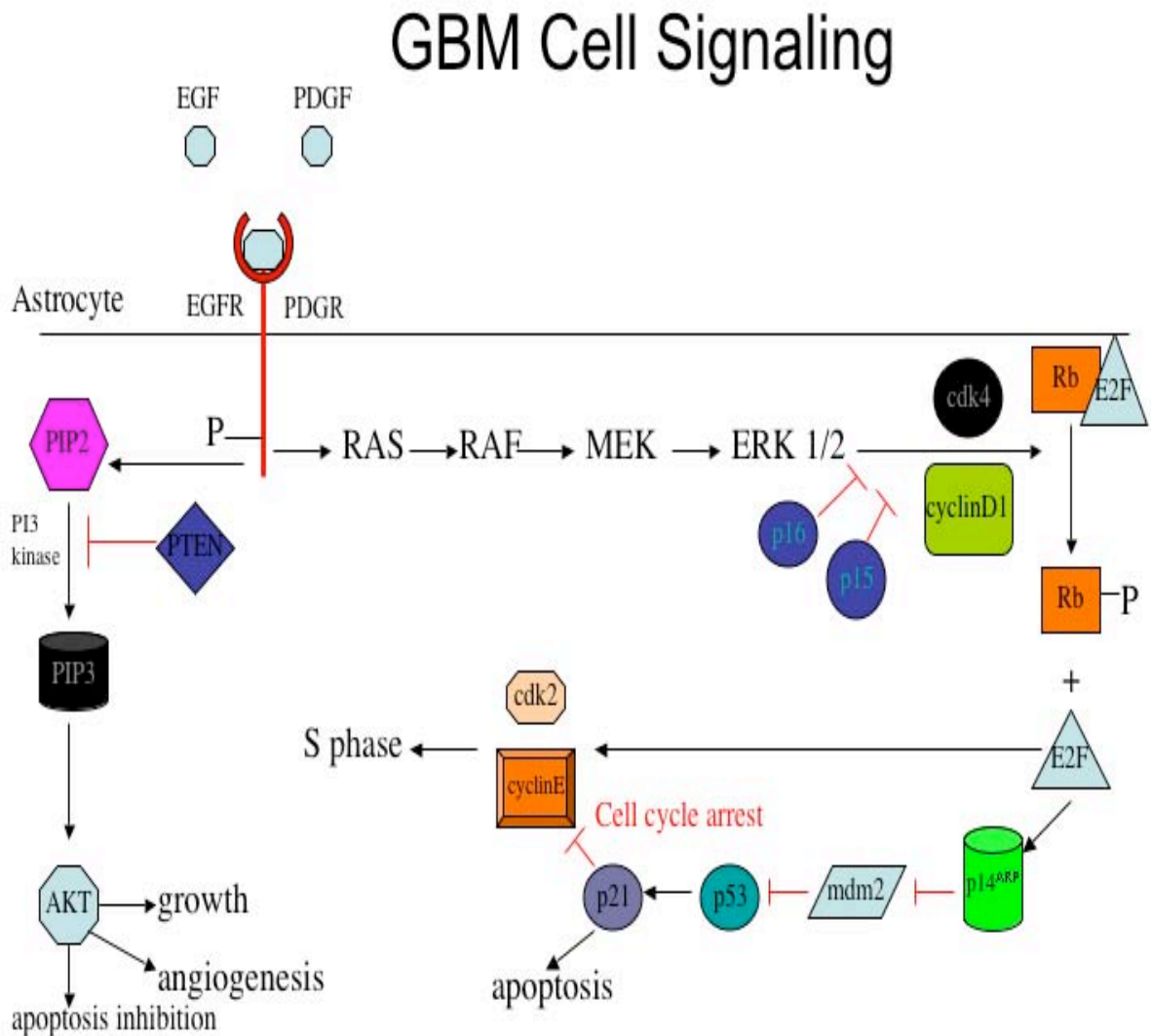


Figure 1. GBM cell signaling.

1.2.2.1. Growth Factor Signaling Pathways, Mouse Modeling, and GBM

The frequent overexpression of growth factors and their receptors or activating mutations of these receptors in GBM suggests the constitutive activation of receptor tyrosine kinase signaling pathways in these tumors (63). Elevated RAS and AKT activities, which are downstream targets of tyrosine kinase receptors, occur in GBM cells (Fig. 1) (121, 123). Activation of the RAS pathway is causally related to tumorigenesis in a mouse model. Overexpression of an active

form of RAS from the glial fibrillary acidic protein (GFAP) promoter in astrocytes induces astrocytoma formation in mice (75). Similarly, overexpression of v-SRC, which is capable of activating RAS from the same promoter also generates astrocytomas in mice (340, 341).

Simultaneous activation of the RAS and AKT pathways has been shown to induce GBM formation in nestin positive CNS progenitor cells (147). The combination of these two signaling pathways is essential, as gene transfer of neither active K-RAS nor AKT alone into the CNS progenitors is able to induce GBM formation. Even though elevated AKT and RAS activities are present in human gliomas and are causally related to GBM formation in mice, no activating mutations of either RAS or AKT have ever been documented in human GBM tumors (63). Elevation of RAS and AKT activities is due to the sustained activation of upstream receptor tyrosine kinases (207) and the inactivation of key negative regulators for these two signaling pathways, such as PTEN for the PI3K/AKT pathway (306) and RAS-like inhibitor of growth for the RAS/MAPK pathway (83).

1.2.2.2. Deregulation of Cell Cycle Arrest Pathways and GBM

Mutations that lead to disruption of cell cycle arrest pathways are also found in human GBM (63). The most common mutation is deletion of the INK4A-ARF locus (155). The INK4A-ARF locus, known to encode both p16^{INK4A} and p14^{ARF} proteins (p19^{ARF} in mice), is one of the major regulators of cell cycle progression (Fig. 1). Homozygous deletion of the INK4A-ARF locus in mice results in the breakdown of G1/S and G2/M cell cycle checkpoints (148).

The p53 gene is another target mutated in human GBM tumors (Fig. 1) (163). Mutations of p53 are frequently associated with either amplification of CDK4 or loss of retinoblastoma (Rb) activity, indicating disruption of both pathways is important in the biology of GBM (247).

1.2.3. GBM Clinical Features, Prognosis, and Histopathology

The clinical history of the disease is usually short (less than 3 months in more than 50% of cases), unless the neoplasm has developed from a lower-grade astrocytoma. Patients often present after an epileptic seizure with non-specific neurological symptoms, headache, and personality changes. As the tumor rapidly enlarges, brain distortion by tumor mass effect and resultant edema can lead to an elevation in intracranial pressure. Patients with large tumors can present with motor/sensory symptoms and/or a change in the level of consciousness.

The median life expectancy of patients with GBM is 12 months; only 5% of patients or fewer will be alive at five years after diagnosis (25, 331) despite treatment. Several variables affect the prognosis of patients with GBM, including age (36), preoperative performance status (115), tumor location (110), reoperation for recurrent tumor (8, 135), and whether the patient receives radiation therapy (331).

GBM tumors occur most often in the subcortical white matter of the cerebral hemispheres. Tumor infiltration extends into adjacent cortex, the basal ganglia, and the contralateral hemisphere. Glioblastomas of the brainstem are infrequent and often affect children. GBM tumors are composed of poorly differentiated neoplastic astrocytes that are pleomorphic and contain nuclear atypia with brisk mitotic activity (171). Tumors are quite vascular characterized by microvascular proliferation, consisting of smooth muscle/pericyte and endothelial cell proliferation. The association of microvascular proliferation and necrosis is a histopathological hallmark of glioblastomas.

Glioblastomas are notorious for their rapid invasion of neighboring brain structures (37). A very common feature is extension of the tumor through the corpus callosum into the contralateral hemisphere, creating the image of a bilateral symmetrical lesion ('butterfly

glioma'). Similarly, rapid spread is observed in the internal capsule, fornix, anterior commissure, and optic radiation. These structures may be enlarged and distorted, serving as a 'passageway' for the formation of new tumor masses in other sites of the brain leading to multifocal glioblastoma. Metastasis of GBM to other sites of the body is very rare.

1.2.4. GBM and Surgical Resection

The goals of surgical resection of GBM include histologic diagnosis, relief of tumor mass effect, and cytoreduction. Due to the work of Kelly et al., complete surgical resection of GBM tumors was determined unlikely because of tumor infiltration with normal brain (165, 166). Kelly described three contiguous regions of a GBM tumor: (1) the contrast-enhancing portion on MRI that corresponds to the tumor cell mass without intervening brain parenchyma, (2) the area found in the center of the enhancing mass on MRI that represents necrotic tumor cells, and (3) the areas of increased signal intensity surrounding the enhancing portion of the tumor, which represent isolated tumor cell infiltration into the brain parenchyma. The density of infiltrating cells may vary in these areas from nearly all tumor cells to rare scattered cells with a predominance of edema. Surgical resections of GBM are aimed at removing the enhancing portion of the tumor along with the necrotic center. All resections of GBMs leave behind nonenhancing infiltrative tumor cells that reside away from the primary tumor mass. These tumor cells are ultimately responsible for recurrence of GBM tumors almost always in a local fashion.

The extent of tumor resection that should be undertaken in patients with GBM is controversial. Rigorous reviews of the literature have revealed there is little scientific evidence that aggressive surgical management significantly prolongs survival (141, 234, 268). One recent multivariate analysis of 416 patients with GBM revealed a significant survival advantage in

patients who underwent surgical resection of 98% or more of their tumor volume (184). The median survival for patients undergoing $\geq 98\%$ of the enhancing portion of the tumor was 13.4 months, whereas for patients with lesser resections, the median survival was 8.8 months. The optimal extent of resection in any patient depends on the tumor size and location, the patient's general and neurological status, and the experience of the surgeon.

1.2.5. GBM and Ionizing Radiation

The first promising data demonstrating the efficacy of radiotherapy after surgery for malignant gliomas in a randomized clinical trial was reported in 1976 by the Brain Tumor Study Group (BTSG), also known as the Brain Tumor Cooperative Group (BTCG) (329, 330). The BTSG established a benefit for postoperative radiotherapy after demonstrating a 37.5 week median survival in whole-brain radiotherapy alone versus 17 and 25 weeks for patients treated with conventional care and chemotherapy (BCNU, also known as carmustine), respectively. BCNU and whole-brain radiation therapy produced a 40.5 week median survival (330). GBM constituted 90% of patients in this trial. Sixty Gy IR in fractionated doses remains the standard of care for patients with newly diagnosed GBM.

Over the last 20 years, attempts have been made to improve the efficacy of IR through dose escalation using increased doses of standard fractionation, hyperfractionation, interstitial brachytherapy, three-dimension conformal radiotherapy, and stereotactic radiosurgery. Unfortunately, no significant increase in survival has been shown with these strategies. Partial brain radiotherapy has replaced whole-brain radiotherapy for patients with GBM based on data showing recurrence of GBM occurs within 2 cm of the primary tumor site in 90% of cases (145).

The limited efficacy of IR treatment is believed to arise from the poor apoptotic response to IR by the tumor cells and the hypoxic environment present within tumors (84, 164, 167, 353,

356). Glioma cells show an absence of either significant induction of bax or repression of bcl-2 and bcl-X_L after irradiation (176, 298). Strategies reported to enhance apoptosis after irradiation of malignant glioma cells include exogenous transfer of p53, APAF-1, and caspase 9 (116, 186, 297). Radiation-induced apoptosis in most cell types other than glial cells has been shown to depend on the presence of wild-type (wt) p53 (200). The presence or absence of wt p53 has not been shown to have a significant impact on the radiosensitivity of GBM cells (14, 125). Recently, autophagic cell death has been introduced as a possible mechanism for GBM cell death after IR, characterized by the accumulation of acidophilic vesicular organelles (AVOs) in the cytoplasm (353). Studies have shown that GBM cells with wt p53 exhibit a radiation-induced cell-cycle G1 arrest in contrast to cells lacking wt p53 (125, 356). These cells resume proliferation after several weeks, correlating with results from clinical studies demonstrating transient inhibition of tumor growth followed by regrowth within 6 to 8 months after irradiation of the lesion (125, 353). A deficit in G1-checkpoint after IR may be a mechanism for radioresistance in GBM cells lacking wt p53 (124). Radioresistance of GBMs with wt p53 may be due to a dysfunctional p53 pathway with overexpression of p21 and failure of transcriptional activation of p21 in response to irradiation (176). Nevertheless, IR continues to be the primary adjuvant treatment modality and standard of care for GBM patients as survival is modestly increased (331).

1.2.6. GBM and Chemotherapy

Chemotherapy has produced little success in the treatment of GBM (256). Nitrosoureas are the main chemotherapeutic agents used in the treatment of malignant gliomas. At present, chemotherapy usually is reserved for the palliative treatment of patients who have recurrent disease. Even though the blood-brain barrier is not entirely intact in these tumors, the blood-

tumor barrier prevents many chemotherapy agents from reaching the tumor in sufficient concentration (343). The invasive nature of GBM results in malignant cells at the periphery of the tumor being associated with a normal blood-brain barrier, providing protection from chemotherapeutic agents. Intra-arterial infusion of chemotherapeutic agents after blood-brain barrier disruption has been attempted resulting in continued toxicity and limited clinical success (77, 239, 294). Biodegradable wafers impregnated with BCNU (GLIADEL; Guilford Pharmaceuticals, Inc.) can be used to line the resection cavity after GBM resection is performed. Modest prolonged survival has been shown with the use of GLIADEL wafers in GBM patients (34, 35, 322). The U.S. Food and Drug Administration has approved the use of these wafers for the treatment of recurrent and newly diagnosed GBM tumors.

Temozolomide (TMZ; Schering-Plough, Inc.), a novel alkylating agent, recently has been introduced to the clinical setting and demonstrated activity in recurrent gliomas (104, 311, 357). After oral administration, TMZ is rapidly absorbed with almost 100% bioavailability (238). It readily crosses the blood-brain barrier and achieves effective concentrations in the cerebrospinal fluid (CSF). In a phase II trial in patients with recurrent GBM, the 6-month progression-free survival rate in temozolomide-treated patients was 18% and the 6-month overall survival rate was 46% (29). A total of 53% of patients experienced a clinical benefit with TMZ treatment. Resistance to TMZ is mediated in part by the DNA repair enzyme, methylguanine-DNA methyltransferase (MGMT). This enzyme has been found to be a major determinant of TMZ cytotoxicity in vitro and continuous exposure to TMZ leads to depletion of MGMT (105). Methylation of the MGMT promoter has been associated with greater overall survival in GBM patients treated with TMZ (138, 139).

1.2.6.1. GBM and Chemoradiation

The combination of TMZ and IR, termed chemoradiation, has been shown to have additive and synergistic activity in vitro against glioblastoma cells (324, 337). It has been shown that TMZ induces a G2-M arrest in glioma cells allowing for cell cycle synchronization in a radiosensitive phase (142). Chemoradiation is a new standard of care now evolving for patients with newly diagnosed GBM (312, 313). Based on promising results from a randomized phase III trial, the use of concomitant and adjuvant TMZ chemotherapy and radiotherapy significantly improves progression-free and overall survival in GBM patients (312, 313). Patients randomized between standard IR treatment versus IR treatment and concomitant TMZ followed by up to 6 cycles of adjuvant TMZ had an increase in median survival of 3 months ($P<.0001$) in the TMZ-treated group.

1.2.6.2. Convection-Enhanced Delivery

Distribution of therapeutic agents within the CNS has been problematic. Systemic delivery is limited by the blood-brain barrier, nontargeted distribution, and systemic toxicity. Diffusion-dependent methods that deliver substances by “push-pull” catheters (232), intrathecal injection (181), miniosmotic pumps (201), and drug-impregnated polymers (211) (34) can result in nontargeted distribution and a volume of distribution (V_d) that is limited by molecular weight and infusate diffusivity. CED is an approach developed to overcome the obstacles associated with current CNS agent delivery (26, 230) and is increasingly used to distribute therapeutic agents for treatment of malignant gliomas. Currently, multiple clinical trials involve CED for the treatment of recurrent GBM (182, 326, 336, 338). In CED, a small hydrostatic pressure differential imposed by a syringe pump to distribute infusate directly to small or large regions of the CNS is used in a safe, reliable, targeted, and homogeneous manner (60). CED relies on bulk

flow that is driven by a small gradient to distribute molecules within the interstitial spaces of the CNS. CED allows for a clinically effective V_d that is linearly proportional to the volume of infusion (V_i). Convection is not limited by the infusate's molecular weight, concentration, or diffusivity (26, 230, 310). Since CED directly distributes molecules within brain parenchyma, it can be used to target select regions of the CNS in a manner that bypasses the blood-nervous system barrier (253).

1.2.7. Gene Therapy for GBM

Malignant brain tumors were one of the earliest targets for human gene therapy. Brain tumor cells represent islands of high mitotic activity on the background of a predominantly postmitotic environment in the adult brain. Treatments with selective tumor toxicity can be designed accordingly. The best explored approach has been insertion of a genetic sequence into tumor cells which renders these and their clonal progeny sensitive to drug treatment (226). The transgene/vector system widely used in the past decade was the herpes simplex virus thymidine kinase (HSV-tk) gene transferred by a replication-incompetent retrovirus vector (97, 227, 251). Tumor cell transduction with HSV-tk together with gancyclovir administration allows for tk phosphorylation of gancyclovir to form a toxic nucleotide analog that is incorporated into replicating DNA causing strand termination and cell death by apoptosis (22). Terminally differentiated cells, such as neurons in the brain, are spared because their DNA does not replicate. In addition, sufficient activated gancyclovir can be transmitted across cell gap junctions to destroy neighboring untransduced tumor cells, a phenomenon known as the "bystander effect" (101, 348). Early clinical trials using retrovirus vectors in combination with gancyclovir revealed the inability of these vectors to achieve a useful tumor transduction rate (293). Also, low viral titers (typically $1 \times 10^5 - 10^7$ infectious particles/ml) and instability of the

virus particles have limited the clinical usefulness of retroviral vectors (27). Other nonreplicating recombinant viruses used in the treatment of GBM include HSV-1. These viruses are deficient in immediate-early genes and express other HSV-1 genes (HSV-tk) and transgenes that can lyse tumor cells (244).

Viruses have also been used as vectors and as oncolytic agents for human GBM tumors (48). Replication conditional HSV-1 and adenovirus vectors have been engineered to replicate in mitotic cells only (e.g., HSV-1) or in cells lacking functional tumor-suppressor proteins such as p53 or Rb (e.g., adenovirus) (7, 208, 222).

1.3. Ionizing Radiation

1.3.1. Types and Quantity of Ionizing Radiation

Radiation includes any kind of energy that is emitted from a source in the form of rays or waves.

The absorption of energy from radiation in biological material may lead to excitation or to ionization. The raising of an electron in an atom or molecule to a higher energy level without actual ejection of the electron is called excitation. If the radiation has sufficient energy to eject one or more orbital electrons from the atom or molecule, the process is called ionization, and that radiation is said to be “ionizing radiation”. The important characteristic of IR is the localized release of large amounts of energy. The energy dissipated per ionizing event is approximately 33 eV, which is more than enough to break a strong chemical bond. For example, the energy associated with a C=C bond is 4.9 eV (130). IR is classified as electromagnetic or particulate. Particulate radiation includes charged particles such as electrons, protons, α -particles, deuteron, negative π -mesons, and heavy charged ions. Neutrons, which are uncharged, are also considered particulate radiation.

Electromagnetic radiation includes x- or γ -rays, radio waves, radar, radiant heat, and visible light. X- and γ -rays do not differ in nature or in properties (130). The designation x or γ reflects simply the way in which they are produced. X-rays are produced extranuclearly, while γ -rays are produced intra-nuclearly. X-rays are produced in an electrical device that accelerates electrons to high energy and then stops them abruptly in a target, usually made of tungsten or gold. Part of the kinetic energy of the electrons is converted into x-rays. Gamma-rays are emitted by radioactive isotopes and represent excess energy that is given off as the unstable nucleus breaks up and decays in its efforts to reach a stable form. Both x- and γ -rays act in the same manner in biological systems. They both may be thought of as a stream of photons, or “packets” of energy. When x- or γ -rays are absorbed in living material, energy is deposited in the tissues and cells. The energy is deposited unevenly in discrete packets. The energy in a beam of x- or γ -rays is quantized into large individual packets, each of which is big enough to break a chemical bond and initiate the chain of events that culminates in a biological change.

Quantity of IR is expressed in roentgens, rads, or gray. The roentgen (R) is the unit of exposure and is related to the ability of x- or γ -rays to ionize air. The rad is the unit of absorbed dose and corresponds to an energy absorption of 100 ergs/g. In the case of x- and γ -rays an exposure of 1 R results in an absorbed dose in water or soft tissue roughly equal to 1 rad. Officially, the rad has been replaced as a unit by the gray (Gy), which corresponds to an energy absorption of 1 joule/kg. Consequently, 1 Gy = 100 rads.

1.3.2. Absorption and Action of Ionizing Radiation

Ionizing radiation may be classified as directly or indirectly ionizing. Charged particles, or particulate radiation, can directly disrupt the atomic structure of the biologic tissue through which they pass and produce chemical and biological changes. Electromagnetic radiation (x-

and γ -rays) is indirectly ionizing. They do not produce chemical and biological damage themselves, but when absorbed in the material through which they pass, they give up their energy to produce fast-moving charged particles.

When x- or γ -rays, charged or uncharged particles are absorbed in biological material, there is a possibility they will interact directly with the critical targets in the cells. The atoms of the target itself may be ionized or excited, leading to biological change. This is what is termed the direct action of radiation and is the dominant process with neutrons or α -particles. In direct action a secondary electron resulting from absorption of an x- or γ -ray photon interacts with cellular DNA to produce DNA damage. Alternatively, radiation may interact with other atoms or molecules in the cell (mainly water) to produce free radicals that are able to diffuse far enough to reach and damage critical targets. This is called the indirect action of radiation, which is the predominant mechanism of damage by x- or γ -rays. A free radical is a free (not combined) atom or molecule carrying an unpaired orbital electron in the outer shell, which is highly reactive. The major effector free radical, after radiation interaction with water, is a highly reactive hydroxyl radical ($\text{OH}\cdot$). Hydroxyl radicals are responsible for DNA damage after IR, producing DNA double- and single-strand breaks. Approximately two thirds of DNA damage from x- or γ -rays is from the hydroxyl radical (130).

1.3.3. DNA Double-Strand Breaks and Cell Response

DNA double-strand breaks (DSBs) are the most critical form of DNA damage that may result in loss or rearrangement of genomic material and thereby lead to mutations, genomic instability, cancer development, or cell death (74, 146, 259, 347). DSBs arise spontaneously during normal cell metabolism, such as meiotic and V(D)J recombination, but can also be induced by DNA damaging agents, such as IR and certain chemicals.

DNA DSBs activate an extensive array of responses that lead to damage repair and continuation of cellular life (Fig. 2) (157). Ataxia telangiectasia mutated (ATM) protein is regarded as the primary activator of this network (296). ATM is missing or inactivated in patients with the genetic disorder ataxia-telangiectasia (A-T), characterized by cerebellar degeneration, immunodeficiency, radiation sensitivity, chromosomal instability and cancer predisposition (21, 109). Following the induction of DSBs, ATM's kinase activity is enhanced and it phosphorylates key proteins in numerous signaling pathways, including the checkpoint kinases Chk1 and Chk2 and the DNA repair proteins 53BP1, BRCA1, and p53 (296). The phosphorylation and accumulation of p53 after IR results in G1/S cell cycle arrest and p21 induction (15, 39). ATM's activation was recently shown to involve dimer dissociation and intermolecular autophosphorylation on the serine 1981 residue (12). ATM has also been shown to phosphorylate the histone variant, H2AX (38). H2AX is rapidly phosphorylated (within seconds) when DSBs are introduced into mammalian cells, resulting in discrete γ -H2AX (phosphorylated-H2AX) foci at DNA damage sites (276). Concomitant with ATM activation, a fraction of the nuclear content of ATM adheres to the DSB sites (9). The mode by which the DSB signal is conveyed to ATM is not clear, nor are the proteins that function in the DSB response between damage induction and ATM activation.

The MRN complex, whose core contains the Mre11, Rad50, and Nbs1 proteins, is involved in the initial processing of DSBs due to its nuclease activity and DNA binding capability (Fig. 2) (62). These activities reside in the Mre11 protein, and partially depend on Mre11's interaction with the Rad50 ATPase. The Nbs1 protein is thought to be involved in the nuclear localization and proper assembly of the complex at DSB ends, probably via its ability to interact directly with γ H2AX (173). The MRN complex adheres to the sites of DSBs

immediately following their induction, and this process is independent of ATM (223). The order in which ATM and the MRN complex act in the early phase of the DSB response is unclear. Functional MRN is required for ATM activation and timely activation of ATM-mediated pathways (321).

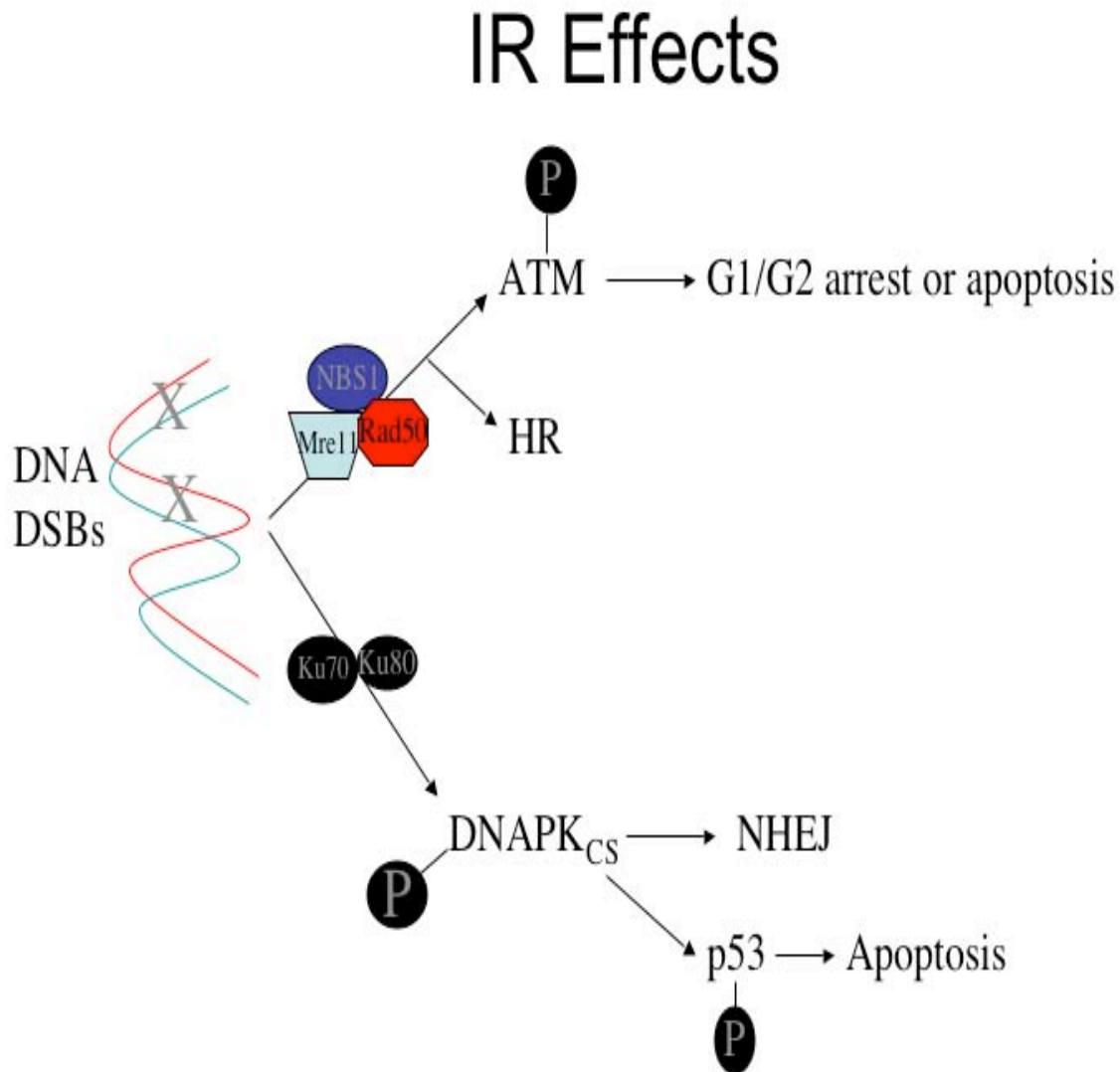


Figure 2. Production of DNA DSBs, cellular response, and repair.

1.3.4. DNA Double-Strand Break Repair

DNA DSBs are repaired in eukaryotes by the concerted action of two repair pathways, homologous recombination (HR) and nonhomologous end-joining (NHEJ) (Fig. 2). The MRN complex plays a role in both modes of repair, particularly in the HR pathway. DSB repair by HR requires an undamaged template that contains a homologous DNA sequence, typically on the sister chromatid in the S or G2 phase of the cell cycle. HR in higher eukaryotes is mediated by the gene products of the homologs to the *Saccharomyces cerevisiae* RAD52 epistasis group (275). In contrast to HR, NHEJ of two double-stranded ends does not require an undamaged partner and does not rely on extensive homologies between the recombining ends (192). NHEJ is active in all cell-cycle phases and is thought to repair the majority of DSBs in mammalian cells. Defects in the NHEJ pathway can cause increased cell death secondary to DSBs generated by IR or restriction endonucleases (45, 278). Additionally, defective or deregulated NHEJ may result in chromosomal aberrations, genomic instability, and ultimately contribute to cancer development (146, 347).

1.3.4.1. NHEJ and DNA DSBs

NHEJ can be an error-free or error-prone process, which is in part determined by different types of DNA ends. Complementary cohesive ends typically generated by restriction endonucleases can be rejoined in an error-free manner by precise ligation. NHEJ is commonly regarded as an error-prone process due the occurrence of end-processing (192). This involves the alignment of overhanging ends by pairing along nucleotides of 1-4 bp microhomology that flank the break site, followed by gap filling or trimming of a few bases and subsequent ligation. The repair of IR-induced DSBs is generally error-prone because IR destroys sequence information by causing complex DNA damage sites (347), thereby requiring end-modification prior to rejoining. It is

largely unknown which regulatory proteins control the extent of DNA sequence alteration during repair.

The DNA-dependent protein kinase (DNA-PK) complex and the XRCC4/DNA ligase IV complex are required for NHEJ (58). DNA-PK, consisting of the Ku heterodimer (which consists of the Ku70 and Ku80 subunits) and the catalytic subunit (DNA-PK_{CS}), is activated by DNA *in vitro* (Fig. 2) (301). DNA-PK_{CS} is a member of the phosphatidylinositol-3 (PI-3)-like kinase family that includes ATM. Ku binds to DNA ends with very high affinity and is thought to function as the DNA-binding and regulatory subunit that stimulates DNA-PK_{CS} activity (118). The kinase activity of DNA-PK is required for the repair of DSBs by the NHEJ pathway (183).

Recently, autophosphorylation of DNA-PK_{CS} has been shown to occur *in vivo* in a Ku-dependent manner in response to IR and is required for DSB repair (44). Phosphorylated DNA-PK_{CS} has been shown to colocalize with both γ H2AX and 53BP1 at sites of DNA DSBs.

When assembled on a suitable DNA molecule *in vitro*, DNA-PK_{CS} becomes activated and phosphorylates many transcription factors, including p53 (10). DNA-PK_{CS} serves as an upstream effector for p53 activation in response to IR, linking DNA damage to apoptosis (332). IR induction of apoptosis and Bax is significantly suppressed in the absence of DNA-PK_{CS}.

1.4. Herpes Simplex Virus

1.4.1. Clinical HSV Infection and Treatment

HSV is a well-adapted pathogen, demonstrated by its widespread prevalence in humans, its only known natural hosts. Over 75% of all adults in the United States have antibodies to HSV-1 or 35% to HSV-2. Approximately 40 million infected individuals will experience recurrent herpes disease due to reactivation of their own “personal” viruses sometime in their lifetime. HSV

initially gains access to the host via infection of epithelial cells at skin and/or mucosal surfaces leading to the production of characteristic painful vesicular lesions. HSV-1 is associated with oral infection and is transmitted via oral and respiratory secretions while HSV-2 is generally associated with genital infection.

HSV infection is associated with other infectious processes, including herpes keratitis and encephalitis. Herpes keratitis can result in corneal blindness. Due to HSV neurotropism, access to the CNS can cause encephalitis. Herpes simplex encephalitis (HSE) occurs relatively infrequently, with an incidence of one case per 250,000 population/year in the United States (344). It is the most commonly identified cause of acute viral encephalitis, comprising 20% of all cases (320). There is a bimodal distribution of HSE, with 1/3 of cases occurring in those less than 20 years of age and 1/2 in those aged 50 years or more. HSE occurs predominantly in neonates and immunocompromised individuals and is caused by HSV-2. In immunocompetent adults, greater than 90% of cases of HSE result from infection with HSV-1, with the remainder due to HSV-2 infection. HSV produces an acute, microhemorrhagic, necrotizing encephalitis with surrounding brain edema. Predilection for bilateral temporal and orbitofrontal lobes of the brain occurs. Asymmetric involvement of the insular cortex and cingulate gyrus can occur. A proposed explanation for the typical pattern of involvement of the temporal and frontal lobes of the brain is the presence of the latent virus within the gasserian ganglion in Meckel's cave (236). Reactivated virus may spread along the meninges around the temporal lobes and the undersurface of the frontal lobes. A good outcome from HSV encephalitis relies on early diagnosis. Delay in therapy or untreated HSV encephalitis has a high mortality rate (50% to 75%), with little chance of full neurologic recovery (320).

Acyclovir is a nontoxic, prodrug antiviral that is highly efficacious against productive HSV infection (82). Acyclovir is a nucleoside analog similar to guanosine, but contains an acyclic sugar group. The drug requires three different kinases to be present in the cell to convert acyclovir to a triphosphate derivative, the actual antiviral drug. High selectivity of the drug occurs with HSV-infected cells. The first kinase that is required is a virus-encoded kinase called thymidine kinase (tk), which is not found in uninfected cells. After initial phosphorylation by tk, subsequent phosphorylation is completed by cellular enzymes and acyclovir triphosphate is incorporated into DNA by the viral DNA polymerase. DNA replication is blocked as acyclovir lacks a 3'-OH group. In addition, inactivation of viral DNA polymerase occurs. Derivatives of acyclovir have been developed, including valacyclovir and famciclovir, which are used predominantly due to their greater efficacy from improved oral bioavailability (133).

1.4.2. HSV Structure and Genome

HSV consists of linear double-stranded DNA packaged into an icosadeltahedral capsid (106, 149). The capsid is surrounded by an amorphous tegument layer that is held within a trilaminar envelope containing glycoprotein spikes (122) (18, 304). Glycoproteins are embedded in the trilaminar envelope of the mature virion (280).

The HSV genome consists of 152 kilobase pairs comprising 84 genes and an excess of 90 open reading frames (ORFs) (20, 169, 339). Viral genes encode proteins that affect the coordinated expression of the viral genome. In addition, proteins are expressed for viral replication and for virion surface and envelope components. The viral genome is separated by a unique long (U_L) and unique short (U_S) sequence flanked on each end by terminal inverted repeat sequences (214, 215). The U_L and U_S sequences are covalently joined by internal repeat

sequences. The U_L and U_S sequences can randomly invert relative to each other so the HSV genome actually can exist in four equimolar isomers (136).

1.4.3. HSV Life Cycle

1.4.3.1. HSV Cell Entry

HSV-1 infection involves virus attachment to the cell surface, fusion of the viral envelope with the plasma membrane, and entry of the viral capsid into the cytoplasm (228, 304). The initial binding of HSV to the cell surface occurs by heparan sulfate (HS) proteoglycans present on the surface of most types of vertebrate cells (350). HSV glycoproteins, B (gB) and C (gC) have been shown to be involved in the initial attachment phase through the interaction of positively charged glycoprotein structures with negatively charged HS moieties located on cell surface proteoglycans (187). Removal of HS from the cell surface, either by enzymatic treatment or by selection of cell lines defective in the pathway HS, renders cells at least partially resistant to HSV infection by reducing virus attachment to the cell surface (119, 295).

Following the initial adsorption event, a secondary binding event occurs between viral glycoprotein D and cellular receptors identified as herpesviral entry mediators, or HVEMs (114, 225). These include HveA, HveB (nectin-2), and HveC (nectin-1). Fusion of the viral envelope with the cell membrane occurs after the binding of gD to its cognate cell surface receptor (228). Three other HSV glycoproteins have been implicated in the fusion process, including gB, gH, and gL (68, 72, 281). Once fusion occurs, the nucleocapsid is released into the cell cytoplasm and viral capsids are transported to nuclear pores where viral DNA is released into the nucleus and viral gene expression can occur. In certain cell types, HSV entry is dependent on

endocytosis and exposure to a low pH (242). Inhibition of endocytosis has been shown to prevent uptake of HSV from HeLa and Chinese hamster ovary cells.

1.4.3.2. HSV Pathogenesis

Initial infection results in productive viral replication in cells of the epidermis and dermis (280).

HSV may gain access to nerve termini of sensory neurons and is transmitted to the neuronal cell body by retrograde transport (55). HSV can cause a latent infection in which the viral genome adopts a persistent, quiescent state. Establishment of latency occurs predominantly in terminally differentiated, nondividing neurons of the peripheral nervous system that innervate the initial site of infection. Neurons of sensory and autonomic ganglia are infected following primary rounds of replication in cells of mucosal or epidermal surfaces. Since neurons neither replicate their DNA nor divide, the HSV genome does not need to replicate to persist. HSV latent infection of peripheral neurons is an effective survival mechanism, as there are no vaccines or antivirals that can attack the latent infection. Consequently, once the host is infected with HSV, the host is infected for life.

Latency occurs when the cell represses immediate-early (IE) viral gene expression, inhibiting the cascade of early (E) and late (L) viral gene expression that lead to lytic infection (87). In the latent state, the HSV viral genome circularizes (108, 156, 262), becomes associated with nucleosomes in a chromatin structure (73), and persists extrachromosomally (219). Viral gene expression during latency is limited to a set of nontranslated RNA species, the latency associated transcripts (LATs), which are expressed as stable lariat intron RNA molecules and are detectable in the nuclei of latently infected neurons (59, 87, 305, 308). Viral genomes can remain in this state in the nucleus of neurons for the lifetime of the host. Alterations in the host-

virus interaction may cause “reactivation” of the viral infection from a quiescent state to a productive, lytic cycle of viral replication. Expression of ICP0 and various types of stress can trigger reactivation (40, 117, 128, 129, 190, 282). During latency, however, ICP0 is not expressed, and reactivation is thought to occur when stress stimuli derepress ICP0, promoting viral gene expression and lytic infection (87). Productive infection results in a lytic cascade of viral gene expression and the production of mature virions which can then travel back down the nerve axon via anterograde transport and establish infection at mucocutaneous surfaces innervated by the infected neuron (55). At least 76 of the total 84 HSV-1 genes are expressed during lytic infection (213). Cell lysis and release of mature virions allows for spread of the virus. Recurrent cutaneous infections occur due to reactivation of the virus from latency in neurons at different time points throughout the life of the individual.

1.4.3.3. HSV Gene Expression

If lytic infection occurs after HSV nuclear entry, viral genes are expressed in a tightly regulated temporal cascade in which three classes of viral genes are sequentially expressed: immediate early (IE) or α , early (E) or β , and late (L) or γ (150, 151). All viral genes are expressed as cellular RNA polymerase II transcription units utilizing the host cellular transcription machinery. Each class of genes differs with respect to its promoter structure, which decreases in complexity from IE to L genes (339). Early promoters differ from IE promoters in that they lack the virus-specific TAATGARAT sequences present in IE promoters. Both E and IE promoters contain a TATA box and retain upstream cellular activating sequences, such as Sp1 and CCAAT boxes, that contribute to activation of these genes (86, 113). L promoters contain a TATA box and are devoid of any essential upstream activating sequences (98). Only two known elements

downstream from the TATA box are important for late gene expression, the initiator element (INR), which overlaps the transcriptional start site, and the downstream activating sequence (307). These class-specific differences in promoter structure may be important in determining the ability to nucleate the assembly of stable preinitiation complexes at various phases of infection, in part mediating kinetic class-specific transcription (328, 359).

The IE genes are the first viral genes expressed upon infection and possess the main regulatory activities of viral gene expression. The resultant IE proteins are necessary for the subsequent expression of the E and L gene classes. The E genes encode proteins involved in nucleotide metabolism and viral DNA replication. HSV encodes its own DNA replication machinery. The third class of viral gene expressed, the L genes, encode mainly structural components of the virus particle.

The temporal nature of the cascade of events during HSV gene expression with lytic infection is well defined (150, 151). IE gene expression is detectable within 30 minutes of infection, with maximal protein accumulation occurring between 2-4 hours post-infection (hpi). The E genes reach peak rates of synthesis between 5-7 hpi. Viral DNA replication is detectable as early as 3 hpi and continues through 12-15 hpi. L gene expression can be detected soon after initiation of viral DNA replication and peak levels of L proteins occur after 8 hpi. During lytic infection, the eclipse period is 5 hours and progeny virus is released throughout the remainder of the replication cycle, which is approximately 18 hours.

1.4.3.4. HSV Immediate-Early Proteins

There are five HSV IE proteins expressed by designated infected cell polypeptide 0 (ICP0), ICP4, ICP22, ICP27, and ICP47. The IE genes are expressed in the absence of de novo viral

protein synthesis. During HSV lytic infection, the viral transactivator, VP16, enters the cell as a component of the virion tegument (318). VP16 complexes with host cellular factors, Oct-1 and host cell factor (HCF), bind TAATGARRAT motifs present in all HSV-1 immediate early (IE) promoters (99, 179, 180, 248, 266, 319). This complex recruits transcriptional activators and RNA polymerase II to IE promoters, which subsequently express the five infected cell polypeptides (ICP). In addition to a TATA box and TAATGARAT elements, sites exist for several cellular *cis*-acting factors such as Sp1 and others that contribute to enhanced transcription or transcription in the absence of VP16 (112).

Gene expression during lytic infection progresses in a regulated cascade in which the five IE gene products, ICP0, ICP4, ICP22, ICP27, and ICP47, are the first viral proteins synthesized upon infection, with the exception of ICP47, encode the primary regulatory functions of the virus necessary for the efficient and timely expression of early and late gene expression (53, 151, 258). Of the five IE proteins, only ICP4 and ICP27 are absolutely essential for productive viral replication (69, 76, 212). The remaining IE proteins ICP0, ICP22, and ICP47 fulfill accessory roles to optimize viral replication.

ICP47 is the only IE protein that does not function directly in regulating viral gene expression. The role of ICP47 during infection is in the down-modulation of the host immune response. ICP47 functions to limit the presentation of antigens via the major histocompatibility (MHC) class I pathway (100, 355). This occurs as a consequence of interaction between ICP47 and the transporter associated with antigen processing (TAP). TAP passes peptides to the endoplasmic reticulum (ER) lumen for assembly onto MHC-1 and the interaction with ICP47 impedes this function. As a result, MHC Class I molecules are retained in the endoplasmic

reticulum/cis-Golgi apparatus within hours after infection. The infected cell is thus prevented from displaying Class I antigens and is preserved from lysis by CD8⁺ T lymphocytes.

ICP22 is thought to function during infection by facilitating L gene expression, thereby promoting the switch from E to L gene expression. ICP22 enables full expression of a subset of L viral genes by causing cdc2 cyclin-dependent kinase activity to survive the degradation of its physiologic partners cyclins A and B, by an aberrant partnership with the U_L42 DNA polymerase processivity factor (2, 3, 6). Optimal transcription of late genes requires binding and posttranslational modification of topoisomerase II α by ICP22 and cdc (5). ICP22 is not essential for virus replication, and phenotypic effects on virus replication and gene expression are highly cell-type dependent (290). ICP22 has been shown to affect the stability of the ICP0 transcript as well as splice site usage during processing of ICP0 mRNA (43). ICP22 is associated with the aberrant phosphorylation state of the C-terminal domain of cellular RNA Pol II in HSV infected cells (273), and is thought that this phosphorylation pattern affects the targeting and activity of the RNA Pol II transcription complex on viral promoters.

ICP27 is required for viral replication, and appears to be multifunctional during infection (285). ICP27 is generally associated with activating E and L gene expression (212). In addition to this transactivation function, ICP27 is also associated with the repression of gene expression (218, 273, 291) which likely aids in the orderly transition from IE, E, and L gene expression. ICP27 exerts additional regulatory influences post-transcriptionally by modulating mRNA processing of both viral and cellular transcripts (132, 217, 289) and with poly-A site usage (216). ICP27 has been shown to block RNA splicing but not transport of unspliced RNA early in infection (287). ICP27 also has been shown to affect the export of certain classes of mRNA (260, 303), as well as the shut-off of host protein synthesis (131, 289). ICP27 is active as a

chaperone of newly made viral mRNA across the nuclear membranes at late times after infection. ICP27 has been demonstrated to affect the post-transcriptional processing of ICP0 (131, 132) and the post-translational modification of ICP4 (218, 273) which may play a role in ICP27 modulation of E and L gene expression.

ICP4 is the major regulatory protein of the virus and is absolutely required for the transition of viral gene transcription from the IE to the E phase due to its role as a transcriptional activator of early and late genes (76, 265, 335). ICP4 is located in the U_S repeat sequences and is thus present in two copies in the viral genome. It can function as a repressor (70, 120, 221) or activator (70, 88, 113) of transcription by forming multiple contacts with basal transcription factors (42, 120, 300, 358). Transcriptional regulation by ICP4 involves complex interactions with the cellular transcription machinery (19, 56). One such interaction involves the ICP4 C-terminal activation domain which interacts with RNA Pol II general transcription factor, TFIID, via its TATA binding protein (TBP) associated factor 250 (TAF250) subunit (42). Although ICP4 contains a DNA binding region that is essential to activation (71), no specific ICP4 binding sites have been identified on early and late promoters that are responsible for activation (86). Deletion of ICP4 eliminates expression of early and late genes (69). However, certain mutations in ICP4 that have no effect on early gene transcription do not allow late gene expression, suggesting ICP4 may act differently on early and late promoters (71).

ICP0 has been described as a promiscuous transactivator of both viral and cellular promoters in transient assays. ICP0 activates a specific subset of cellular genes, including p53-responsive genes that it activates independently of p53 (143). ICP0 is the only viral protein capable of transactivating all three classes of viral genes (47). ICP0 activates transcription of viral genes in synergy with or independent of ICP4 (88, 111, 160). ICP0 has been shown to

interact with ICP4, and this interaction is believed to mediate cooperative activation of gene expression, as it maps to a region of ICP0 that contains the domain involved in synergy with ICP4 (352). HSV mutants deficient for ICP0 function are severely growth impaired and do not efficiently reactivate from latency in animal models (40, 52, 117). The role of ICP0 during infection is generally considered to be in promoting lytic cycle events and inhibiting latency. Recently, ICP0 has been shown to inhibit circularization of the HSV-1 genome and promote lytic infection (156, 288). ICP0 does not bind DNA, but activates gene expression at the level of mRNA synthesis by increasing the rate of transcription (162, 286). ICP0 interacts with host cellular proteins and pathways by complex interactions. In fact, ICP0 targets many cellular proteins for destruction, including nuclear structures known as ND10, which contain the promyelocytic protein (PML) and Sp100 (46, 93). Other proteins targeted for destruction by ICP0 include the catalytic subunit of the DNA-dependent protein kinase (DNA-PK_{CS}) (189, 255) and centromeric proteins C and A (91, 197). ICP0 has been shown to function as an E3 ubiquitin ligase (28, 87) conjugating ubiquitin onto proteins, in a RING finger-dependent manner, and targeting them for degradation by the ubiquitin-dependent proteasome degradation pathway (93).

1.4.3.5. HSV DNA Replication and Recombination

Replication of HSV occurs within the nucleus of the infected cell. HSV encodes over 80 gene products that contribute to viral replication in either cultured cells or animal hosts (280). Due to the limited size of the HSV-1 genome, the virus cannot code for every function required for its propagation. HSV-1 must rely upon factors supplied by the host cell for replication. For example, HSV exclusively uses the host cell RNA polymerase II for transcription of viral genes (57).

Viral DNA synthesis takes place within globular domains in called replication compartments (269), which contain the seven essential viral DNA replication proteins: the origin-binding protein (UL9), the single-stranded-DNA-binding protein (UL29 or ICP8), the helicase-primase heterotrimer (UL5/UL8/UL52), the viral polymerase (UL30), and its processivity factor (UL42)(342). Other viral proteins that are found in the replication centers include ICP4, ICP27, and the major capsid protein VP5 (67, 172, 195, 261). Cellular proteins that have been shown to localize within replication compartments include p53, Rb, and the DNA-binding replication protein A (RPA) (345). Recently, various cellular proteins involved in DNA recombination/repair have also been shown to localize within replication compartments such as DNA-PK_{CS}, Ku86, BLM, Nbs1, PCNA, BRCA1, MSH2, Rad50, Rad51, and WRN (317, 346).

Initially, viral DNA replication was thought to occur via a rolling circle mechanism that generated head-to-tail concatamers of viral genomes (23, 158, 159). HSV genome circularization was believed to be a prerequisite for viral DNA replication that involved recombination of the terminal repeats, resulting in a θ replication mode for the initial round of replication, providing the template for a rolling circle mode of replication (279, 299).

Recently, our group has challenged the concept of HSV genome circularization as a requirement for viral DNA replication. Jackson and DeLuca have shown that genome circularization does not occur in productive infection but instead may occur during the establishment of latency as a function of ICP0 expression (156, 288). ICP0 appears to prevent the formation of circular HSV-1 DNA molecules. HSV-1 mutants defective for ICP0 expression resulted in the predominance of circular HSV-1 genomes during infection. The finding that ICP0 appears to prevent the formation of circular molecules may explain why replication of

HSV-1 is greatly reduced in HSV-1 mutants defective in ICP0 at low multiplicities of infection (283, 309). Jackson and DeLuca have postulated that linear HSV molecules rather than circles might serve as the initial templates for HSV-1 replication. Genome replication may proceed from the three origins of HSV-1 DNA replication, oriL and two copies of oriS, to produce highly branched structures that might then be resolved by recombination or during packaging of viral DNA.

Several lines of evidence indicate that the process of HSV-1 DNA replication is linked to recombination. For example, recombination is a frequent event within the HSV-1 genome as well as between infecting genomes and is stimulated on HSV-1 infection (78, 79). Newly replicated DNA is larger than unit length and adopts a highly complex structure, the formation of which is presumed to require recombination (203). Newly replicated DNA also undergoes genomic inversion (17). Viral proteins may function to promote recombination and it is likely that recombination during HSV-1 infection also may involve cellular recombination pathways (243, 354).

1.4.3.6. HSV Infection, ND10 Domains, and DNA Damage Response

HSV DNA replication is closely associated with nuclear matrix-bound multiprotein domains called ND10 domains (also called promyelocytic leukemia [PML] nuclear bodies), which are defined and organized by the PML protein (11, 154, 210). Upon entry into the nucleus, parental viral genomes are found adjacent to ND10 domains (210) early in infection, and the IE protein, ICP0, induces degradation of PML and the dispersal of ND10 domains and associated proteins (94, 209).

ND10 domains have been shown to contain host recombination/repair proteins (235) and participate in the cell's response to DNA damage (41). ND10 domains are redistributed in response to DNA damage (41), and it has been proposed that ND10 may store and release proteins in response to certain external insults such as viral infection and DNA damage (235). For example, the ND10-associated proteins PML, Mre11, γ H2AX, Rad50, NBS1, RPA, and TopBP1 are redistributed to double-strand DNA repair foci induced by ionizing radiation (16, 41, 351). Recently, HSV infection has been shown to induce a cellular response to DNA damage with recruitment of recombination and repair proteins to HSV-1 DNA (193, 346). Activation and exploitation of a cellular DNA damage response has been shown to aid viral replication in nonneuronal cells (193). Activation of ATM, Chk2, 53BP1, and Nbs1 have been shown after HSV-1 infection. ATM activation appears to be an early event that precedes signaling to other proteins and expression of ICP0. In contrast to adenovirus infection, HSV-1 infection does not alter steady-state levels of Mre11/Rad50/Nbs1. ATM, Nbs1, and Rad50 proteins have been shown to accumulate at sites of HSV-1 replication. Lilley and Weitzman have suggested that when the DNA damage response is absent, HSV-1 replication is impaired (193). In cell lines harboring mutations in Mre11 or ATM, viral yield was shown to be decreased. The defect in HSV-1 growth in the absence of a DNA damage response is even more marked with infection by an ICP0-null virus. In neuronal cells, HSV-1 infection is unable to elicit a DNA damage response which is consistent with prior reports that neurons are inefficient at DNA repair (246). Inability to mount a DNA damage response and viral replication compromise may contribute to the establishment of viral latency in neuronal cells.

Recently, our group has suggested the ends of the HSV-1 linear genome could be treated as DNA double-strand breaks, which could be repaired as circular genomes (156). The

expression of ICP0 early during lytic infection would inhibit the repair process by ND10 body disruption and degradation of the catalytic subunit of DNA-dependent protein kinase (DNAPK_{cs}). As a result, circularization of HSV-1 DNA would not proceed and replication of linear HSV-1 genomes can occur.

1.4.3.7. HSV Assembly and Release

The replication of HSV-1 does not produce genomic DNA molecules, but rather concatemers containing many head-to-tail copies of the viral genome. Individual genomes are therefore liberated from the concatemers. Cleavage of viral DNA at terminal repeat sequences into genome length segments can then be packaged into preformed capsids (220). These particles, or nucleocapsids, are non-infectious and unstable until they acquire an envelope. The mature nucleocapsid that is assembled within the nucleus initially acquires an envelope by budding through the inner nuclear membrane (100). Upon fusion with the outer nuclear membrane, this membrane is lost as unenveloped nucleocapsids are released from the cytoplasm (220). Envelope glycoproteins are initially added in the first stage of the secretory pathway, the endoplasmic reticulum. The final envelope is acquired upon budding of tegument-containing structures into a late compartment of the secretory pathway in the transgolgi network. The viral particles then reach the cellular plasma membrane and are released into the extracellular space via cellular secretory and trafficking pathways in which the capsids may exchange envelope moieties with other cellular membrane bound compartments.

1.4.4. ICP0

ICP0 is required for both HSV lytic viral infection and efficient reactivation from latency in vitro and in vivo (40, 117, 128, 129, 190, 282). ICP0 is a promiscuous transactivator shown to

enhance the expression of genes introduced into cells by infection or transfection (127). ICP0 is critical for viral replication in cultured cells infected at low multiplicity, but is not essential in cells infected at high multiplicity (283, 290). One copy of the ICP0 gene exists on each end of the U_L sequence of the HSV-1 genome within the repeat sequences. ICP0 is a 110 kDa (775 amino acids in length) protein translated from a spliced mRNA containing three exons encoding 19, 222, and 534 amino acids (127). ICP0 is extensively posttranslationally processed (1). It is phosphorylated by the viral protein kinase U_L13 (249) and the cell cycle kinase cdc2 (6) and nucleotidylated by casein kinase II (224). Modifications of ICP0 are sequential and are associated with specific locations of the protein within cellular compartments (3). Newly synthesized ICP0 accumulates initially at or near ND10 structures (209). As the amount of ICP0 increases, the protein spreads out and fills the nucleus. Late in infection, after the onset of viral DNA synthesis, ICP0 is found in the cytoplasm (198). ICP0 appears to shuttle between the nucleus and cytoplasm and may linger rather than reside in the cytoplasm at late times after infection (127).

ICP0 participates in many cellular processes that lead to transactivation of gene expression indirectly even though it does not bind DNA (90, 96). Activation of gene expression by ICP0 is considered to occur at the level of mRNA synthesis (162, 286). Mutational analysis has demonstrated the importance of an N-terminal C3HC4 (RING finger) motif in ICP0 activity, and such domains are thought to mediate protein-protein interactions (85, 89, 95, 102, 103).

1.4.4.1. ICP0 Conquest of Host Cell Metabolism

ICP0 is a multifunctional protein whose multitude of interactions with cellular metabolic functions translates into dysregulation of cell metabolism and cytotoxic effects. Infection with

HSV-1 has been linked to inhibition of cellular DNA synthesis associated with cell cycle arrest (66). ICP0 has been shown to cause cell cycle arrest at both G1/S and G2/M checkpoints (143). ICP0 expression in cells results in the induction of p53-responsive genes p21, gadd45, and MDM2. ICP0 has also been shown to induce these genes in the absence of cellular p53. The histone deacetylase (HDAC) inhibitor, trichostatin A (TSA), is able to reproduce many of the effects of ICP0 on viral and cellular gene expression (143). Low level expression of ICP0 (1,000-fold lower relative to the level of expression from HSV-1 vectors) from an adenovirus construct, has been shown to not affect cellular division, perturb cellular metabolism, or cell survival (144).

ICP0 has been shown to function as an E3 ubiquitin ligase (28, 87) conjugating ubiquitin onto proteins, in a RING finger-dependent manner, and targeting them for degradation by the ubiquitin-dependent proteasome degradation pathway (93). As a viral protein that stimulates viral gene expression by targeting cellular proteins for degradation, ICP0 is thought to target cellular proteins that repress viral gene expression (87). ICP0 has been shown to target proteins, such as PML and Sp100, that are major constituents of ND10 bodies (93). ND10 bodies are discrete nuclear foci where HSV-1 genomes may localize early during infection (210). Recent studies have suggested that these foci are sites of DNA double-strand break (DSB) repair and inhibition of HSV genome circularization by ICP0 (41, 156). Other proteins targeted for degradation include centromere proteins, CENP A (197) and CENP-C (92, 196), the E2 ubiquitin-conjugating enzyme cdc34 (UbcH3) (127), and the catalytic subunit of DNA-dependent protein kinase (DNA-PK_{cs}) (189, 255).

1.4.4.2. ICP0 Degradation of DNA-PK_{CS}

HSV-1 infection causes the active degradation of DNA-PK_{CS}, a major player in the NHEJ pathway of DSB DNA repair. This process is reliant on the expression of the IE protein, ICP0 (189, 255). The extent of DNA-PK_{CS} degradation is cell-type specific and it has been shown that degradation occurs between 2 and 6 hours post-infection by HSV-1. The RING finger domain of ICP0 is required for DNA-PK_{CS} degradation (255). The proteasome pathway is responsible for the virus-induced degradation of DNA-PK_{CS}, and in the presence of a proteasome inhibitor, degradation of DNA-PK_{CS} is inhibited. ICP0 does not directly affect the enzyme activity of the DNA-PK and does not physically interact with DNA-PK_{CS}. Parkinson et al., have shown that degradation of DNA-PK_{CS} does not appear to be spatially regulated like the PML protein in ND10 bodies (255). At the time DNA-PK_{CS} degradation is observed, ICP0 is not present in a punctate, ND10-related pattern but is diffuse throughout the nucleus.

1.4.5. HSV-1 and NHEJ

Evidence suggests the cellular NHEJ pathway inhibits HSV replication. Disruption of this pathway has been shown to enhance viral replication (255, 317). Parkinson et al., have shown that ICP0-induced degradation of DNA-PK_{CS} and loss in DNA-PK activity appears to be beneficial to HSV-1 infection, as virus replication is more efficient in cells lacking DNA-PK_{CS}, especially at low multiplicities of infection (255). Taylor and Knipe have recently shown in cells whose NHEJ pathway is disrupted, HSV-1 growth is increased (317). Viral yields were shown to increase 30- to 50 fold in murine embryonic fibroblasts deficient in Ku70.

1.4.6. HSV-1 Replication-Defective Mutants

Recombinant HSV-1 mutants have been constructed with deletions in IE genes to reduce cell toxicity, permit transgene expression, and inhibit viral replication (284, 349). In ICP4 mutant

backgrounds, expression of viral early and late genes is dramatically reduced, inhibiting viral replication (69). This has led to the consideration of such backgrounds as starting points for the construction of replication incompetent HSV-1 gene transfer vehicles. Despite the limited expression of the HSV genome in ICP4 mutant backgrounds, such mutants are very toxic to cells. This is due to the overexpression of the remaining IE proteins in the absence of ICP4 (69). Improved cell survival has been shown by further reduction in IE gene expression after deletion of other IE genes in the HSV-1 genome (161, 284, 286). Both ICP0 and ICP22 contribute to toxicity, as demonstrated by the improved survival of infected cells when either ICP0 or ICP22 is deleted in viruses already deficient in ICP4 and ICP27 expression (286, 349). At high multiplicities of infection (MOI), both of these triple mutants remain toxic to cells. Elimination of all IE gene and protein expression (ICP 0, 4, 22, 27, and 47) results in a virus that is nontoxic at high MOI and is capable of long-term persistence in nonneuronal cells.

The degree of transgene expression in different IE-deficient HSV mutants has been shown to be dependent on the ICP0 protein (284). Green fluorescent protein (GFP) transgene expression has been shown to be abundant in cells infected with a recombinant HSV-1 virus that expresses only ICP0. In the absence of all of the HSV IE proteins, the level of GFP transgene expression is low. Transgene expression of cells infected by a complete IE-deficient virus can be stimulated by ICP0.

1.4.6.1. d106 and d109 (Fig. 3)

The mutant virus, d106, is defective in the expression of all of the IE viral genes (ICP4- ICP22- ICP27- ICP47-) except that which encodes ICP0 (284). The d106 virus overexpresses ICP0 relative to wild-type HSV-1 (81). The mutant virus d109 is an isogenic mutant of d106 and does

not express any of the IE viral genes necessary for HSV-1 genome expression. This virus, d109, is non-toxic to cells at high multiplicities of infection (MOI) and can persist in a repressed, quiescent state in cultured nonneuronal cells. Low levels of ICP0 can effectively activate gene expression in trans and promote persistent transgene expression in cis from otherwise silent promoters contained on persisting d109 viral genomes (144). Construction of the viruses, d106 and d109, proceeded in a series of steps that generated and utilized a set of mutants defective in sets of IE genes (284). Deletion mutations have been placed in the coding sequences of ICP0/4/27 while ICP22/47 have a TAATGARAAT deletion introduced into their promoters. In place of the deletion of ICP27, a GFP gene under the control of the human cytomegalovirus (HCMV) IE promoter was inserted.

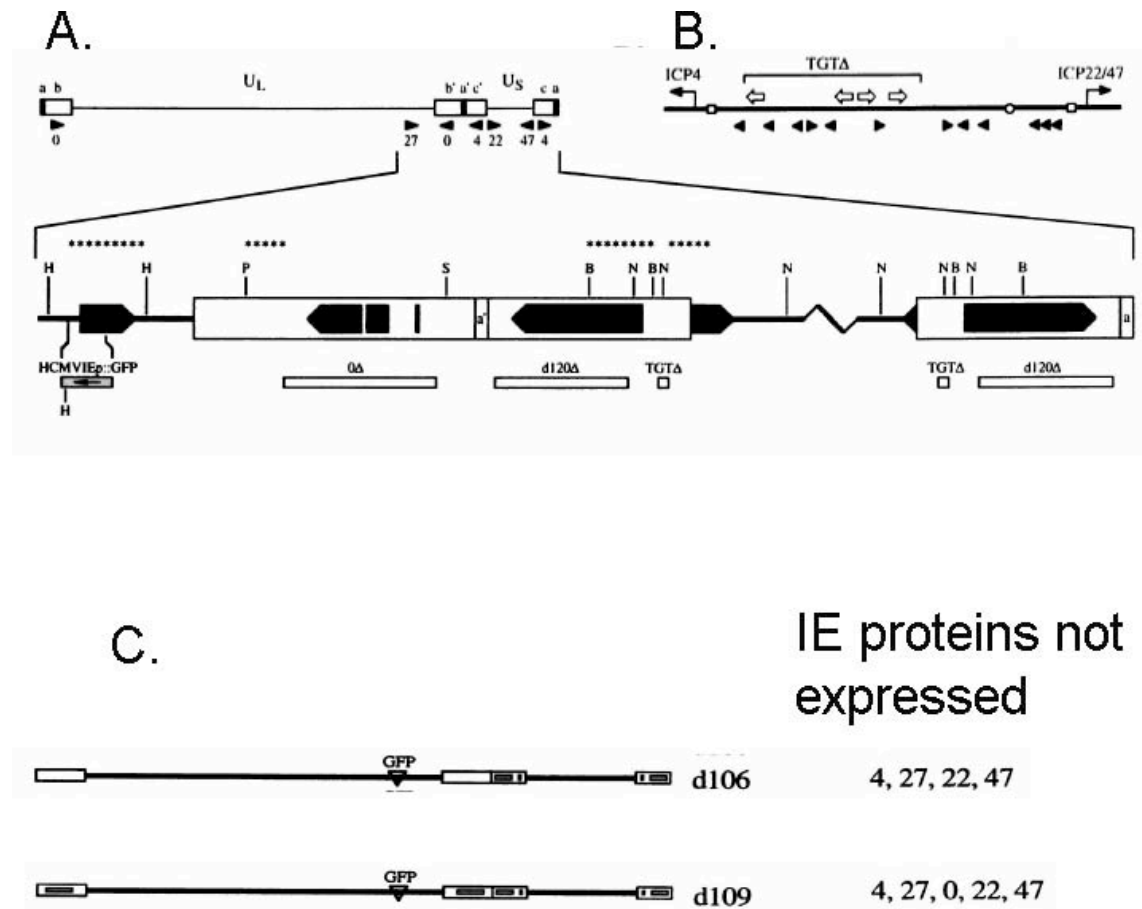


Figure 3. Structures of the isogenic HSV-1 mutants, d106 and d109. A. The HSV-1 viral genome is represented with the unique long (U_L) and short (U_S) regions bounded by terminal and internal repeats (white boxes). The genomic locations and directions of transcription of the IE genes are indicated (arrowheads). Expanded map of the right end of the d109 genome, showing coding sequences of the IE genes (solid arrows) and the deletion mutations (white bars) in ICP4 (d120), ICP0 (0Δ), and the ICP22/47 promoter (TGTA Δ). The transgene cassette containing the GFP reporter gene under the control of the HCMV IE promoter substituted into the deletion in ICP27 is represented by a shaded bar, with the arrow inside indicating the direction of transcription. The relevant restriction sites are as follows: H, *HpaI*; P, *PstI*; S, *SacI*; B, *BamHI*; and N, *NcoI*. B. The TAATGARAT deletion, TGTA (bracketed), introduced into the promoter regions of ICP22/47. The positions of the TAATGARAT elements (open arrows), binding sites for the transcription factor Sp1 (arrowheads), TATA boxes (open squares), and oriS (open circle) are shown relative to the transcription start sites of ICP4 and ICP22/47 promoter (TGTA Δ). C. Genomic structures of d106 and d109. The deletion mutations in ICP4, ICP0, and the ICP22/47 promoter present in both virus mutant strains are indicated by the shaded bars inside the white boxes representing the repeat sequences. The GFP substitution in ICP27 is also shown (inverted triangles). The mutant designations are indicated on the right along with a list of the IE proteins not synthesized by the viruses in the absence of complementation. (Figures adapted with permission from Samanieo et al. *J Virol* 72(14), p 3310, 1998)

1.4.7. HSV-1 Replication-Conditional (Oncolytic) Viruses

Replication-conditional HSV-1 viruses, also known as oncolytic viruses, have been genetically engineered to replicate and grow in tumor cells and cause their demise (194). A number of different genetically engineered oncolytic viruses have been constructed with deletions or mutations in one or more HSV genes ($\gamma_134.5$, U_L39 , tk, and UTPase) in an effort to decrease the toxicity of HSV to the CNS and provide a condition for viral replication only in replicating cells that can provide cellular homologues (49, 51, 54, 152, 175, 208, 222, 267).

The first study of a genetically-engineered virus used as an HSV-1 oncolytic agent was a tk deletion HSV-1 mutant, dlsptk (208). This virus was previously constructed and determined to lack neurovirulence (54). In a mouse glioma model, dlsptk demonstrated antiglioma effects with tumor growth inhibition and increases in animal median survival. Shortcomings of the dlsptk virus included acyclovir resistance, due to the tk deletion, and long-term surviving animals had evidence of low-grade encephalitis. Another HSV-1 oncolytic virus was generated containing a 1 kb deletion in both copies of the diploid viral gene, $\gamma_134.5$, located in the terminal α repeats of the U_L segment (49). R3616 was found to be aneurovirulent at the highest doses obtainable after intracerebral inoculation in susceptible mouse species (51). HSV1716 was also developed which had both copies of the RL1 gene deleted encoding the protein ICP34.5 (271). The $\gamma_134.5$ gene has been determined to encode for the neurovirulence elicited by HSV infection, and has been termed the neurovirulence factor. The carboxy terminus of this factor is responsible for evading a stereotypical antiviral response of the host cell by the shutdown of all protein synthesis in the cell. While this results in cell death, the purpose of the response is to prevent further spread of viral infection to other cells in the host organism (50).

Other HSV-1 oncolytic viruses have been developed based on 1 kb deletions of both copies of $\gamma_134.5$ (222, 254). Using R3616 as a parent virus, G207 was developed after creation

of an additional mutation to the virus by introduction of a lacZ reporter gene in the U_L39 gene locus (222). U_L39 encodes for the large unit of HSV's ribonucleotide reductase gene, ICP6, which is necessary for replication of the viral DNA in non-replicating cells.

Phase I clinical studies in humans with malignant gliomas have demonstrated modest antitumor effect with the HSV-1 oncolytic viruses G207 and 1716 (134, 206, 271). Safety has been established when viruses are injected into the brains of patients with malignant gliomas. Delivery of HSV-1 vectors in all clinical trials has been by multiple stereotactic intratumoral or peritumoral injections after surgical resection (134, 206). Such techniques are problematic as viral delivery is unable to produce widespread and uniform distribution within tumors.

1.4.7.1. Oncolytic HSV-1 and Ionizing Radiation

Advani et al., have shown the conditionally-replicative HSV-1 mutant, R3616, has greater oncolytic effects and increased replication when exposed to IR (4). In their study, human U87-MG xenografts in mice underwent significantly greater reduction in tumor volume or total regression when tumors were inoculated with the R3616 mutant and irradiated. Increased spread of the virus was seen with in-situ hybridization with DNA probes to the virus. Other studies have confirmed the enhanced tumoricidal effect of HSV when combined with IR (30, 205).

2. STATEMENT OF THE PROBLEM

Despite the use of conventional therapeutic modalities such as surgery, chemotherapy, and IR, the prognosis in patients with GBM remains poor. To improve this dismal prognosis, novel treatment approaches are required which attack the molecular and biological features of malignant gliomas. Since these tumors rarely metastasize away from the nervous system and the majority recur in a local fashion, local tumor control must be achieved to significantly extend the survival of patients with GBM. Enhancement of the effects of IR, the primary adjuvant treatment for GBM, may serve this purpose.

DNA DSBs are known to occur with IR exposure of cells (168). DNA double-strand breaks (DSBs) are the most critical form of DNA damage that may result in loss or rearrangement of genomic material and thereby lead to mutations, genomic instability, cancer development, or cell death (74, 146, 259, 347). DNA DSBs activate an extensive array of responses that lead to damage repair and continuation of cellular life (157).

HSV-1 is a large, neurotropic DNA virus that affects many aspects of host cell metabolism during infection. During lytic cell infection, HSV-1 has been shown to induce a host DNA damage response with recruitment of recombination and repair proteins to HSV-1 genomes present in the nucleus (156, 193, 346). Activation and exploitation of a cellular DNA damage response has been shown to aid viral replication (193).

HSV-1 DNA replication is closely associated with ND10 domains, which are defined and organized by the PML protein (11, 154, 210). ND10 domains have been shown to contain host recombination/repair proteins (235) and participate in the cell's response to DNA damage (41). ND10 domains are redistributed in response to DNA damage (41), and it has been proposed that

ND10 may store and release proteins in response to certain external insults such as viral infection and DNA damage (235). For example, the ND10-associated proteins PML, Mre11, γ H2AX, Rad50, NBS1, RPA, and TopBP1 are redistributed to DNA DSB repair foci induced by IR (16, 41, 351). The phosphorylated form of the NHEJ DNA repair protein, DNA-PK_{cs}, has also been shown to localize to sites of DNA DSBs (44).

Upon entry into the nucleus, parental HSV-1 genomes are linear in structure and are found adjacent to ND10 domains (156, 210). The ends of the HSV-1 linear genome may be treated as cellular DNA DSBs, and repaired by NHEJ, forming circular genomes that are associated with viral latency (156). The expression of the IE protein, ICP0, during early lytic infection can inhibit the DNA repair process by ND10 body disruption and degradation of DNAPK_{cs} (94, 189, 209, 255). As a result, circularization of HSV-1 DNA cannot occur and replication of linear HSV-1 genomes can proceed.

The isolation of HSV-1, deleted for all IE genes except ICP0, can be used to study the effect of ICP0 on cellular DNA repair and survival after IR exposure and viral infection. The HSV-1 mutant, d106, is essentially restricted to the expression of ICP0 and the transgene, GFP (284). The d106 virus may be evaluated as a potential viral vector for delivery to the brain and ultimate treatment of GBM tumors by ICP0 DNA repair inhibition after IR.

The aims of this study are to identify the ICP0 protein as a potential candidate for DNA DSB repair inhibition and radiosensitivity enhancement of experimental GBM. Specifically, the aims are: **(1) To determine the effect of HSV-1 infection and IR, on human GBM cell survival and proliferation *in vitro*; (2) To determine whether the degradation of DNA-PK_{cs} by ICP0 occurs after HSV-1 infection and contributes to altered DNA DSB repair in GBM cells *in vitro*; (3) To determine whether CED is an optimal method of HSV-1 delivery to**

the brain in a mouse model; (4) To determine whether the HSV-1 mutant, d106, enhances the radiosensitivity of mouse intracranial human GBM xenografts after CED.

3. INHIBITION OF DNA REPAIR BY A HERPES SIMPLEX VIRUS VECTOR ENHANCES THE RADIOSENSITIVITY OF HUMAN GLIOBLASTOMA CELLS

A modified version of the data presented in Chapter 3 appeared in “Inhibition of DNA repair by a herpes simplex virus vector enhances the radiosensitivity of human glioblastoma cells,” Costas G. Hadjipanayis and Neal A. DeLuca, *Cancer Research*, 2005, volume 65 (12), pages 5310-5316, copyright © 2005, American Association of Cancer Research. All rights reserved.

3.1. Abstract

Expression of the herpes simplex virus (HSV) protein, ICP0, from the viral genome, rendered two radioresistant human glioblastoma multiforme (GBM) cell lines more sensitive to the effects of ionizing radiation (IR). Using the MTT and clonogenic survival assays, U87-MG and T98 cell survival was more greatly decreased as a function of IR dose when ICP0 was preexpressed in cells compared to when ICP0 was not expressed. Consistent with previous results, we found that the catalytic subunit of DNA-dependent protein kinase (DNA-PK_{cs}) was degraded as a function of ICP0 in both cell types. This most likely resulted in the inhibition of DNA repair as inferred by the persistence of γ H2AX foci, or DNA double-strand breaks (DSBs). Enhanced apoptosis was also found to occur following irradiation of U87-MG cells preinfected with the ICP0-producing HSV-1 mutant, d106. Our results suggest that expression of ICP0 in human GBM cells inhibits the repair of DNA DSBs after IR treatment, decreasing the survival of these cells in part by induction of apoptosis.

3.2. Introduction

Glioblastoma multiforme (GBM) is the most common malignant primary brain tumor in adults (64). Despite the use of conventional therapeutic modalities such as surgery, chemotherapy, and ionizing radiation (IR) treatment, the prognosis in patients is poor. Radiation therapy remains the sole agent that increases the survival of patients with GBM but provides modest benefit (191). Both adult primary (de novo) and secondary GBMs are remarkably resistant to IR treatment. The limited efficacy of radiation treatment is believed to arise from the poor apoptotic response to IR by the tumor cells (167, 353, 356). New therapeutic strategies need to be developed for improved long-term management of these tumors. Enhancement of the effects of IR, the primary adjuvant treatment for GBM, may increase patient survival and quality of life.

DNA DSBs are known to occur with IR exposure of cells (168). One repaired DSB can be sufficient to kill a cell if it inactivates an essential gene or triggers apoptosis (274). The repair of DSBs is performed by two pathways in mammalian cells, nonhomologous end-joining (NHEJ) and homologous recombination (HR). The serine/threonine kinase, DNA-dependent protein kinase (DNA-PK), is an important component of NHEJ, consisting of a large catalytic subunit (DNA-PK_{cs}) and a Ku heterodimer (Ku70 and Ku80 subunits). In response to IR, Ku-dependent phosphorylation of DNA-PK_{cs} is required for the repair of DSBs by NHEJ. DNA-PK_{cs} contributes to the repair of DSBs by assembling the broken ends of DNA molecules and serves as a molecular scaffold for recruiting DNA repair factors to DNA DSBs (10, 118, 183).

Herpes simplex virus (HSV) is a large, neurotropic DNA virus that affects many aspects of host cell metabolism during infection. The HSV-1 immediate early (IE) protein, ICP0, has been found to induce the degradation of the catalytic subunit of DNA-dependent protein kinase (DNA-PK_{cs}) by the ubiquitin-dependent proteasome degradation pathway (189, 255). The extent

of DNA-PK_{cs} degradation is cell-type specific and it has been shown that HSV replication is increased in cells lacking DNA-PK_{cs} (255). Therefore, HSV infection may affect NHEJ.

ICP0 is a promiscuous transactivator shown to enhance the expression of genes introduced into cells by infection or transfection (127). ICP0 is critical for viral replication in cultured cells infected at low multiplicity, but is not essential in cells infected at high multiplicity (283). Recently, ICP0 has been shown to be an E3 ubiquitin ligase (28) and has been proposed to promote lytic infections by destabilizing cellular proteins that inhibit the lytic viral life cycle. ICP0 is required for both lytic HSV viral infection and efficient reactivation from latency in vitro and in vivo (129). In addition to DNA-PK_{cs} degradation, ICP0 has been shown to induce the degradation of proteins associated with nuclear domain 10 (ND10) bodies in a RING finger-dependent manner (93). ND10 bodies are discrete nuclear foci where HSV-1 genomes may localize early during infection (210). Recent studies have suggested that these foci are sites of DNA DSB repair and inhibition of HSV genome circularization by ICP0 (41, 156).

Replication-defective mutant HSV-1 viruses were used to study the effect of ICP0 on DNA repair after IR in human GBM cells. The mutant virus d106, is defective in the expression of all of the IE viral genes except that which encodes ICP0 (284). The mutant virus d109 is an isogenic mutant of d106 and does not express any of the IE viral genes necessary for HSV-1 genome expression. Both of these mutant viruses were used to infect human GBM cells prior to irradiation to determine the effect of ICP0 on cell survival, proliferation, DNA-PK_{cs} protein levels, DNA DSB repair, and apoptosis.

3.3. Material and Methods

3.3.1. Cells and Viruses

The human GBM cell lines T98 and U87-MG were obtained from the American Type Culture Collection (ATCC) and maintained in Dulbecco's modified Eagle medium (DMEM) supplemented with sodium pyruvate, non-essential amino acids, antibiotics, and 10% fetal bovine serum (FBS) (Life Technologies, Inc., Gaithersburg, MD). The HSV-1 IE mutant viruses, d106 and d109, are derived from the wild-type strain KOS and have been previously described (284). Each mutant was grown and assayed for infectivity (PFU/ml) in the appropriate complementing cell lines (F06 and E11) as previously described (284). AdS.11E4(ICP0), an adenovirus vector that expresses ICP0, and AdS.11D, the empty adenoviral vector, were provided by Douglas Brough (GenVec, Gaithersburg, MD) and have been described (144).

3.3.2. HSV-1/Adenovirus Infection, IR, and Cell Survival/Proliferation

Tumor cells were seeded in triplicate at 2×10^3 cells/well (0.1 ml) in 96-well flat-bottomed plates and incubated overnight at 37° C. Confluent monolayers of T98 and U87-MG cells were infected with the HSV-1 viruses, d106 or d109, at an MOI of 10 for 24 hours prior to irradiation. U87-MG cells were also infected with 10^4 particles/cell with the adenoviruses AdS.11E4(ICP0) or AdS.11D. IR treatment was delivered at room temperature in a ^{137}Cs irradiator (Gammacell40, Atomic Energy of Canada Limited, Ontario, Canada) at a dose rate of .87 Gy/min. Cells were subsequently returned to the incubator.

To assess cell survival and proliferation after viral infection and IR treatment, an MTT [3-(4,5-dimethylthiazol-2-yl)-2,5-diphenyltetrazolium bromide] cell proliferation assay (ATCC, Bethesda, MD) (231) was performed at 0, 2, 4, and 6 days after cell irradiation. MTT reagent was added (.02 ml) to each well and cells were placed in the incubator for 1 hour. A solubilizing cell detergent (ATCC, Bethesda, MD) was added (0.1 ml) to the cells and the formazan reaction

product was measured with a microtiter plate reader (Dynateck, Alexandria, VA). Absorbance values are presented as the mean of three wells per treatment \pm the standard deviation (SD).

Clonogenic survival assays were performed on U87-MG cells after d106 infection and IR treatment. Exponentially growing cells were seeded at a density of 10^5 cells/well in six well flat-bottomed plates overnight. Cells were either mock infected or infected with d106 at an MOI of 10 PFU/cell for 24 hours. Cells were irradiated at 10 Gy and placed in the incubator overnight. Trypsinized cells were serially diluted and plated in triplicate on six well plates. Cells were left to grow colonies for 2 weeks with routine changing of serum-containing medium twice a week. Cells were fixed and stained with a crystal violet/formalin solution and colonies were counted. Cell survival was estimated from the number of colonies (defined as a cluster of >50 cells) formed and expressed as a fraction of the number of cells seeded multiplied by the plating efficiency (PE). The PE was determined by the number of colonies formed in the mock infected group of cells that did not receive IR and expressed as a fraction of the number of cells seeded (PE= 0.9).

3.3.3. Western Blot Analysis of DNA-PK_{cs} and Cleaved Caspase-3

For Western blot analysis of DNA-PK_{cs}, U87-MG and T98 cells were infected with either d109 or d106 and cell lysates were harvested at 6 and 24 hpi. T98 and U87-MG cells were mock or d106-infected for 24 h and then irradiated (0 or 10 Gy) for Western blot analysis of cleaved caspase-3. Cell lysates were collected at 48 h after irradiation. Lysates were harvested into Laemmli buffer and loaded onto denaturing polyacrylamide gels using standard protocols. Due to the large size of the protein (460 kDa), 8% bisacrylamide gels were used to resolve DNA-PK_{cs}. The large fragment of cleaved caspase-3 (17/19 kDa) was resolved on 10-20% Tris-HCL gradient gels (Bio-Rad, Hercules, CA). After electrophoresis, proteins were electrotransferred

onto polyvinylidene difluoride membranes (Amersham Biosciences, Piscataway, NJ) and probed for DNA-PK_{cs} (mouse monoclonal at a dilution of 1:1000 in 5% nonfat dry milk/TBS-Tween solution; Upstate Biotechnology, Lake Placid, NY) and cleaved caspase-3 (rabbit monoclonal at a dilution of 1:1000 in 5% nonfat dry milk/TBS-Tween solution; Cell Signaling Technology, Beverly, MA). This was followed by binding of peroxidase-conjugated goat antimouse/rabbit antibody and detection of proteins by enhanced chemiluminescence (Amersham Biosciences, Piscataway, NJ).

3.3.4. Apoptosis

A carboxyfluorescein poly-caspase detection kit (APO LOGIX, Cell Technology Inc., Mountain View, CA) was used to detect active caspases in cells undergoing apoptosis (302). U87-MG cells were seeded in triplicate at a density of 10^5 cells/well in six well flat-bottomed plates overnight and were mock or d106 infected for 24 hours and then irradiated. U87-MG cells were irradiated with 0, 5, 10, and 20 Gy. Active caspases 1, 2, 3, 6, 8, 9, and 10 were detected with a carboxyfluorescein (FAM)-labeled peptide fluoromethyl ketone (FMK) caspase inhibitor 24 hours after irradiation. Quantitation of cells with active caspases undergoing apoptosis was performed with single color flow cytometry (Beckman-Coulter Epics XL, Fullerton, CA) after cell fixation (Fixative Solution, Cell Technology Inc., Mountain View, CA). Data acquisition and analysis was performed with the EXPO32 ADC software (Beckman Coulter, Fullerton, CA).

Staurosporine (A.G. Scientific, San Diego, CA), a potent apoptosis inducing agent, was used as a positive control for apoptosis in U87-MG cells for Western analysis of cleaved caspase-3 levels. Staurosporine was dissolved in anhydrous DMSO and diluted to a concentration of 0.01 $\mu\text{M/L}$ in medium prior to treatment of U87-MG cells for 2 hours.

3.3.5. Indirect Immunofluorescence for γ H2AX and ICP0

Confluent monolayers of U87-MG and T98 cells were grown on circular 18 mm coverslips. Cells were mock or d106-infected (MOI 10) for six hours and then irradiated (8 Gy). At 2, 6, and 24 hours after IR treatment, cells were fixed and permeabilized in cold methanol (-20°C) for 5 minutes. Cells were then treated with deionized water for 20 minutes and then 10% phosphate-buffered saline (PBS) for 15 minutes. Cells were washed in 1% bovine-serum albumin (BSA) three times for 10 minutes each. Anti- γ H2AX (rabbit polyclonal at a dilution of 1:200 in PBS; Upstate Biotechnology, Lake Placid, NY) and anti-ICP0 (mouse monoclonal at a dilution of 1:500 in PBS; Goodwin Institute for Cancer Research) antibodies were added and cells were incubated at room temperature for 1 hour. Cells were washed in PBS five times for 10 minutes each before incubating in the dark with FITC-labeled secondary antibodies at a dilution of 1:500 in PBS. Cells were washed again in PBS six times 10 minutes each in the dark and coverslips were mounted with an antifade solution (Gelvatol, Simon C. Watkins Laboratory, University of Pittsburgh). Slides were examined on a Nikon Diaphot 300 photomicroscope (Melville, NY). Images were captured by a SPOT RT camera (Diagnostic Instruments, Sterling Heights, MI) and imported into the SPOT version 3.5.9 for MacOS image analysis software package (Diagnostic Instruments, Sterling Heights, MI) running on a Macintosh G3 computer (Apple, Cupertino, CA). Final image analysis was performed with Adobe Photoshop. For each treatment condition, γ H2AX foci were determined in at least 50 cells.

3.3.6. Statistical Analysis

Cell proliferation and viability data represent the average of three independent absorbance values on day 6 of the MTT assay. Statistical proliferation and viability differences were assessed using

an unpaired two-sample Student t-test assuming equal variance. A probability value less than 0.05 was considered significant.

3.4. Results

3.4.1. Effect of ICP0 and IR on Human GBM Cell Survival and Proliferation: MTT Assay

To determine the effect of ICP0 on human GBM cell survival and proliferation after IR treatment, U87-MG and T98 cells were infected at an MOI of 10 PFU/cell with two replication-defective HSV-1 viruses, d106 or d109, 24 h prior to single-dose irradiation (0, 5, 10, or 20 Gy). The MTT assay was performed at 0, 2, 4, and 6 days after cell irradiation (Fig. 1). Both cell lines used are radioresistant and the U87-MG cell line contains wild-type p53 while T98 contains mutant p53 protein. Both cell lines when irradiated, but not infected with virus, showed a dose-dependent decrease in cell survival and proliferation in comparison to cells which received no IR ($P < 0.005$). The U87-MG cell line appears more radioresistant than the T98 cell line in this study (Fig. 1). Infection of U87-MG and T98 cells by the ICP0-producing virus, d106, followed by IR treatment, resulted in a dose-dependent decrease in cell proliferation and survival after 6 days in comparison to cells receiving only IR ($P < 0.005$) (Fig. 1). The greatest decrease in cell survival and proliferation occurred at the highest IR dose of 20 Gy ($P < 0.005$). The largest decline in cell survival occurred between 2 and 4 days after IR treatment of U87-MG cells and infection with d106. T98 cells showed a decline in cell survival immediately after IR. Infection of both cell lines by the IE-deficient virus, d109, did not result in a dose-dependent decrease in cell proliferation and survival after IR treatment. Cell proliferation occurred in both cell lines after d109 infection in the absence of irradiation consistent with the documented lack of toxicity

upon d109 infection (284). Infection of both cell lines with d106 resulted in cell toxicity as proliferation and cell viability decreased soon after infection ($P < 0.05$) (143). Cell toxicity with d106 infection was greatest in the T98 cell line (Fig. 1B).

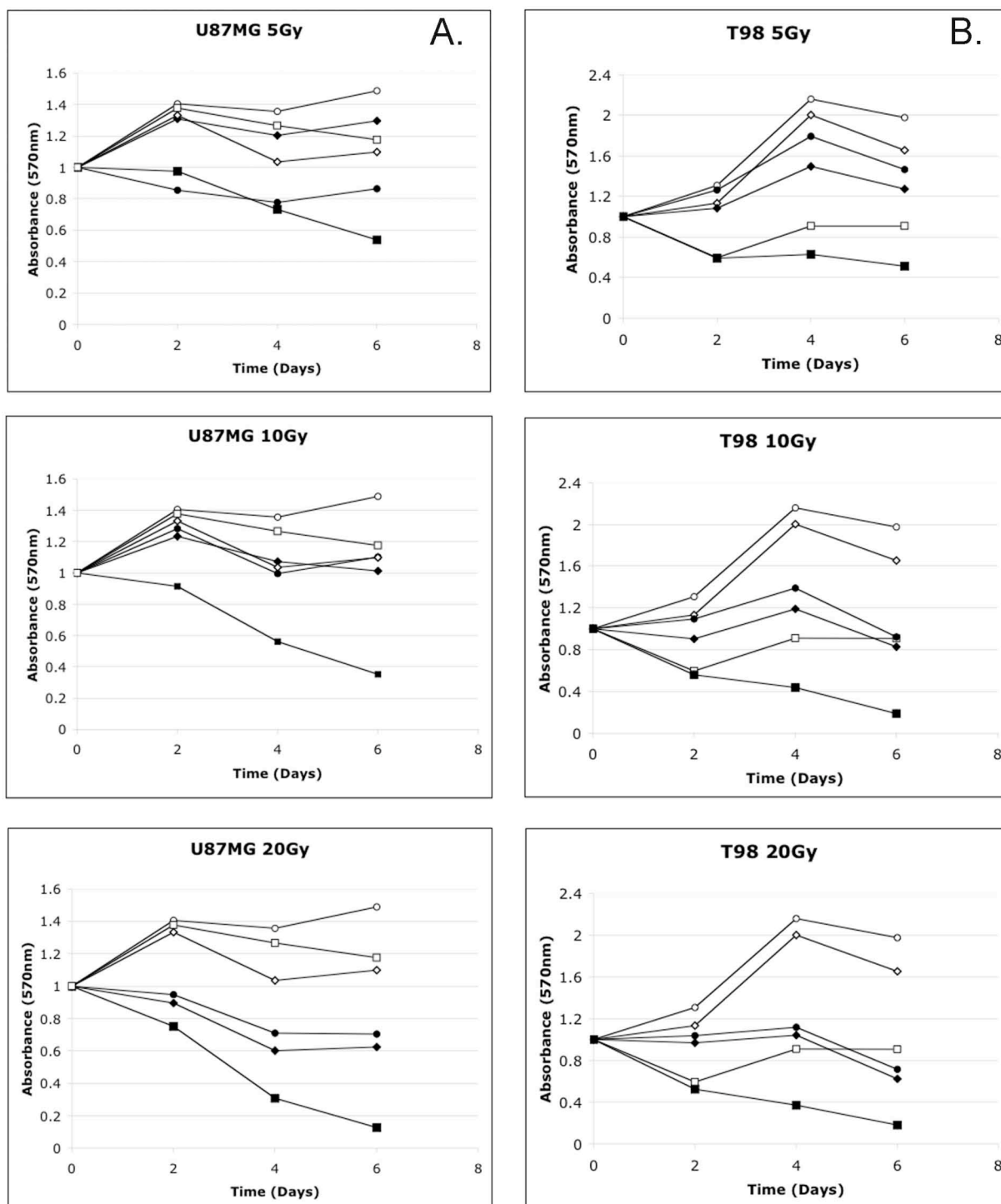


Figure 4. Effect of HSV mutant viruses and escalating doses of ionizing radiation (IR) on U87-MG and T98 cell proliferation and survival using the MTT assay. U87-MG or T98 cells were mock infected or infected with HSV mutant viruses, d106 or d109, at 10 PFU per cell. The MTT assay was performed 0, 2, 4, 6 days after irradiation. A. Effect of 5, 10, and 20 Gy IR exposure 24 hours postinfection (hpi) with mock, d106, and d109 infected U87-MG cells. B. Effect of 5, 10, 20 Gy IR exposure 24 hpi with mock, d106, d109 infected T98 cells. (◆ Mock IR, ● d109 IR, ■ d106 IR, ◇ Mock, ○ d109, □ d106)

3.4.1.1. Adenovirus Expression of ICP0

To confirm the effect of ICP0 on cell survival and proliferation in GBM cells after irradiation, U87-MG cells were infected with 10^4 particles/cell with two replication-defective adenoviruses, AdS.11E4(ICP0) or AdS.11D, 24 h prior to a single-dose of IR (20 Gy). The MTT assay was performed at 0, 2, 4, and 6 days after irradiation. AdS.11E4(ICP0) is an E1⁻ E3⁻ E4⁻ adenovirus vector with ICP0 expression controlled from the endogenous adenoviral E4 promoter. One-thousand fold less ICP0 is expressed from this construct relative to the level of expression from d106 (144). AdS.11D is an empty E1-E3-E4- adenovirus vector that does not express ICP0. U87-MG cells infected with the ICP0-producing adenovirus, AdS.11E4(ICP0), showed a decrease in cell survival and proliferation after irradiation in comparison to cells which were only irradiated ($P < 0.005$)(Fig. 2).

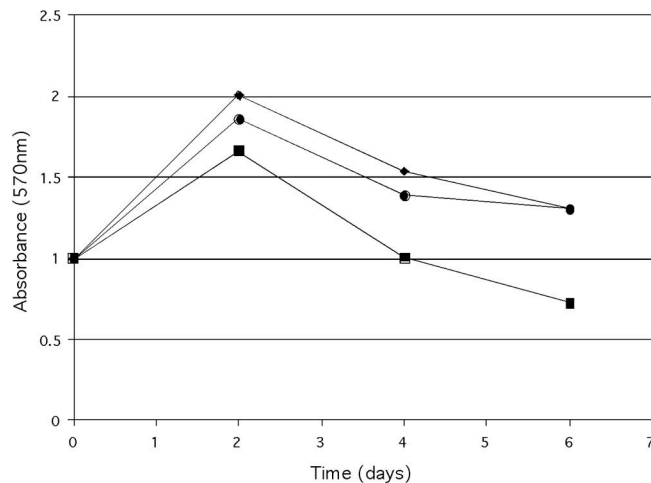


Figure 5. Effect of empty adenovirus (AdS.11D) and ICP0-producing adenovirus [AdS.11E4(ICP0)] on U87-MG cell proliferation and viability after IR. A. U87-MG cells were mock infected or infected with AdS.11D or AdS.11E4(ICP0) at 10,000 particles/cell for 24 hours prior to 20 Gy IR exposure. The MTT assay was performed 0, 2, 4, 6 days after irradiation. (● Mock, ◆ AdS.11D, ■ AdS.11E4(ICP0))

3.4.2. Effect of ICP0 and IR on Human GBM Cell Survival: Clonogenic Survival Assay

Clonogenic survival assays were performed to confirm the results of the MTT assay with d106 infection of U87-MG cells and subsequent irradiation. Cells were serially diluted and plated

after d106 infection and 10 Gy of IR treatment. After two weeks of growth, cell survival was estimated from the number of colonies formed and expressed as a fraction of colonies resulting from uninfected, unirradiated cells (Fig. 3). The survival fraction was lowest among cells that were infected by d106 and irradiated (0.001). U87-MG cells that only received IR had an impaired ability to form colonies with a low survival fraction (0.01). Cells that did not receive IR but were infected with d106 had a higher survival fraction (0.2). These results support the data from the MTT assay showing an enhanced decrease in GBM cell survival with ICP0 production and subsequent irradiation.

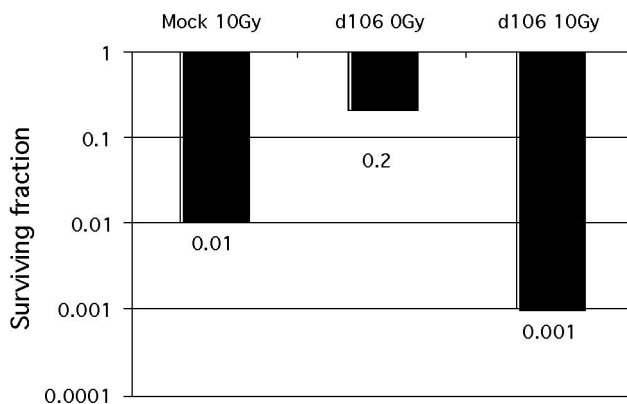


Figure 6. Clonogenic survival performed on U87-MG cells after d106 infection and IR treatment plotted on a logarithmic scale. Cells were mock or d106 infected at 10 PFU/cell for 24 hours and irradiated (0 or 10 Gy). Trypsinized cells were serially diluted and left to grow colonies for 2 weeks. Cell survival was estimated from the number of colonies (defined as cluster >50 cells) formed and expressed as a fraction of the number of colonies in the control (PE 0.9).

3.4.3. Apoptosis as a Mode of GBM Cell Death with ICP0 Production and IR

To determine whether apoptosis is a mode of GBM cell death with ICP0 production and IR, Western blot analysis was performed on U87-MG cells after d106 infection and irradiation (10 Gy). The blot was probed with an antibody specific to cleaved caspase-3. Caspase-3, a key executioner of apoptosis, is activated by cleavage into two subunits (p17 and p12) (241). Levels of cleaved caspase-3 (p17) were detected in U87-MG cells that were infected by d106 and

irradiated (Fig. 4A). Lower levels of cleaved caspase-3 were found in cells that were d106 infected but did not undergo irradiation. Both groups of cells that were mock infected and did or did not receive IR had minimal detectable levels of cleaved caspase-3.

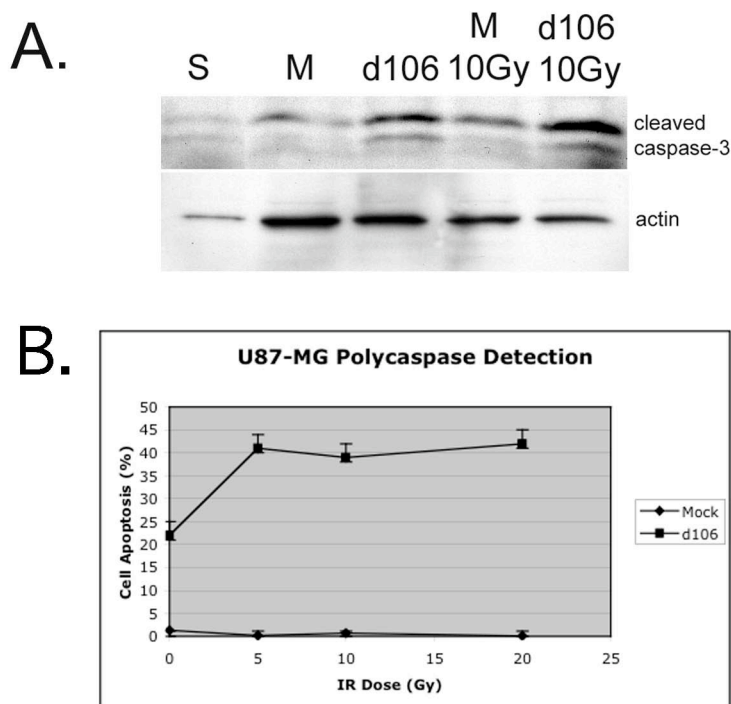


Figure 7. Apoptosis as a mode of GBM cell death with ICP0 production and IR. **A.** Cleaved caspase-3 levels after d106 infection and IR treatment. U87-MG cells were mock (M) infected or infected with d106 at 10 PFU per cell for 24 h and then irradiated (0 or 10 Gy). At 48 hours post-irradiation, cells were harvested into Laemmli buffer and samples were analyzed by Western blotting. The blot was probed with rabbit monoclonal anti-cleaved caspase-3 and mouse monoclonal anti-actin at a dilution of 1:1000. Staurosporine (S), was used as a positive control for apoptosis in cells. **B.** Percentage of U87-MG cells undergoing apoptosis after d106 infection and IR treatment. U87-MG cells were mock infected or infected with d106 at 10 PFU per cell for 24 h and then irradiated (0, 5, 10, or 20 Gy). Carboxyfluorescein poly-caspase detection was performed by flow cytometry 24 h after irradiation to quantitate cells undergoing apoptosis. (◆ Mock, ■ d106)

Carboxyfluorescein poly-caspase detection was performed with flow cytometry in order to quantify the number of U87-MG cells undergoing apoptosis after d106 infection and IR treatment (Fig. 4B). Flow cytometry was performed 24 hours after cell irradiation. Minimal apoptosis was detected in mock infected cells that did or did not undergo irradiation, confirming the results of our Western analysis of cleaved caspase-3 levels (Fig. 4A). U87-MG cells that

were d106 infected and received subsequent IR treatment underwent apoptosis in greater numbers than d106 infected cells that were not irradiated. The percentage of d106-infected cells undergoing apoptosis were very similar 24 h after irradiation at 5, 10, or 20 Gy (Fig. 4B).

Our results confirm apoptosis as a mode of cell death with cell ICP0 production and irradiation. At 24 h after irradiation, a large portion of U87-MG cells infected with d106 undergo apoptosis. Other modes of cell death such as necrosis or autophagy may also occur (353). Our results support other studies showing irradiation alone causes a poor apoptotic response in GBM cells. Most importantly, these results show enhanced GBM cell apoptosis with d106 infection and subsequent irradiation.

3.4.4. ICP0 Degradation of DNA-PK_{cs} in Human GBM Cells

To determine whether degradation of DNA-PK_{cs} by ICP0 occurs in human GBM cells, Western blot analysis was performed on U87-MG and T98 cells after d106 or d109 infection. The blot was probed with anti-DNA-PK_{cs} and degradation was found to occur between 6 and 24 hpi with d106 in U87-MG cells (Fig. 5). Degradation of DNA-PK_{cs} in T98 cells occurred at 6 hpi with d106 and complete degradation was found at 24 hpi (Fig. 5). No degradation of DNA-PK_{cs} occurred with d109 infection of the U87-MG or T98 cell lines.

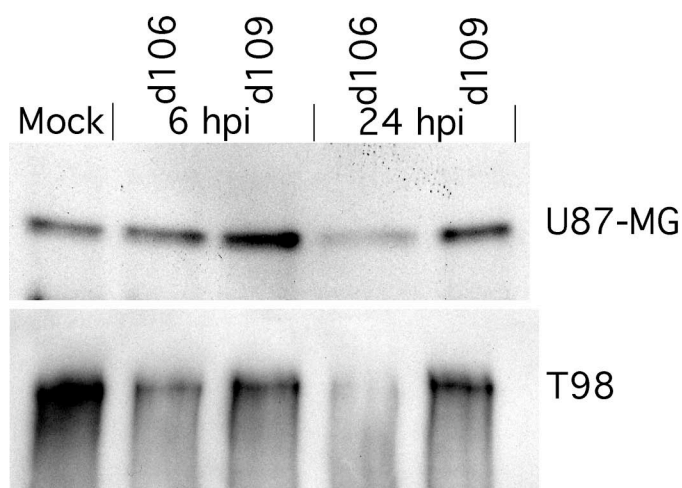


Figure 8. Effect of HSV mutant viruses on DNA-PK_{CS} protein levels in U87-MG and T98 cells. Cells were mock infected or infected with d106 or d109 as shown at 10 PFU per cell. At 6 and 24 hpi, cells were harvested into Laemmli buffer and samples were analyzed by Western blotting. The blot was probed with a mouse monoclonal anti- DNA-PK_{CS} at a dilution of 1:1000.

3.4.5. Persistent DNA DSBs with ICP0 Production and IR in Human GBM Cells

To determine whether DNA DSB repair is inhibited by ICP0, indirect immunofluorescence was performed on U87-MG and T98 cells infected with d106 for 6 hours, irradiated, and incubated for 2, 6, and 24 hours (0 or 8 Gy)(Fig. 6). Cells were labeled with antibodies to ICP0 and γ H2AX, the phosphorylated form of a histone H2A variant (H2AX) found at sites of DNA DSBs (38, 277). Phosphorylation of H2AX appears to play a critical role in the recruitment of repair or damage-signaling factors to sites of DNA damage in the nucleus (257). The repair of DNA DSBs after IR correlates with the loss of γ -H2AX foci (233). Prior reports have shown the loss of γ -H2AX foci in cells within 6 hours after irradiation (233).

U87-MG and T98 cells that were mock infected and did not receive IR had undetectable γ -H2AX foci, or DNA DSB (Fig. 6). Mock-infected cells, which underwent IR treatment, had detectable γ -H2AX foci at 2 h post irradiation but reduced foci at 6 and 24 h. The loss of γ -H2AX foci at 6 and 24 h post-irradiation indicates the repair of dsDNA breaks. Both T98 and

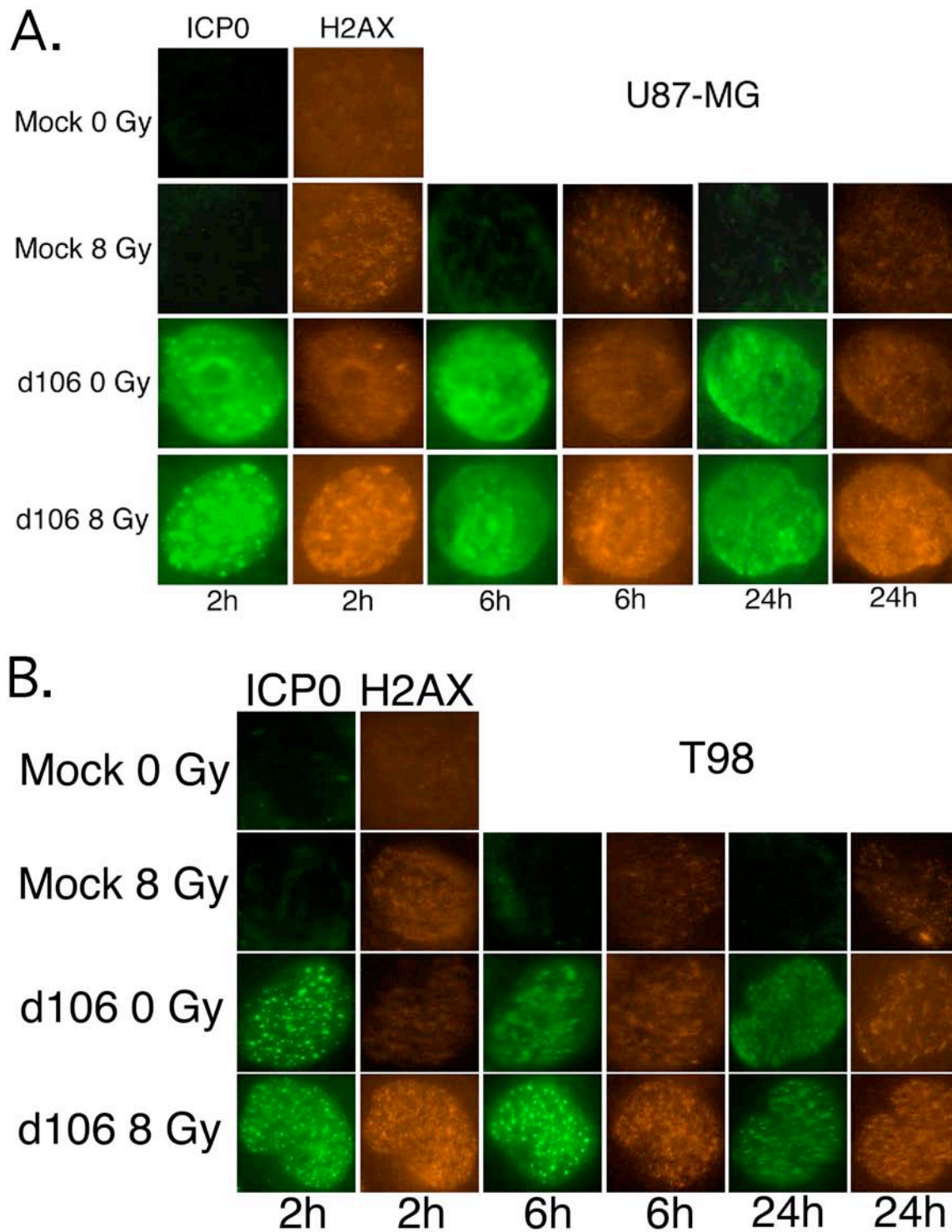


Figure 9. Indirect immunofluorescence for γ H2AX and ICP0 in U87-MG and T98 cells. Cells were mock or d106 infected for 6 h and then irradiated (0 or 8 Gy). At 2, 6, and 24 h post-IR, cells were permanently fixed and labeled with anti- γ H2AX (rabbit polyclonal) and anti-ICP0 (mouse monoclonal). FITC-labeled secondary antibodies (red

for γ H2AX and green for ICP0) were then added. The presence of γ H2AX foci, or DNA DSBs, are more numerous and persistent with d106 infection and IR treatment of cells at 24 h after irradiation. A. U87-MG cells. B. T98 cells. U87-MG cells infected with d106, which did not receive IR, had detectable γ -H2AX foci at 6 and 24 h post irradiation. These results suggest linear HSV-1 genomes present after infection may be treated as DNA DSB with formation of γ -H2AX foci (156, 279). Abundant γ -H2AX foci, or DNA DSBs, were found in d106-infected cells at 2, 6, and 24 h after IR treatment (Fig. 6). Persistent γ -H2AX foci at 24 h suggests ICP0 inhibits DNA repair.

3.5. Discussion

Both primary and secondary GBMs are very resistant to the effects of IR. GBM cells have a poor to absent apoptotic response to IR (167, 356) (353). Glioma cells show an absence of either significant induction of bax or repression of bcl-2 and bcl-X_L after irradiation (176, 298). Strategies reported to enhance apoptosis after irradiation of malignant glioma cells, include exogenous transfer of p53, APAF-1, and caspase 9 (116, 186, 297). Radiation-induced apoptosis in most cell types other than glial cells has been shown to depend on the presence of wild-type p53 (200). The presence or absence of wild-type p53 has not been shown to have a significant impact on the radiosensitivity of GBM cells (14, 125). Recently, autophagic cell death has been introduced as a possible mechanism for GBM cell death after IR, characterized by the accumulation of acidophilic vesicular organelles (AVOs) in the cytoplasm (353). Nevertheless, IR continues to be the primary adjuvant treatment modality for GBM patients as survival is modestly increased.

It has been firmly established that DNA-PK_{cs} plays an important role in DNA end joining, especially DNA DSB repair after IR. Prior reports have shown that inhibition or deficiency in DNA-PK_{cs} leads to decreased DNA DSB repair and increased radiosensitivity, both

in vitro and in vivo (183, 188, 316, 325). The repair of DNA DSBs after IR may account for the poor apoptotic response and ultimate radioresistance of malignant glioma cells. Degradation of DNA-PK_{cs} has been shown to occur after HSV-1 infection and is dependent on expression of the virus IE protein ICP0 (189). We present evidence that an HSV-1 vector inhibits DNA DSB repair and enhances the radiosensitivity of human GBM cells possibly due to the degradation of DNA-PK_{cs}. Persistence of DNA DSBs with ICP0 production in GBM cells and irradiation is indicative of the disruption of the NHEJ repair pathway after degradation of DNA-PK_{cs} by ICP0. The inhibition of DNA DSB repair by ICP0 may account for the enhanced apoptosis of GBM cells after ICP0 production and irradiation. ICP0 may have many effects on cells. It has also been shown that ICP0 induces cell cycle arrest in G1 and G2/M independently of p53 (143). Therefore, while ICP0 may inhibit DNA repair, it may also affect the survival of cells via other pathways.

HSV-1 has been studied for use in the therapy of human GBM. A number of different genetically engineered viruses have been constructed with deletions or mutations in 1 or more HSV genes in an effort to decrease toxicity of HSV to the CNS and provide a condition for viral replication only in replicating cells that can provide cellular homologues (206, 208). Other HSV mutants have been constructed that are defective for immediate-early (IE) gene expression, resulting in replication-incompetent viruses. Various genes have been inserted in these modified viruses for expression in infected cells (178, 244). In our study, we found the HSV-1 virus alone can enhance the radiosensitivity of GBM.

Advani et al., have shown the conditionally-replicative HSV-1 mutant, R3616, has greater oncolytic effects and increased replication when exposed to IR (4). In their study, human U87-MG xenografts in mice underwent significantly greater reduction in tumor volume or total

regression when tumors were inoculated with the R3616 mutant and irradiated. Increased spread of the virus was seen with in-situ hybridization with DNA probes to the virus. Other studies have confirmed the enhanced tumoricidal effect of HSV when combined with IR (30, 205).

We believe targeting the repair of DNA DSBs in malignant glioma cells may be an important method to enhance the tumoricidal effect of IR. Inhibition of DNA repair may also play a role in the chemotherapeutic treatment of GBM. Use of an HSV-1 vector, which solely produces ICP0, may form the basis of future gene therapy strategies against human GBM.

4. INTRACEREBRAL CONVECTION-ENHANCED DELIVERY OF A HERPES SIMPLEX VIRUS VECTOR IN A MOUSE MODEL

4.1. Abstract

The less than optimal tissue distribution of HSV-1 vectors in the brain remains a limiting factor when considering the efficacy of various HSV-1 constructs for treatment of malignant gliomas. Convection-enhanced delivery (CED) of the replication-defective mutant, d106, resulted in homogeneous cell infection and extensive viral distribution in the mouse brain 48 hours after infusion. Persistent transgene expression occurred up to 6 days after CED. In addition, minimal viral reflux occurred along the catheter needle tract. Heparin or dextran sulfate co-infusion diminished HSV-1 cell infection and viral spread. Toxicity studies of intracerebral CED of d106 revealed a local inflammatory response occurring within 6 days of infusion that resolved 21 days after infusion. Local *in vivo* apoptosis was present on day 7 after d106 CED that was absent with Hanks' balanced salt solution CED. No animals showed any external signs of toxicity. The ICP0-producing mutant, d106, may form the basis of future gene therapy studies for malignant gliomas by CED.

4.2. Introduction

Herpes simplex virus-1 (HSV-1) recombinant vectors have been tested in multiple human clinical trials for the treatment of malignant gliomas (134, 252, 271). The less than optimal tissue distribution of HSV-1 vectors in the brain remains a limiting factor when considering the efficacy of various HSV constructs for the treatment of malignant gliomas. Delivery of HSV-1 vectors in all clinical trials has been by multiple manual stereotactic intratumoral or peritumoral injections after surgical resection (134, 206). Viral particles accumulate adjacent to the needle tract, and limited dispersal of particles occurs by diffusion. The binding of viral particles to the heparan sulfate proteoglycans found abundantly in the extracellular matrix and glycocalyx in the brain may contribute to limited dispersal (350).

Convection-enhanced delivery (CED) is an approach developed to overcome the obstacles associated with current CNS agent delivery (26, 230) and is increasingly used to distribute therapeutic agents for treatment of malignant gliomas. Currently, multiple clinical trials involve CED for the treatment of recurrent GBM (182, 326, 336, 338). In CED, a small hydrostatic pressure differential, imposed by a syringe pump to distribute infusate directly to small or large regions of the CNS, is used in a safe, reliable, targeted, and homogeneous manner (60). CED relies on bulk flow that is driven by a small gradient to distribute molecules within the interstitial spaces of the CNS. Convection is not limited by the infusate's molecular weight, concentration, or diffusivity (26, 230, 310).

Limited use of CED for viral vector delivery to the brain has been reported, mainly with the adeno-associated virus type 2 (AAV-2) (13, 61, 240). In one study, the authors suggested heparin co-infusion significantly increased the volume of distribution of AAV-2 by blocking the

binding of virus to heparan sulfate proteoglycans in the extracellular matrix (240). In the present study, we chose to deliver a replication-defective HSV mutant, d106, by intracerebral CED in a mouse model to determine cell infection, viral spatial distribution, and viral reflux along the needle tract. Heparin or dextran sulfate co-infusion was also performed to determine whether viral spatial distribution could be augmented. In addition, intracerebral viral toxicity was assessed after CED of the d106 virus.

4.3. Material and Methods

4.3.1. Animals and HSV-1 Vector

Six- to 7-week old female BALB/c mice (Charles River Laboratories, Wilmington, MA) were used, and all procedures were performed in accordance with the guidelines of the Institutional Animal Care and Use Committee of the University of Pittsburgh. The HSV-1 IE mutant virus, d106, is derived from the wild-type strain KOS and has been previously described (284). The HSV-1 mutant, d106, is defective in the expression of all of the immediate-early (IE) viral genes except that which encodes ICP0 (284). In place of the deletion of infected cell polypeptide (ICP) 27, a green fluorescent protein (GFP) gene under the control of the human cytomegalovirus (HCMV) IE promoter is present. GFP transgene synthesis is abundant in d106-infected cells, in which ICP0 is expressed (284).

4.3.2. CED Apparatus

The infusion apparatus consisted of a hydraulic drive serially connected to a syringe pump (Sage Apparatus, ATI Orion, Boston, MA, Model 361) (Fig. 7). This depressed the plunger of three 50 μ l oil-filled Hamilton syringes connected by cannulae made from polyetheretherketone (PEEK)

tubing (inner diameter 0.51 mm; Cole-Parmer Instrument Company, Vernon Hills, IL). The distal end of each cannula was fitted with a 30-gauge hypodermic needle (Fisher Scientific, Hanover Park, IL) and glued in place. The length of each cannula was measured to hold a volume of 120 μ l. HSV suspension or Hanks' balanced salt solution (HBSS; Gibco Invitrogen Life Technologies, Inc., Grand Island, NY) was used to fill each cannula prior to attachment to each Hamilton syringe needle tip. Each cannula end was secured to the electrode manipulator of a small animal stereotaxic instrument (Model 900, David Kopf Instruments, Tujunga, CA).

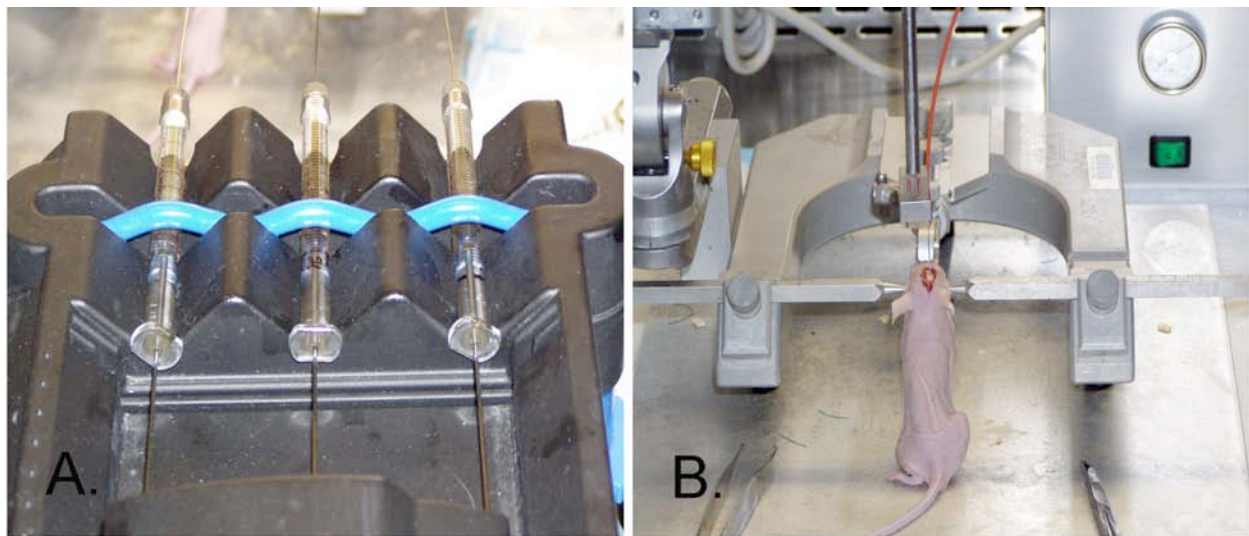


Figure 10. Convection-enhanced delivery mouse model. A, Infusion apparatus holding three 50 μ l Hamilton syringes filled with oil connected distally to cannulae made from PEEK tubing. B, Anesthetized mouse placed in a small animal stereotaxic instrument and the CED cannula secured to the electrode manipulator of the stereotaxic instrument.

4.3.3. HSV-1 CED and Heparin or Dextran Sulfate Co-infusion

Mice were anesthetized with a ketamine/acepromazine mixture administered by the intraperitoneal route. Anesthetized mice were placed in a stereotaxic instrument and an incision was made in the midline from the glabella to the occiput. The underlying skull was exposed and a 2 mm burr hole was placed 0.5 mm anterior and 3 mm to the right of bregma. Mice were

randomized into 4 groups of three animals each: (1) CED of d106, (2) CED of HBSS, (3) CED of d106 and heparin, (4) CED of d106 and dextran sulfate (10 or 100 µg).

The CED cannula needle was inserted stereotactically through the burr hole to a depth of 3 mm below the dural surface. All animals underwent CED of 10 µl of d106 (3×10^7 pfu) suspension, HBSS, d106 (3×10^7 pfu) and heparin (1 unit), or d106 (3×10^7 pfu) with dextran sulfate (10 or 100 µg), at a rate of 1 µl/min. After infusion completion, the cannula was left in place for 5 minutes to minimize any infusate leakback. The cannula was then withdrawn at a rate of 1 mm/min and the craniotomy was sealed with bone wax and the scalp was re-approximated by suture. All animals were sacrificed 48 hours after CED. Mouse brains were harvested and fixed with 10% neutral buffered formalin for histologic analysis.

4.3.4. Persistent HSV-1 Transgene Expression and In vivo Toxicity

Two separate groups of mice, 12 animals each, were randomized to undergo stereotactic intracerebral CED of 10 µl of d106 or HBSS at a rate of 1 µl/min. Mice were sacrificed at 4, 6, 7, and 21 days after CED. Mouse brains were harvested and fixed with 10% neutral buffered formalin for histologic analysis.

4.3.5. Histologic Analysis

Upon brain fixation with formalin, coronal sections of each brain were made at the level of the needle tract to mark the center of virus or HBSS delivery. Serial sections of the cerebral hemisphere were examined from each animal. Tissue blocks were embedded in paraffin and sectioned (8 µm). All sections were stained with hematoxylin and eosin.

GFP immunohistochemistry was performed after deparaffination of tissue sections. Drying of tissue sections was performed initially. Slides were then rinsed in deionized water and

placed in a slide holder and a Tissue-Tek staining dish filled with Antigen retrieval solution (Abcam Inc., Cambridge, MA). Slides were heated in a microwave oven until the antigen retrieval solution came to a boil and then were allowed to cool. Slides were rinsed in phosphate buffered solution (PBS) prior to treatment with proteinase K. Repeat rinsing with PBS was performed before the addition of 0.3% hydrogen peroxide to the slides to block endogenous peroxidase activity. After rinsing with PBS, a permeabilizing/blocking solution consisting of PBS, 2% horse serum, and 0.2% Triton-X was added. The blocking solution was removed and a primary rabbit polyclonal GFP antibody (sc-8334; Santa Cruz Biotechnology, Santa Cruz, CA), diluted 1:100 in PBS, was added in addition to 2% horse serum and 0.05% Tween 20 and incubated overnight at 4° C. Slides were rinsed in PBS prior to addition of a biotinylated anti-rabbit secondary antibody (dilution 1:100) provided in a rabbit ABC staining system (sc-2018; Santa Cruz Biotechnology, Santa Cruz, CA). Incubation was performed for 30 minutes prior to rinsing of slides with PBS. Incubation with a biotinylated horseradish peroxidase reagent was performed for 30 minutes and rinsing of slides was repeated with PBS. Tissue sections were incubated in 1-3 drops of peroxidase substrate for 2-15 minutes until stain intensity was optimal. Counterstaining of tissue sections was performed in Mayer's hematoxylin for 5 minutes prior to washing in running tap water. Permanent mounting medium was added to each slide prior to glass coverslip placement.

A terminal deoxynucleotidyl transferase-mediated dUTP-biotin nick end-labeling (TUNEL) assay was performed day 7 after CED of either d106 or HBSS on sections in accordance with the manufacturer's instructions (Chemicon, Temecula, CA) and analyzed in a blinded fashion at 40X magnification by use of a light microscope.

Tissue sections were examined by light microscopy using a Nikon Diaphot 300 photomicroscope (Melville, NY). Images were captured by a SPOT RT camera (Diagnostic Instruments, Sterling Heights, MI) and imported into the SPOT version 3.5.9 for MacOS image analysis software package (Diagnostic Instruments, Sterling Heights, MI) running on a Macintosh G3 computer (Apple, Cupertino, CA).

4.4. Results

4.4.1. HSV-1 Cell Infection, Spatial Distribution, Reflux, and Transduction After CED

The CED parameters chosen included a viral suspension volume of 10 μ l infused at a rate of 1 μ l/min through a 30-gauge needle tip. GFP transgene expression was used as a marker for cell infection in the brain. Abundant cellular GFP expression has been shown *in vitro* 24 hours post-infection by the d106 virus (284). Intracerebral GFP expression was determined 2, 4, 6, 7, and 21 days after stereotactic CED of d106 alone (Fig. 8). Strong, homogeneous GFP staining was found adjacent to the needle tip, suggestive of uniform cell infection in the brain 2 days after CED. Extensive viral spatial distribution within the gray matter of the brain was found away from the needle tip. White matter tract distribution of HSV-1 was found distal to the needle tip and minimal infusate reflux occurred. Persistent GFP expression, or cell infection, was found up to 6 days after CED of d106 (Fig. 9).

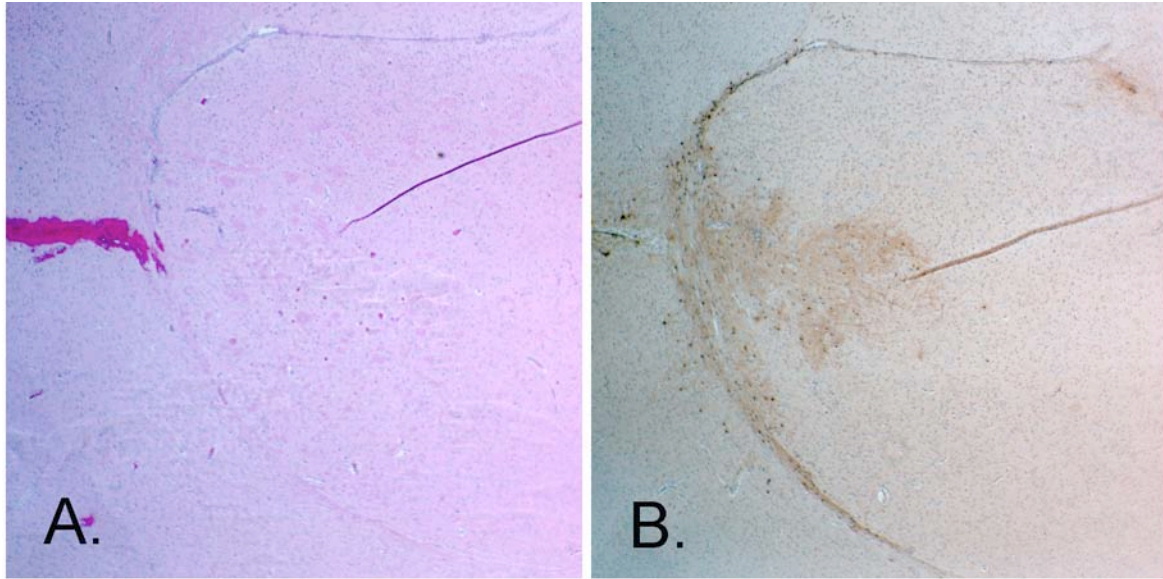


Figure 11. Photomicrographs of mouse brain sections 48 hours after CED of d106. Magnification, 40X. A, Hematoxylin/eosin-stained section showing the catheter needle track on the left. B, GFP-stained section showing viral cell infection and spatial distribution within the gray matter and white matter tracts.

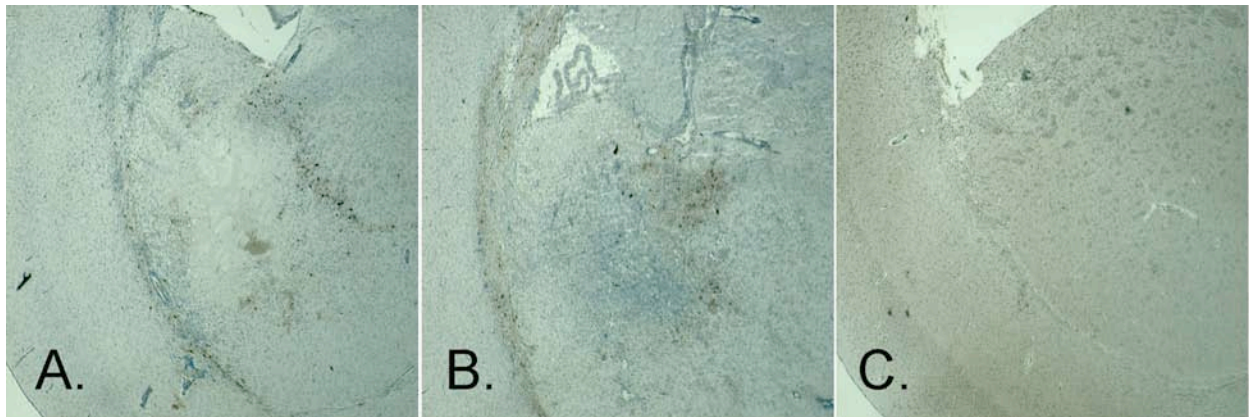


Figure 12. Photomicrographs of mouse brain sections stained with GFP 4, 6, and 21 days after d106 CED. Persistent cell infection is present for 6 days. Magnification, 40X. A, Section day 4 after d106 CED. B, Section day 6 after d106 CED. C, Section day 21 after d106 CED revealing no GFP cell positivity.

4.4.2. HSV-1 CED and Heparin or Dextran Sulfate Co-infusion

The initial binding of HSV-1 to the cell surface occurs by heparan sulfate proteoglycans present on the surface of most types of vertebrate cells (350). A potential problem in the delivery of HSV-1 by CED may be the binding of viral particles to the heparan sulfate proteoglycans found abundantly in the extracellular matrix and glycocalyx in the brain. A prior report on CED of

AAV-2 to the rat brain, revealed abundant attachment of AAV-2 particles to cells adjacent to the injection tract limiting the distribution of AAV-2 when infused into the CNS parenchyma (240). Heparin co-infusion (2.5 units) significantly increased the volume of distribution of AAV-2 as demonstrated by immunoreactivity to a transgene product 6 days after infusion into the rat striatum. No intracerebral hemorrhage was reported with heparin-coinfusion.

In our study, we chose to administer a lower dose of heparin (1 unit) with d106 into the mouse brain by CED to determine intracerebral infection and viral spatial distribution. Intracerebral GFP expression was determined 2 days after stereotactic CED. Minimal cell infection occurred after CED of d106 and heparin together (Fig. 10). Our results are consistent with prior *in vitro* studies, showing heparin inhibition of HSV-1 cell infection by masking the heparin sulfate binding domains on the virus envelope (350). No intracerebral hemorrhage occurred in the animals that underwent heparin-coinfusion in our study.

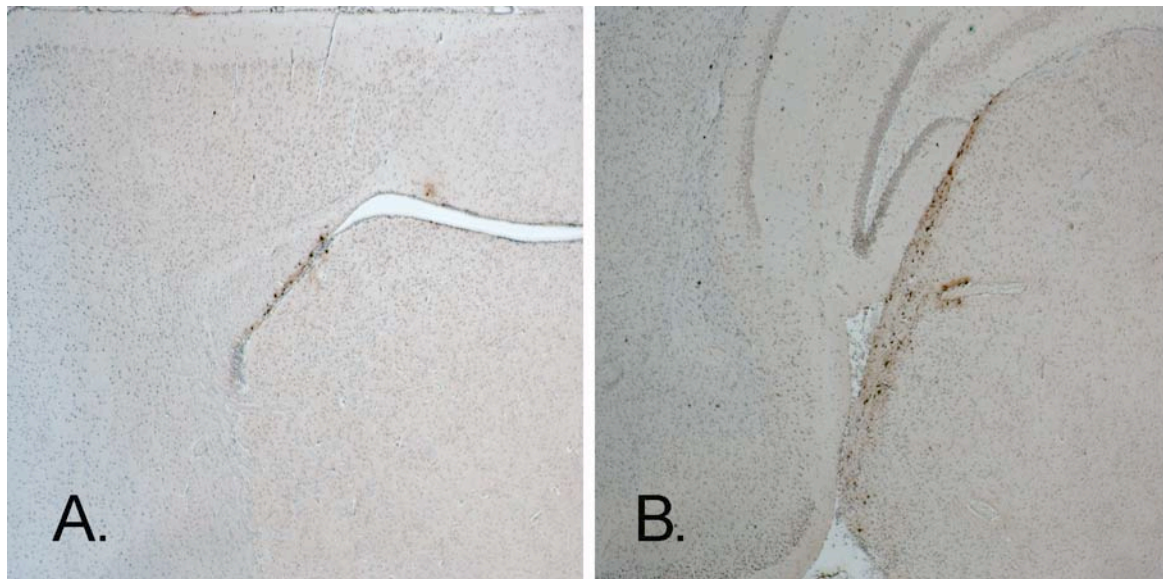


Figure 13. Photomicrographs of mice brain sections after heparin or dextran sulfate (10 µg) co-infusion with d106. Immunohistochemistry staining for GFP was performed. Magnification, 40X. A, CED of d106 and heparin. B, CED of d106 and dextran sulfate.

Co-infusion of dextran sulfate with d106 was also performed to determine if cell infection and viral spatial distribution could be enhanced. Dextran sulfate may serve as a substitute for heparin, which is not associated with anticoagulative effects. In a prior report, dextran sulfate has been shown to interact with both HSV-1 virions and cells (80). In that paper, a mutant cell line unable to produce glycosaminoglycans was treated with DS either prior to or during infection with HSV-1. The use of dextran sulfate (10 or 100 μ g) added either prior to or during inoculation stimulated HSV-1 infection by up to 35 fold. Their results were consistent with a model in which DS effectively substitutes for heparan sulfate as a matrix to initiate viral adsorption at the cell surface.

We chose to co-infuse either 10 or 100 μ g of dextran sulfate with d106 into the mouse brain. Intracerebral GFP expression was determined 2 days after stereotactic CED. All three of the animals that underwent CED of d106 and the higher dose of dextran sulfate (100 μ g) died within 6 hours after infusion. Co-infusion of the lower dose of dextran sulfate (10 μ g) resulted in limited HSV-1 cell infection and viral distribution (Fig. 10). Distribution of virus was found only along the needle tract. Neither heparin or dextran-sulfate co-infusion resulted in any increase in cell infection or viral distribution in comparison to d106 CED alone. Instead, heparin or dextran-sulfate co-infusion diminished cell infection and viral spread.

4.4.3. Intracerebral Toxicity of d106 After CED

We have previously shown in vitro that d106 infection of cells results in decreased cell survival in part by apoptosis induction (126, 284). In addition, prior reports have confirmed the immunogenicity of HSV-1 replication-defective viruses both in vitro and in vivo (32, 33). We chose to evaluate the toxicity of d106 in the mouse brain at 4, 6, 7, and 21 days after CED.

Inflammation, or encephalitis, was determined after hematoxylin/eosin preparation of brain sections. *In vivo* apoptosis was determined on brain sections with TUNEL staining day 7 after CED. No animals showed any signs of external toxicity such as weight loss or paresis.

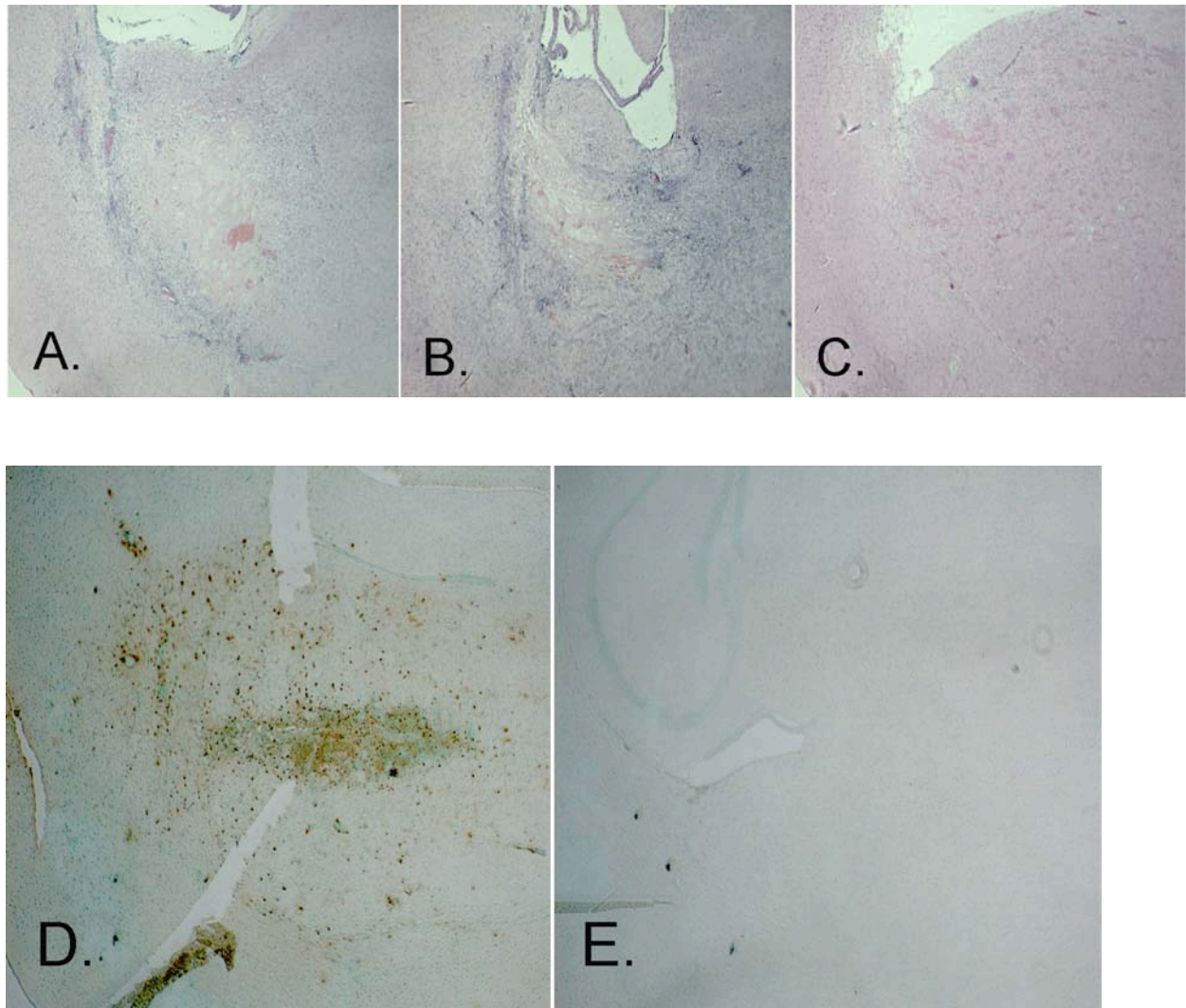


Figure 14. Intracerebral toxicity of d106 after CED. Photomicrographs of mice brain sections 4, 6, 7, and 21 days after d106 CED. Magnification, 40X. A-C, Hematoxylin/eosin-stained sections on days 4, 6, and 21. D, *In vivo* apoptosis by TUNEL staining on day 7. E, TUNEL staining after CED of HBSS on day 7.

On day 4 after CED of d106, cell necrosis was present within the area of brain infused with d106 with minimal surrounding inflammation (Figs. 11 and 9). GFP cell expression was found at the periphery of the area of cellular necrosis. A substantial inflammatory cell response adjacent to

the area of viral delivery was present on day 6 after d106 CED. No intracerebral inflammation was present 21 days after d106 CED. No intracerebral inflammation was present on days 4, 6, 7, and 21 days after HBSS CED.

In vivo apoptosis was present on day 7 after CED of d106 (Fig. 11). The greatest number of apoptotic cells was found immediately adjacent to the catheter needle tip. Cells undergoing apoptosis were found distal to the needle tip in a circumscribed, homogeneous distribution. No *in vivo* apoptosis was present after CED of HBSS (Fig. 11).

4.5. Discussion

The method of HSV-1 delivery to tumors within the brain is critical to determining the efficacy of various recombinant constructs in the treatment of malignant gliomas. In studies to date, manual stereotactic injection is the delivery method used (134, 206, 252, 271). Such a technique is unlikely to result in widespread and uniform distribution of HSV-1 within tumor tissue as well as surrounding, tumor-invaded brain. In addition, reflux of viral dose along the injection tract is an important problem that could impact on the dose of virus that reaches the tumor (204). Intra-arterial delivery has been examined as a potential mechanism of delivery for HSV-1, but obtaining adequate delivery of vector was also difficult via this route (153).

We believe convection-enhanced delivery of HSV-1 is an optimal delivery approach to the brain. Cell infection and distribution of HSV-1 appears relatively homogeneous in the brain after CED with a moderate dose of virus (3×10^7 pfu/10 μ l). Spread of viral particles occurs within the gray matter and along white matter tracts in the brain. In addition, minimal viral reflux occurs along the catheter needle tract maximizing the viral dose available for cell infection. Delivery of HSV-1 with heparin or dextran sulfate does not enhance cell infection and

viral distribution in the brain. Instead, diminished cell infection and viral spatial distribution occurs after heparin or dextran sulfate co-infusion.

The potential use of replication-defective HSV-1 vectors in human trials for the therapy of malignant gliomas exists. Prior to the use of any of these vectors in the clinic, adequate toxicity studies need to be performed. The ICP0-producing mutant, d106, does elicit an initial local inflammatory response in the mouse brain that subsides 21 days after viral delivery. An apoptotic mode of cell death is triggered within the area of viral infusion after 7 days. No animals that underwent CED of d106 showed any external signs of toxicity such as weight loss or paresis.

Recently, we have shown the HSV-1 mutant, d106, inhibits DNA repair and enhances the radiosensitivity of human GBM cells in vitro (126). We believe the replication-incompetent d106 virus may form the basis of future gene therapy studies for malignant gliomas by convection-enhanced delivery.

5. A HERPES SIMPLEX VIRUS VECTOR ENHANCES THE RADIOSENSITIVITY OF MOUSE INTRACRANIAL HUMAN GLIOBLASTOMA XENOGRAFTS AFTER CONVECTION-ENHANCED DELIVERY

5.1. Abstract

Improving the efficacy of herpes simplex virus 1 (HSV-1) therapy for malignant gliomas may require combination therapy with other treatment modalities and a change in the delivery of virus to tumor cells in the brain. The goals of this study were the following: (1) To compare convection-enhanced delivery (CED) of HSV-1 to stereotactic manual injection in viral spatial distribution, cell infection, and viral suspension reflux in the mouse brain; (2) To determine U87 MG xenograft infection and viral transduction in a mouse intracranial human glioma model after CED of the ICP0-producing HSV mutant, d106; (3) To determine whether radiosensitivity enhancement of intracranial malignant glioma xenografts occurs after CED of d106 in combination with whole-brain irradiation. Stereotactic manual intracerebral injection and CED of HSV-1 was performed on BALB/c mice. The volume for each method of delivery was 10 μ l of d106 suspension (3×10^9 plaque forming units (pfu)/ml). The rate of infusion for CED was 1 μ l/minute. Viral spatial distribution and cell infection in the brain were determined by brain immunohistochemistry for enhanced green fluorescent protein (EGFP). Intracranial U87-MG human GBM xenografts were established in athymic nude mice. Mice were randomized to undergo intracranial CED (10 μ l) of the replication-defective d106 virus (3×10^9 pfu/ml) or Hanks' balanced salt solution (HBSS), at a rate of 1 μ l/min prior to whole-brain irradiation (0 or 10 Gy). Superior brain viral spatial distribution and cell infection was found after CED of d106 in comparison to stereotactic manual injection. Minimal viral suspension reflux occurred during CED while reflux happened frequently with stereotactic injection. Optimal xenograft infection

and persistent cell infection was found after CED of d106. Combination therapy of d106 CED and irradiation resulted in xenograft regression and greater overall survival ($P < 0.01$) in animals. CED is superior to stereotactic injection of HSV-1 in viral delivery to the mouse brain. Combination therapy of d106 CED and whole-brain irradiation resulted in optimal xenograft HSV-1 delivery and enhancement of the effects of radiation in an intracranial malignant glioma model.

5.2. Introduction

Herpes simplex virus 1 (HSV-1) is a double-stranded DNA virus that has been studied for use in the treatment of human malignant gliomas, the most devastating and therapy-resistant central nervous system (CNS) tumors in adults. A number of different genetically engineered oncolytic viruses have been constructed with deletions or mutations in one or more HSV genes ($\gamma_134.5$, U_L39 (ribonucleotide reductase), tk , and $UTPase$) in an effort to decrease the toxicity of HSV to the CNS and provide a condition for viral replication only in replicating cells that can provide cellular homologues (49, 51, 152, 175, 208, 222, 267). Phase I clinical studies in humans with malignant gliomas have demonstrated modest antitumor effect with HSV-1 oncolytic viruses (134, 206, 271). Other HSV mutants have been constructed that are defective for immediate-early (IE) gene expression, resulting in replication-incompetent viruses that are nontoxic to cells (284). Various genes have been inserted in these modified viruses for expression in infected cells (178, 202, 229, 244).

Improving the efficacy of HSV-1 therapy for malignant gliomas may require combination therapy with other treatment modalities and a change in the delivery of virus to tumor cells in the brain. Prior studies have shown that HSV replication and tumor kill in human GBM xenografts is increased when the oncolytic virus, R3616, is administered in conjunction with ionizing radiation (IR) (4). Other studies have confirmed the tumoricidal effect of HSV when combined with IR (30, 205).

In all human Phase I and animal studies, HSV delivery is by direct manual stereotactic injection into the brain (134, 206, 271). In the human studies performed, viral injection is performed multiple times within the contrast-enhancing portion of the tumor or around the

resulting cavity after surgical resection (134, 205, 271). Stereotactic intracerebral injection of HSV-1 vectors has produced limited success in the delivery of the virus to brain tumor cells (206, 229, 270). Besides the difficult task of standardizing distances between injection tracts and applied volumes, reflux of vector suspension from needle tracks is invariably encountered with manual injection (204, 270). Viral particles accumulate adjacent to the needle tract and limited dispersal of particles occurs by diffusion (24). The binding of viral particles to the heparan sulfate proteoglycans found abundantly in the extracellular matrix and glycocalyx in the brain may contribute to limited dispersal (350).

Convection-enhanced delivery (CED) is an approach developed to overcome the obstacles associated with current CNS agent delivery (26, 230) and is increasingly used to distribute therapeutic agents for treatment of malignant gliomas. Currently, multiple clinical trials involve CED for the treatment of recurrent GBM (182, 326, 336, 338). In CED, a small hydrostatic pressure differential, imposed by a syringe pump to distribute infusate directly to small or large regions of the CNS, is used in a safe, reliable, targeted, and homogeneous manner (60). CED relies on bulk flow that is driven by a small gradient to distribute molecules within the interstitial spaces of the CNS. Convection is not limited by the infusate's molecular weight, concentration, or diffusivity (26, 230, 310). Limited use of CED for viral vector delivery to the brain has been reported, mainly with the adeno-associated virus 2 (AAV-2) (13, 61).

We have recently shown the replication-defective HSV-1 vector, d106, inhibits DNA repair and enhances the radiosensitivity of human GBM cells (126). The mutant virus, d106, is defective in the expression of all of the IE viral genes except that which encodes ICP0 (284). Expression of the ICP0 protein by d106 results in degradation of the catalytic subunit of DNA-dependent protein kinase (DNA-PK_{CS}) in human GBM cells. DNA-PK_{CS} is a key component of

the nonhomologous end-joining (NHEJ) DNA repair pathway that is thought to repair the majority of DNA double-strand breaks. Inhibition of the repair of DNA double-strand breaks after IR (5, 10, or 20 Gy) results in a significant decrease in survival of GBM cells in part by induction of apoptosis. ICP0 has also been shown by our group to induce cell cycle arrest in G1 and G2-M independently of p53 (143). In the present study, we chose to deliver d106 by intracerebral stereotactic injection or CED in normal mice to compare cell infection, viral spatial distribution, and viral suspension reflux by each modality. In addition, intracerebral CED of d106 was performed in a mouse glioma model in combination with ionizing radiation (IR) to determine U87 MG xenograft infection and transduction, viral antitumor effect, and mouse survival.

5.3. Material and Methods

5.3.1. Animals, Cells, and HSV-1 Vector

Six- to 7-week old female athymic nude (nu/nu) and BALB/c mice (Charles River Laboratories, Wilmington, MA) were used, and all procedures were performed in accordance with the guidelines of the Institutional Animal Care and Use Committee of the University of Pittsburgh. The human glioblastoma cell line, U87 MG, was obtained from the American Type Culture Collection (ATCC) and maintained in Dulbecco's modified Eagle medium (DMEM) supplemented with sodium pyruvate, non-essential amino acids, antibiotics, and 10% fetal bovine serum (FBS) (Invitrogen Life Technologies, Inc., Gaithersburg, MD). The HSV-1 IE mutant virus, d106, is derived from the wild-type strain KOS and has been previously described (284). In place of the deletion of infected cell polypeptide (ICP) 27, a green fluorescent protein

(GFP) transgene under the control of the human cytomegalovirus (HCMV) IE promoter was inserted. GFP transgene synthesis is abundant in d106-infected cells, in which ICP0 is present

5.3.2. CED Apparatus

The infusion apparatus consisted of a hydraulic drive serially connected to a syringe pump (Sage Apparatus, ATI Orion, Boston, MA, Model 361). This depressed the plunger of three 50 μ l oil-filled Hamilton syringes (Hamilton Co., Reno, NV) connected by cannulae made from polyetheretherketone (PEEK) tubing (inner diameter 0.51 mm; Cole-Parmer Instrument Company, Vernon Hills, IL). The distal end of each cannula was fitted with a 30-gauge hypodermic needle (Fisher Scientific, Hanover Park, IL) and glued in place. The length of each cannula was measured to hold a volume of 120 μ l. HSV solution or Hanks' balanced salt solution (HBSS; Gibco Invitrogen Life Technologies, Inc., Grand Island, NY) was used to fill each cannula prior to attachment to each Hamilton syringe needle tip. Each cannula end was secured to the electrode manipulator of a small animal stereotaxic instrument (Model 900, David Kopf Instruments, Tujunga, CA).

5.3.3. Tumor Inoculation, HSV-1 Convection Procedure, and Irradiation

Mice were anesthetized with a ketamine/acepromazine mixture administered by the intraperitoneal route. Anesthetized mice were placed in the stereotaxic instrument and an incision was made in the midline from the glabella to the occiput. The underlying skull was exposed and a 2 mm burr hole was placed 0.5 mm anterior and 3 mm to the right of bregma. U87 MG cells (5×10^5) in a 5 μ l volume were stereotactically inoculated into the right striatum, 3 mm below the dural surface on day 0, with a 10 μ l Hamilton syringe fitted into a syringe holder microinjection unit (Model 5000, David Kopf Instruments, Tujunga, CA) and secured to

the small animal stereotaxic instrument. After removal of the injection needle, the craniotomy was sealed with bone wax and the scalp was re-approximated by suture. On day 5 post-tumor implantation, mice were randomized into four groups (Table 1): (1) CED of HBSS (untreated control), (2) CED of HBSS and irradiation, (3) CED of d106 alone, (4) CED d106 and irradiation.

Table 1.

Treatment groups (n=10)	Protocol		Median survival (days)	Survival at 80 d (%)
	Day 5	Day 7		
1. HBSS (control)	CED HBSS	0 Gy	23	0
2. HBSS + IR	CED HBSS	10 Gy	39	0
3. d106	CED d106	0 Gy	41	0
4. d106 + IR	CED d106	10 Gy	68	30

Table 1. Summary of treatment group results including number of animals, protocol, median survival, and percent survival at 80 days.

All animals underwent CED of 10 μ l of d106 (3×10^7 pfu) suspension or HBSS at a rate of 1 μ l/min on day 5. Anesthetized mice were placed back in the stereotactic head frame and the previous skin incision was opened. The CED cannula needle was inserted stereotactically through the previous craniotomy using the same coordinates as used earlier for tumor cell implantation. After infusion completion, the cannula needle was left in place for 5 minutes to minimize any infusate leakback. The cannula needle was then withdrawn at a rate of 1 mm/min and the craniotomy was sealed with bone wax and the scalp was re-approximated by suture.

A single dose of IR (10 Gy) was delivered to anesthetized mice on day 7 in a ^{137}Cs animal irradiator (Gammacell40, Atomic Energy of Canada Limited, Ontario, Canada) at a dose rate of .87 Gy/min. A lower dose of ionizing radiation was chosen to have modest antitumor

effect but to not be curative. Perforated collimator plates were used for selective whole-brain irradiation of animals.

5.3.4. Intracerebral HSV-1 CED or Stereotactic Injection Alone

Intracerebral stereotactic CED or injection of d106 was performed in six BALB/c mice after anesthesia and placement in the small animal stereotaxic instrument. CED was performed as described previously. Injection was performed in the same fashion as tumor inoculation described previously. Briefly, 10 μ l of d106 (3×10^7 pfu) suspension was manually injected through a 10 μ l Hamilton syringe secured to the syringe holder microinjection unit attached to the small animal stereotaxic instrument. The syringe needle was stereotactically inserted into a 2 mm burr hole placed 0.5 mm anterior and 3 mm to the right of bregma. Injection was initiated 3 mm below the dural surface. The injection needle was left in place for 5 minutes prior to removal. All animals were sacrificed 48 hours after intracerebral CED or injection and brains were harvested for histologic analysis.

5.3.5. Animal Observation

All mice were observed daily to monitor external appearance, feeding behavior, and locomotion. The contralateral limbs were observed for the development of paresis. Animals were sacrificed at the first sign of an adverse event (paresis, inability to feed) and brains were removed for histological examination. On days 5, 7, 9, 12, 15, and 17, three animals from each group of animals inoculated with tumor were randomly sacrificed for histologic analysis of intracranial tumor burden and U87 MG xenograft d106 infection. All remaining animals surviving 80 days after tumor implantation were sacrificed.

5.3.6. Histologic Analysis

Mouse brains were harvested and fixed with 10% neutral buffered formalin. Coronal sections were made at the level of the needle tract to mark the center of the tumor. Serial sections of the cerebral hemisphere were examined from each animal. Tissue blocks were embedded in paraffin and sectioned (5 μ m). All sections were stained with hematoxylin and eosin.

GFP immunohistochemistry was performed after deparaffination of tissue sections. Drying of tissue sections was performed initially. Slides were then rinsed in deionized water and placed in a slide holder and a Tissue-Tek staining dish filled with Antigen retrieval solution (Abcam Inc., Cambridge, MA). Slides were heated in a microwave oven until the antigen retrieval solution came to a boil and then were allowed to cool. Slides were rinsed in phosphate buffered solution (PBS) prior to treatment with proteinase K. Repeat rinsing with PBS was performed before the addition of 0.3% hydrogen peroxide to the slides to block endogenous peroxidase activity. After rinsing with PBS, a permeabilizing/blocking solution consisting of PBS, 2% horse serum, and 0.2% Triton-X was added. The blocking solution was removed and a primary rabbit polyclonal GFP antibody (sc-8334; Santa Cruz Biotechnology, Santa Cruz, CA), diluted 1:100 in PBS, was added in addition to 2% horse serum and 0.05% Tween 20 and incubated overnight at 4° C. Slides were rinsed in PBS prior to addition of a biotinylated anti-rabbit secondary antibody (dilution 1:100) provided in a rabbit ABC staining system (sc-2018; Santa Cruz Biotechnology, Santa Cruz, CA). Incubation was performed for 30 minutes prior to rinsing of slides with PBS. Incubation with a biotinylated horseradish peroxidase reagent was performed for 30 minutes and rinsing of slides was repeated with PBS. Tissue sections were incubated in 1-3 drops of peroxidase substrate for 2-15 minutes until stain intensity was optimal. Counterstaining of tissue sections was performed in Mayer's hematoxylin for 5 minutes prior to

washing in running tap water. Permanent mounting medium was added to each slide prior to glass coverslip placement.

Tissue sections were examined by light microscopy using a Nikon Diaphot 300 photomicroscope (Melville, NY). Images were captured by a SPOT RT camera (Diagnostic Instruments, Sterling Heights, MI) and imported into the SPOT version 3.5.9 for MacOS image analysis software package (Diagnostic Instruments, Sterling Heights, MI) running on a Macintosh G3 computer (Apple, Cupertino, CA).

5.3.7. Statistical Analysis

Survival data were entered into Kaplan-Meier plots and statistical analysis was performed using a log-rank test. A *P* value of 0.05 was used as the boundary of statistical significance.

5.4. Results

5.4.1. HSV-1 Stereotactic Injection vs. CED

HSV-1 intracerebral cell infection, spatial distribution, and reflux along the needle tract were determined in the normal mouse brain after stereotactic CED or injection. GFP transgene expression was used as a marker for cell infection. Abundant cellular GFP expression has been shown *in vitro* 24 hours post-infection by the d106 virus (284). GFP expression was determined 48 hours after stereotactic CED or injection of d106. A 10 μ l suspension of d106, containing 3×10^7 pfu, was used with each method of delivery. Histologic analysis of tissue sections along either the cannula or syringe needle tract revealed both greater spatial distribution and intensity of GFP staining after CED of d106 in comparison to stereotactic injection (Fig. 12). Strong, homogeneous GFP expression after CED suggests greater cell infection by d106. White matter tract spread of HSV-1 was found after CED but not with stereotactic injection. Vector

suspension reflux along the needle tract was present with manual stereotactic injection while minimal infusate leakback occurred after CED (Fig. 12).

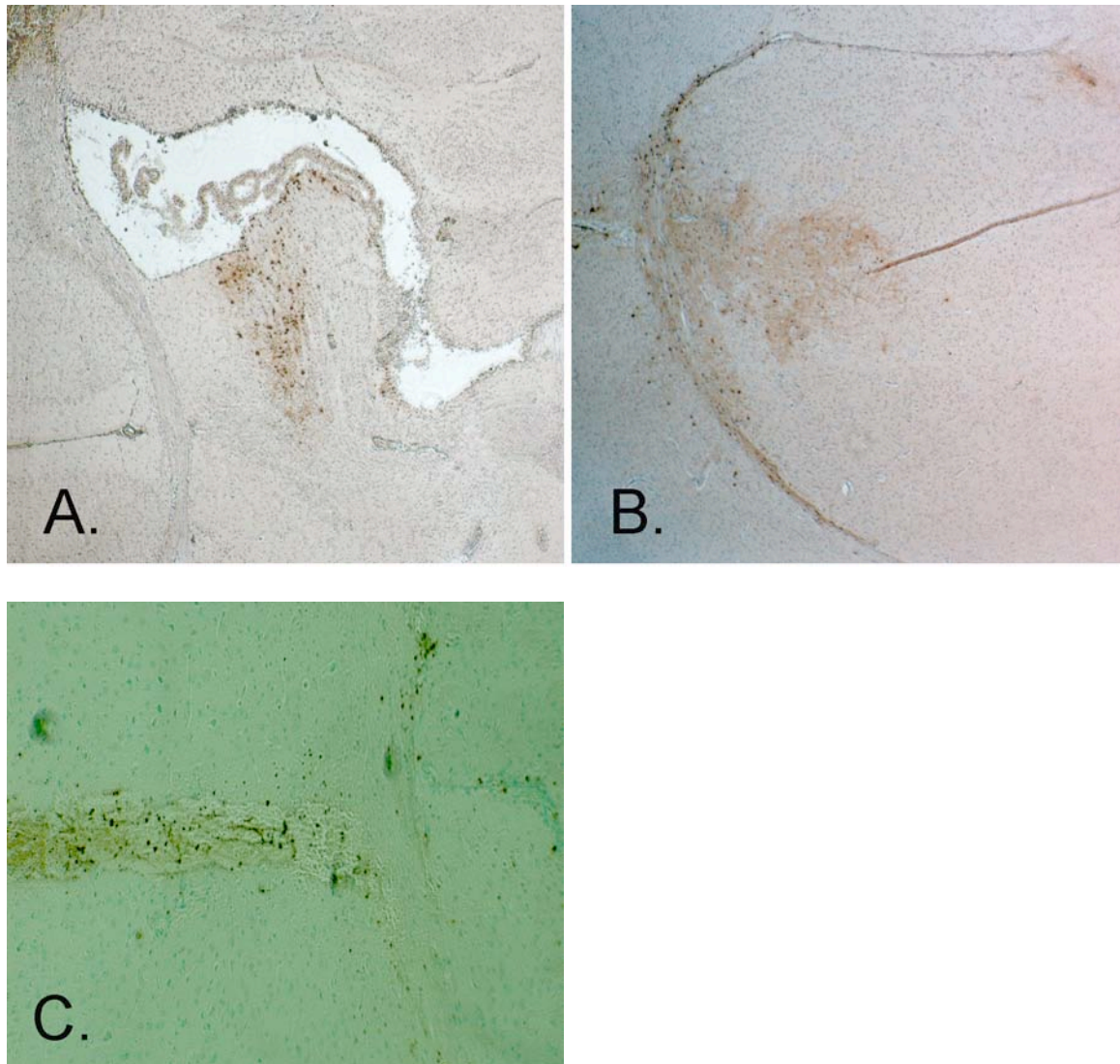
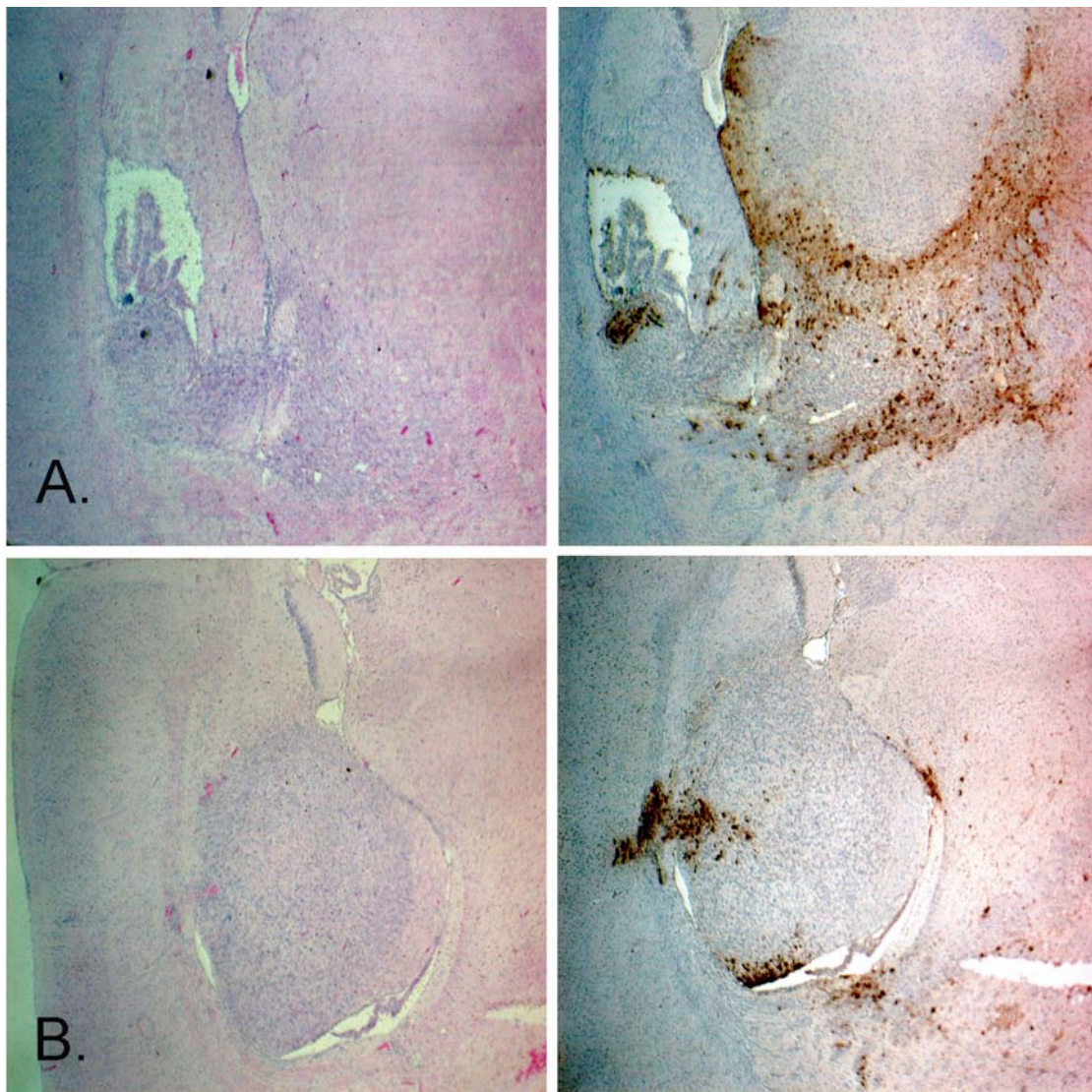


Figure 15. Photomicrographs of BALB/c mice brain sections after immunohistochemistry staining for GFP. A comparison of intracerebral manual stereotactic injection and convection-enhanced delivery (CED) with 10 μ l of d106 viral suspension (3×10^7 pfu) revealing greater cell infection and viral spatial distribution with minimal viral reflux after CED. A. Manual stereotactic injection (Magnification, 40X). B. Stereotactic CED (Magnification, 40X). C. Viral reflux along the needle tract after manual stereotactic injection (Magnification, 100X).

5.4.2. HSV-1 Xenograft Infection and Cell Transduction

After inoculation of athymic nude mice with U87 MG tumor cells, CED of d106 or HBSS was performed 5 days later. Intracerebral GFP expression was determined at 7, 9, 12, 15, and 17 days after xenograft placement (Fig. 13; Table 2). Intratumoral expression of GFP was found in

75% (9 of 12 animals) of the animals that underwent CED of d106 and were randomly sacrificed at 7 and 9 days post-tumor implantation (2 and 4 days after d106 CED) (Figs. 13A and 13C). Two of the 9 animals had minimal intra-tumoral GFP expression (Fig. 13B). All animals that did not have intratumoral expression of GFP had peri-tumoral cell expression of GFP, indicating inadequate penetration of the xenograft by the d106 virus. Persistent cellular GFP transgene expression was found up to 12 days after d106 CED in cells within and surrounding xenograft sites (Fig. 13D) after tumor regression.



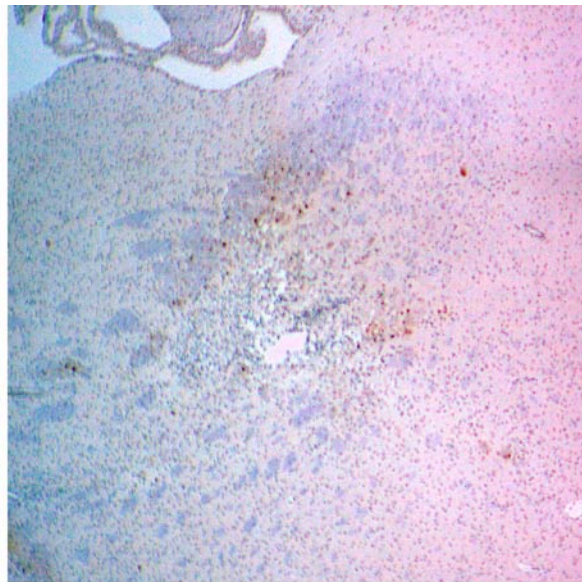
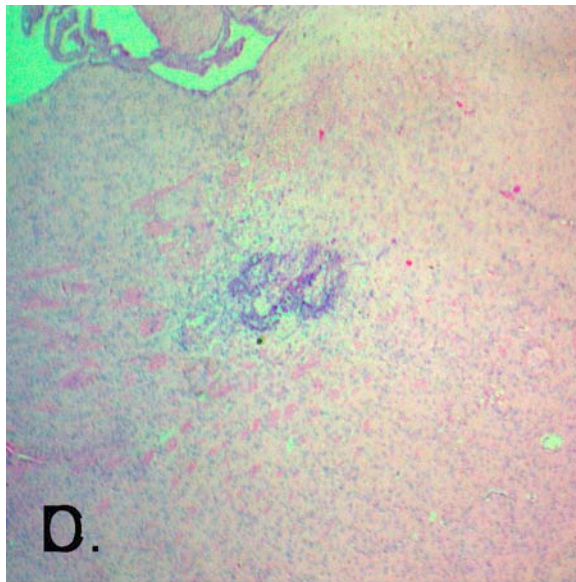
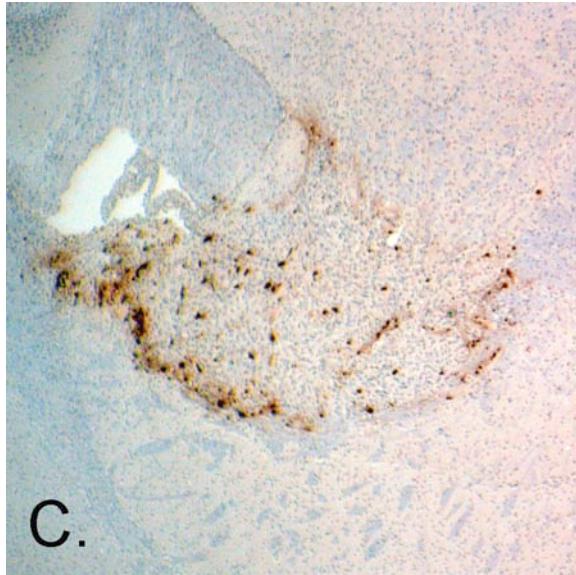


Figure 16. Photomicrographs of athymic nude mice brain sections containing U87 MG xenografts after stereotactic intracerebral CED of d106. Magnification, 40X. A. Hematoxylin/eosin-stained section day 7 after tumor implantation and 2 days after d106 CED revealing boundaries of xenograft (*left*); corresponding GFP-stained section revealing marked xenograft infection and viral spatial distribution into the surrounding brain (*right*). B. Hematoxylin/eosin-stained section day 7 after tumor implantation (*left*) and corresponding GFP-stained section (*right*) revealing minimal xenograft infection and viral spatial distribution. C. GFP-stained section day 7 showing strong xenograft infection and extensive viral spatial distribution within the tumor. D. Hematoxylin/eosin-stained section day 17 after tumor implantation (*left*) and corresponding GFP-stained section (*right*) revealing complete tumor regression and continued GFP expression at the xenograft site suggestive of persistent viral infection.

5.4.3. Antitumor Effect of d106 and IR

Survival studies were performed on animals that underwent CED of HBSS or d106 and whole-brain irradiation (0 or 10 Gy). A total of 4 groups, consisting of 10 animals each, were used for survival analysis at a 80-day post tumor induction survival mark (Table 1). The median survival for control animals that underwent CED of HBSS and no irradiation was 23 days. Those animals that underwent CED of d106 and were not irradiated had a median survival of 41 days. Median survival was significantly increased ($P < 0.01$ by log-rank method) when animals underwent CED of d106 in comparison to control animals. Animals that had HBSS CED and were irradiated (10 Gy) had a median survival of 39 days. Animals that underwent CED of d106 and were irradiated had a median survival of 68 days. Of these animals, 30% were still alive on day 80 when sacrificed. Median survival was significantly increased ($P < 0.01$ by log-rank method) when animals underwent CED of d106 and subsequent whole-brain irradiation (10 Gy) in comparison to animals that underwent CED of HBSS and irradiation (Fig. 14).

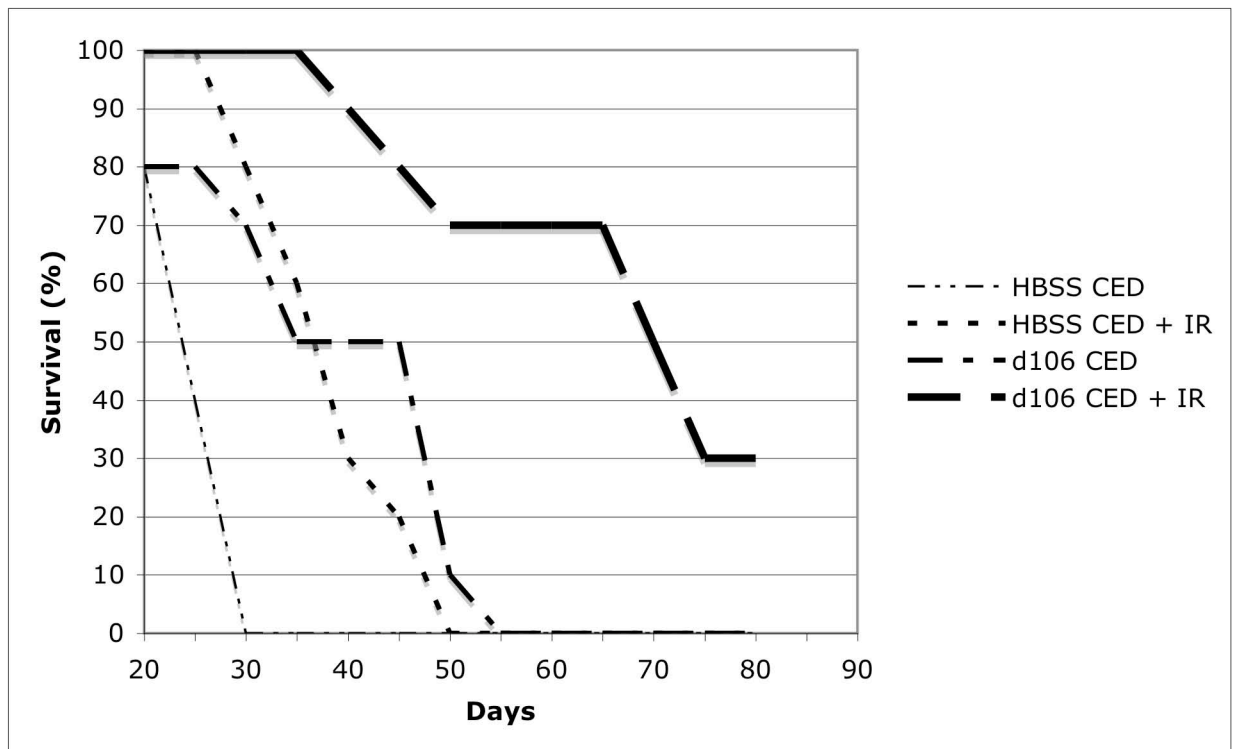


Figure 17. Kaplan-Meier survival curves of athymic nude mice after intracranial implantation of U87-MG cells and treatment by stereotactic CED of d106 or HBSS and irradiation (0 and 10 Gy). Control animals were mice that underwent CED of HBSS and did not receive ionizing radiation. Statistical significance, $P < 0.001$ by log-rank method of CED of d106 and irradiation compared to CED HBSS and irradiation ($n=10$ per group). Animals surviving 80 days post-tumor implantation were sacrificed.

Partial regression of xenograft was found in all three animals randomly sacrificed day 12 post tumor implantation after undergoing d106 CED and irradiation (Fig. 15A; Table 2). Complete tumor regression was found in three of six animals randomly sacrificed on days 15 and 17 post-tumor induction, which underwent d106 CED and irradiation (Figs. 13D and 15B; Table 2). Partial regression of tumor was found in the other three animals.

Table 2.

Intra-tumoral GFP expression days 7/9 after d106 CED (%)	Partial tumor regression day 12 after d106 CED + IR (%)	Complete tumor regression days 15/17 after d106 CED + IR (%)
9/12 (75)	3/3 (100)	3/6 (50)

Table 2. Summary of U87-MG xenograft infection rate and treatment response in animals that underwent d106 CED and whole-brain irradiation that were randomly sacrificed. GFP xenograft infection was determined in animals from treatment groups 3 and 4 on days 7 and 9 post tumor implantation. Treatment response was determined in treatment group 4 on days 12, 15, and 17 post tumor implantation.

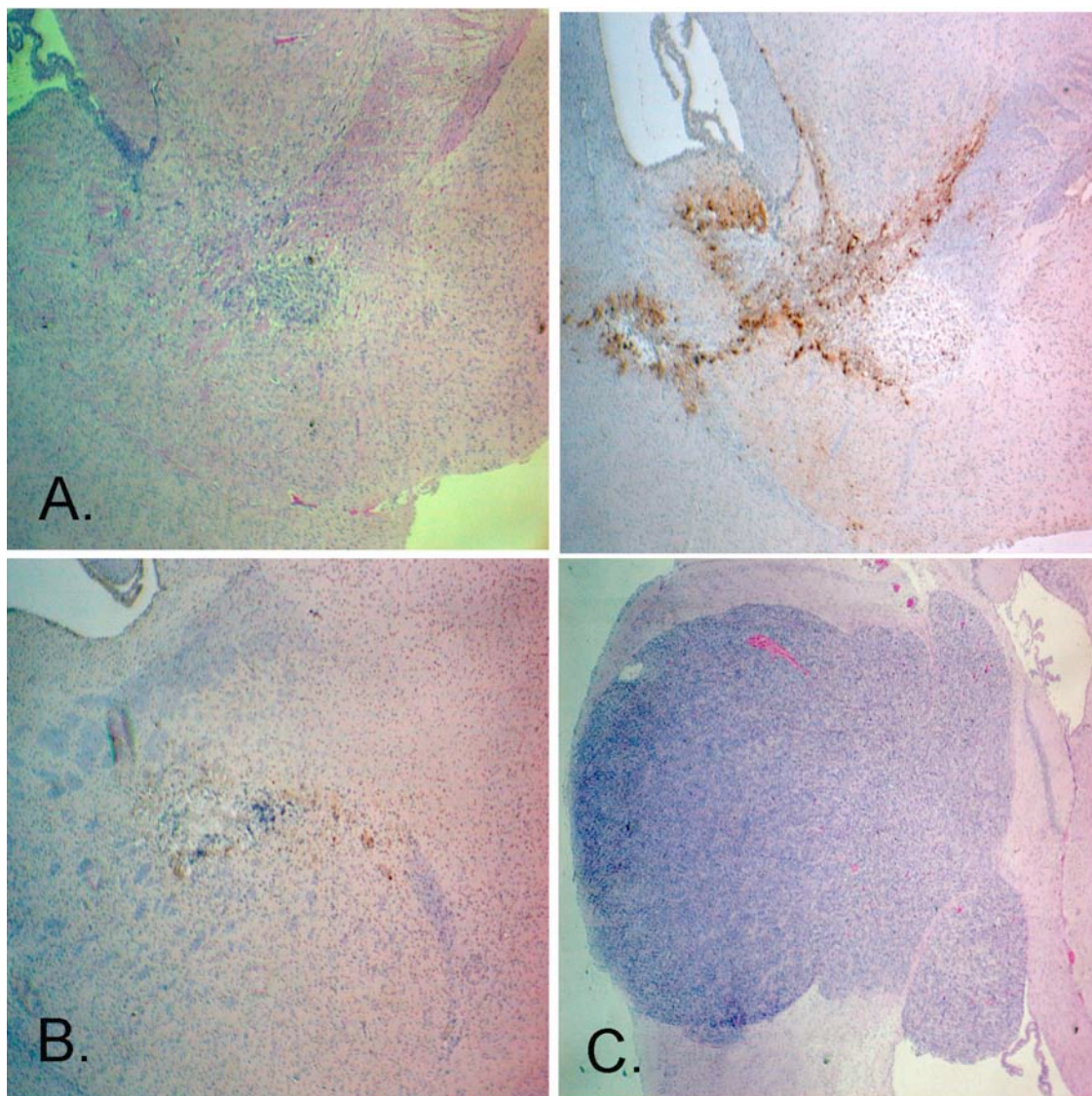


Figure 18. Photomicrographs of brain sections revealing antitumor efficacy of stereotactic CED of d106 in combination with ionizing radiation (10 Gy) in athymic nude mice implanted with U87-MG xenografts. Magnification, 40X. A, Hematoxylin/eosin- (*left*) and GFP-stained (*right*) sections day 12 after tumor implantation and 7 days after d106 CED showing regression of xenograft. B, GFP-stained section revealing complete tumor regression on day 17 after tumor implantation. C, Hematoxylin/eosin-stained section day 17 after tumor implantation in animal that underwent intracerebral CED of HBSS and irradiation showing a large tumor.

5.5. Discussion

Radiation therapy remains the sole agent that increases the survival of patients with GBM but provides modest benefit (191, 330, 331). Combining the effects of ionizing radiation and HSV-1 in the therapy of malignant gliomas has been reported in multiple studies (4, 30, 205) and is currently being developed into a human clinical protocol (204). Both oncolytic and replication-

defective HSV-1 constructs have been used with ionizing radiation. HSV replication and tumor kill is increased with oncolytic viruses utilizing large fractions of IR (20 and 25 Gy) (4, 30). In the case of replication-defective viruses, greater animal survival has been shown with the combination of radiosurgery (margin dose of 15 Gy; center dose of 21.4 Gy) and HSV-1 constructs that express the HSV-1 genes, ICP0 and tk, in addition to multiple transgenes (244, 245). In all these studies, delivery of HSV-1 is by stereotactic intratumoral manual injection resulting in suboptimal delivery of virus to tumor cells.

Our group has recently shown that the HSV-1 immediate-early protein, ICP0, naturally inhibits the repair of DNA double-strand breaks after IR treatment of GBM cells leading to decreased cell survival and induction of apoptosis *in vitro* (126). ICP0 has many effects on cell metabolism and has been proposed to promote lytic HSV infections by destabilizing cellular proteins that inhibit the lytic viral life cycle (127). ICP0 has been shown by our group to inhibit the circularization of HSV-1 genomes and promote lytic infection (156).

We present evidence showing intracerebral CED of the ICP0-producing HSV-1 mutant, d106, in combination with a single fraction of whole-brain irradiation (10 Gy), enhances the survival of animals implanted with U87-MG xenografts. The radiation dose used in our study is approximately half the dose used in other studies (4, 244). We believe optimal intracerebral HSV-1 delivery, by CED, allows for greater xenograft infection, transduction, and ultimate tumor cell demise by radiosensitivity enhancement. Tumor regression is felt to occur by ICP0 targeting of tumor cell repair of DNA double-strand breaks after irradiation and apoptosis induction. Our results show that intracerebral HSV-1 CED does lead to greater cell infection and viral spatial distribution than manual stereotactic injection in the normal mouse brain. In

addition, minimal viral reflux occurs along the catheter needle tract by CED, maximizing the viral dose available for cell infection.

Targeting the repair of DNA after irradiation in tumor cells and maximizing the delivery of HSV-1 to tumor cells and the surrounding brain where tumor-infiltration has occurred may form the basis of future clinical gene therapy strategies against malignant gliomas.

6. SUMMARY AND DISCUSSION

6.1. Summary of Results

The study presented here describes the effects of HSV-1 infection on cellular DNA repair after ionizing radiation exposure. Experiments were designed to identify the HSV IE protein, ICP0, as an inhibitor of DNA repair that enhances the radiosensitivity of experimental GBM. A mouse model was developed to optimize the delivery of HSV-1 to the brain and determine the intracerebral toxicity of the ICP0-producing mutant, d106. Intracerebral CED of the d106 was performed to determine the *in vivo* effects of ICP0 on human GBM xenografts in a mouse model.

In Chapter 3 it was determined that expression of ICP0 in human GBM cells inhibits the repair of DNA DSBs after IR treatment, decreasing the survival and proliferation of these cells in part by apoptosis induction. Infection of two radioresistant human GBM cell lines, U87-MG and T98, by the ICP0-producing virus, d106, followed by IR treatment, resulted in a significant dose-dependent decrease (5, 10, or 20 Gy) in cell proliferation and survival by the MTT assay after 6 days compared with cells receiving only IR. The greatest decrease in cell survival and proliferation occurred at the highest IR dose of 20 Gy ($p < 0.005$). (284). Infection of both cell lines with d106 resulted in cell toxicity as proliferation and cell viability decreased soon after infection ($P < 0.05$). Infection of both cell lines by the IE-deficient virus, d109, did not result in a dose-dependent decrease in cell proliferation and survival after IR treatment. Cell proliferation occurred in both cell lines after d109 infection in the absence of irradiation consistent with the documented lack of toxicity upon d109 infection (284). U87-MG cells infected with the ICP0-producing adenovirus, AdS.11E4(ICP0), showed a decrease in cell survival and proliferation

after irradiation in comparison to cells which were only irradiated ($P < 0.005$), confirming the effect of ICP0 on cell survival and proliferation in GBM cells. One-thousand fold less ICP0 is expressed from this construct relative to the level of expression from d106 (144). Clonogenic survival assays confirmed the cytotoxic effects of ICP0 and IR. The survival fraction was lowest among cells that were infected by d106 and irradiated compared to cells that solely were irradiated or infected with d106. Apoptosis was determined to be a mode of GBM cell death with ICP0 production and IR exposure. Levels of cleaved caspase-3 (p17) were detected in U87-MG cells that were infected by d106 and irradiated. Lower levels of cleaved caspase-3 were found in cells that were d106 infected but did not undergo irradiation. Both groups of cells that were mock infected and did or did not receive IR had minimal detectable levels of cleaved caspase-3. Carboxyfluorescein poly-caspase detection performed with flow cytometry revealed greater numbers of U87-MG cells undergoing apoptosis when infected with d106 and irradiated than when infected or irradiated alone. The percentage of d106-infected cells undergoing apoptosis were very similar 24 h after irradiation at 5, 10, or 20 Gy. Minimal apoptosis was detected in mock infected cells that did or did not undergo irradiation confirming the results of our Western analysis of cleaved caspase-3 levels. Degradation of DNA-PK_{cs} was shown in both GBM cell lines 6 to 24 hours postinfection by d106. Indirect immunofluorescence performed on both cell lines, preinfected with d106, revealed abundant and persistent γ -H2AX foci at 2, 6, and 24 h post irradiation. Cells infected by d106 and not irradiated had persistent γ -H2AX foci at 6 and 24 h post-irradiation. These results suggest linear HSV-1 genomes present after infection may be treated as DNA DSB with formation of γ -H2AX foci. The greater number of γ -H2AX foci and persistence of these foci after irradiation suggests ICP0 inhibits DNA repair in human glioblastoma cells.

In Chapter 4, optimal delivery of HSV-1 to the brain was investigated by CED in a mouse model. GFP transgene expression by the d106 virus, was used as a cell marker for cell infection in the brain. Strong, homogeneous GFP staining was found adjacent to the catheter needle tip, suggestive of uniform cell infection in the brain 2 days after CED. Extensive viral spatial distribution within the gray matter of the brain was found away from the needle tip. White matter tract distribution of HSV-1 was found distal to the needle tip and minimal infusate reflux occurred. Persistent GFP expression, or cell infection, was found up to 6 days after CED of d106. Neither heparin or dextran-sulfate co-infusion with d106 resulted in any increase in cell infection or viral distribution in comparison to d106 CED alone. Instead, heparin or dextran-sulfate co-infusion diminished cell infection and viral spread. Toxicity studies of intracerebral CED of d106 revealed a local inflammatory response occurring within 6 days of infusion that resolved 21 days after infusion. Local *in vivo* apoptosis was present on day 7 after d106 CED that was absent with Hanks' balanced salt solution CED. No animals showed any external signs of toxicity.

In Chapter 5, the use of d106 as a potential antiglioma viral vector was investigated in a mouse glioma model. Initial comparison of intracerebral HSV-1 delivery by manual stereotactic injection and CED in the normal mouse brain revealed greater cell infection and viral distribution after CED. Viral vector suspension reflux along the needle tract occurred after stereotactic manual injection while minimal reflux occurred with CED. The majority of human GBM (U87-MG) xenografts implanted in athymic nude mice were infected by the d106 virus 7 and 9 days post-tumor implantation. Persistent cellular transgene expression, or HSV-1 transduction, was found up to 12 days after d106 CED in cells within and surrounding the xenograft sites. Survival studies were performed on animals that underwent CED of HBSS or d106 and whole-brain

irradiation (0 or 10 Gy). The median survival for control animals that underwent CED of HBSS and no irradiation was 23 days. Those animals that underwent CED of d106 and were not irradiated had a median survival of 41 days. Animals that had HBSS CED and were irradiated (10 Gy) had a median survival of 39 days. Animals that underwent CED of d106 and whole-brain irradiation had a median survival of 68 days. Of these animals, 30% were alive at the 80 day survival mark post tumor implantation. Median survival was significantly increased ($P < 0.01$ by log-rank method) when animals underwent CED of d106 and subsequent whole-brain irradiation (10 Gy) in comparison to animals that underwent CED of HBSS and irradiation. Partial regression of xenograft was found in all three animals randomly sacrificed day 12 post tumor implantation after undergoing d106 CED and irradiation. Complete tumor regression was found in three of six animals randomly sacrificed on days 15 and 17 post tumor induction, which underwent d106 CED and irradiation. Partial regression of tumor was found in the other three animals.

6.2. Role of ICP0 in Cellular DNA Repair

ICP0 has many effects on cell metabolism and has been proposed to promote lytic HSV infections by destabilizing cellular proteins that inhibit the lytic viral life cycle (127). Recently, the concept of HSV genome circularization as a requirement for viral DNA replication has been challenged. Genome circularization does not occur in productive infection but instead may occur during establishment of latency as a function of ICP0 expression (156, 288). ICP0 appears to prevent the formation of circular HSV-1 DNA molecules. HSV-1 mutants defective for ICP0 expression result in the predominance of circular HSV-1 genomes during infection. The finding that ICP0 appears to prevent the formation of circular molecules may explain why replication of

HSV-1 is greatly reduced in HSV-1 mutants defective in ICP0 at low multiplicities of infection (283, 309). Thus, linear HSV molecules rather than circles might serve as the initial templates for HSV-1 replication.

The presence of linear HSV-1 genomes in the nucleus, early in infection, induces a cellular response to DNA damage with recruitment of recombination and repair proteins to HSV-1 DNA (156, 193, 346). Activation and exploitation of a cellular DNA damage response has been shown to aid viral replication. The ends of the HSV-1 linear genomes may be treated as DNA DSBs with cellular repair processes activated to promote circularization of the viral genomes and a viral latent state. ICP0 inhibition of genome circularization by cellular DNA repair disruption may occur by ND10 disruption and degradation of DNA-PK_{CS}. ND10 domains have been shown to contain host recombination/repair proteins (235) and participate in the cell's response to DNA damage (41). ND10 domains are redistributed in response to DNA damage (41), and it has been proposed that ND10 may store and release proteins in response to viral infection and DNA damage (235). Degradation of DNA-PK_{CS} and inhibition of NHEJ, the main DNA DSB repair pathway in mammalian cells, may further aid viral replication and production of viral progeny.

The combination of IR-induced DNA DSBs and cell ICP0 production triggers cell death in human GBM cells in part by apoptosis induction. The mechanism for cell death appears to be the overwhelming persistence of DNA DSBs that go unrepaired due to DNA repair inhibition by ICP0. It is well known, that one unrepaired DSB can be sufficient to kill a cell if it inactivates an essential gene or triggers apoptosis (274).

6.3. Therapy of Human GBM with d106

Phase I clinical studies in humans with GBM tumors have demonstrated modest antitumor effect with HSV-1 oncolytic viruses (134, 206, 271). HSV-1 delivery has been by manual stereotactic injection into the brain. Improving the efficacy of HSV-1 therapy for malignant gliomas requires multimodal therapy and a change in the delivery of virus to tumor cells in the brain. Prior studies have shown an enhanced tumoricidal effect of oncolytic, HSV-1 mutants when combined with IR (30, 205).

In this study, the replication-defective mutant virus, d106, has shown antitumor effects when combined with IR both *in vitro* and *in vivo*. The tumoricidal property of d106 is due to the effects of ICP0, as it does not express any other IE proteins. One important effect of ICP0 may be the inhibition of DNA repair in cells. Combining IR and d106 infection may overwhelm the cell's ability to repair DNA damage, leading the cell to death.

The toxicity of intracerebral d106 infusion in the normal mouse brain has been confirmed in this study. An inflammatory response occurs after d106 delivery to the brain and normal cells undergo apoptosis within the vicinity of d106 infusion. The inflammatory response in the brain resolves as persistent infection is attenuated due to the non-replicative properties of d106.

The delivery of any HSV-1 mutant into the brain for therapy against GBM needs to be critically evaluated. Stereotactic manual injection does not allow for widespread and uniform distribution of HSV-1 within the brain and tumor tissue. Instead, reflux of viral dose occurs along the needle tract that impacts on the dose of virus that reaches tumor. In this study, CED allows for greater cell infection and viral distribution in the normal mouse brain in comparison to stereotactic manual injection. In addition, CED maximizes the local delivery of HSV-1 to human GBM xenografts implanted within the mouse brain.

The effective regression of intracranial glioblastoma xenografts after CED of d106 in combination with whole-brain irradiation may be explained by greater cell infection by convection and uniform irradiation of xenografts. The possibility exists that a “bystander effect” from the ICP0 protein may contribute to xenograft regression since only a fraction of tumor cells appear virally infected after d106 CED. In addition, an inflammatory response generated by d106 viral particles and virally infected cells may contribute to xenograft regression even in the absence of a T-cell mediated immune response in athymic nude mice.

Targeting the repair of DNA after irradiation in tumor cells and maximizing the delivery of HSV-1 to tumor cells and the surrounding brain where tumor-infiltration has occurred may form the basis of future clinical gene therapy strategies against malignant gliomas.

6.4. Future Studies

Inhibition of DNA repair by the HSV protein, ICP0, in combination with IR and chemotherapy (chemoradiation), may serve as a therapeutic model for malignant glioma. Targeting the effects of ICP0 within tumor tissue and limiting the surrounding toxicity in the brain will be the focus of future studies. New generation HSV-1 mutants will be produced that selectively express ICP0. Synthetic hypoxia-response elements (HREs) and chemotherapy/IR-sensitive enhancers (CArG elements) will be used to modify the native HSV-1 ICP0 promoter to create replication-defective viruses that selectively express ICP0 with IR, hypoxia, and/or chemotherapy. Transcriptional targeting of ICP0 by IR, hypoxia, and/or chemotherapy will be performed *in vitro* and *in vivo* after convection-enhanced HSV delivery.

A human clinical trial involving the use of the d106 virus in combination with chemoradiation will be pursued in the therapy of GBM. A Phase Ib trial will initially be

performed to determine human intracerebral toxicity after CED of a high titer of d106 (10^9 pfu) in patients with recurrent GBM tumors who have failed standard treatments. At the time of surgical resection, 3 to 4 CED catheters will be placed in the periphery of the tumor bed. Patients will be randomized to undergo CED of d106 or HBSS within 48 hours after catheter placement. CED of virus or HBSS will be performed over 8 hours. Patients will then undergo a conformal radiotherapy boost (20-30 Gy) to the region of brain with tumor within 24 hours after CED. Patients will have serial MRI scans of the brain every 2-4 weeks to determine intracerebral toxicity and tumor response. If safety and efficacy can be established in recurrent GBM patients who undergo d106 CED and a radiotherapy boost, then a Phase II clinical study will be performed assessing the efficacy of d106 CED in combination with chemoradiation in patients with newly diagnosed GBM.

BIBLIOGRAPHY

BIBLIOGRAPHY

1. **Ackermann, M., D. K. Braun, L. Pereira, and B. Roizman.** 1984. Characterization of herpes simplex virus 1 alpha proteins 0, 4, and 27 with monoclonal antibodies. *J Virol* **52**:108-18.
2. **Advani, S. J., R. Brandimarti, R. R. Weichselbaum, and B. Roizman.** 2000. The disappearance of cyclins A and B and the increase in activity of the G(2)/M-phase cellular kinase cdc2 in herpes simplex virus 1-infected cells require expression of the alpha22/U(S)1.5 and U(L)13 viral genes. *J Virol* **74**:8-15.
3. **Advani, S. J., R. Hagglund, R. R. Weichselbaum, and B. Roizman.** 2001. Posttranslational processing of infected cell proteins 0 and 4 of herpes simplex virus 1 is sequential and reflects the subcellular compartment in which the proteins localize. *J Virol* **75**:7904-12.
4. **Advani, S. J., G. S. Sibley, P. Y. Song, D. E. Hallahan, Y. Kataoka, B. Roizman, and R. R. Weichselbaum.** 1998. Enhancement of replication of genetically engineered herpes simplex viruses by ionizing radiation: a new paradigm for destruction of therapeutically intractable tumors. *Gene Ther* **5**:160-5.
5. **Advani, S. J., R. R. Weichselbaum, and B. Roizman.** 2003. Herpes simplex virus 1 activates cdc2 to recruit topoisomerase II alpha for post-DNA synthesis expression of late genes. *Proc Natl Acad Sci U S A* **100**:4825-30.
6. **Advani, S. J., R. R. Weichselbaum, and B. Roizman.** 2000. The role of cdc2 in the expression of herpes simplex virus genes. *Proc Natl Acad Sci U S A* **97**:10996-1001.
7. **Aleman, R., C. Gomez-Manzano, C. Balague, W. K. Yung, D. T. Curiel, A. P. Kyritsis, and J. Fueyo.** 1999. Gene therapy for gliomas: molecular targets, adenoviral vectors, and oncolytic adenoviruses. *Exp Cell Res* **252**:1-12.
8. **Ammirati, M., J. H. Galicich, E. Arbit, and Y. Liao.** 1987. Reoperation in the treatment of recurrent intracranial malignant gliomas. *Neurosurgery* **21**:607-14.
9. **Andegeko, Y., L. Moyal, L. Mittelman, I. Tsarfaty, Y. Shiloh, and G. Rotman.** 2001. Nuclear retention of ATM at sites of DNA double strand breaks. *J Biol Chem* **276**:38224-30.
10. **Anderson, C. W.** 1993. DNA damage and the DNA-activated protein kinase. *Trends Biochem Sci* **18**:433-7.
11. **Ascoli, C. A., and G. G. Maul.** 1991. Identification of a novel nuclear domain. *J Cell Biol* **112**:785-95.

12. **Bakkenist, C. J., and M. B. Kastan.** 2003. DNA damage activates ATM through intermolecular autophosphorylation and dimer dissociation. *Nature* **421**:499-506.
13. **Bankiewicz, K. S., J. L. Eberling, M. Kohutnicka, W. Jagust, P. Pivrotto, J. Bringas, J. Cunningham, T. F. Budinger, and J. Harvey-White.** 2000. Convection-enhanced delivery of AAV vector in parkinsonian monkeys; in vivo detection of gene expression and restoration of dopaminergic function using pro-drug approach. *Exp Neurol* **164**:2-14.
14. **Barker, F. G., 2nd, M. L. Simmons, S. M. Chang, M. D. Prados, D. A. Larson, P. K. Sneed, W. M. Wara, M. S. Berger, P. Chen, M. A. Israel, and K. D. Aldape.** 2001. EGFR overexpression and radiation response in glioblastoma multiforme. *Int J Radiat Oncol Biol Phys* **51**:410-8.
15. **Barlow, C., K. D. Brown, C. X. Deng, D. A. Tagle, and A. Wynshaw-Boris.** 1997. Atm selectively regulates distinct p53-dependent cell-cycle checkpoint and apoptotic pathways. *Nat Genet* **17**:453-6.
16. **Barr, S. M., C. G. Leung, E. E. Chang, and K. A. Cimprich.** 2003. ATR kinase activity regulates the intranuclear translocation of ATR and RPA following ionizing radiation. *Curr Biol* **13**:1047-51.
17. **Bataille, D., and A. Epstein.** 1994. Herpes simplex virus replicative concatemers contain L components in inverted orientation. *Virology* **203**:384-8.
18. **Batterson, W., and B. Roizman.** 1983. Characterization of the herpes simplex virion-associated factor responsible for the induction of alpha genes. *J Virol* **46**:371-7.
19. **Beard, P., S. Faber, K. W. Wilcox, and L. I. Pizer.** 1986. Herpes simplex virus immediate early infected-cell polypeptide 4 binds to DNA and promotes transcription. *Proc Natl Acad Sci U S A* **83**:4016-20.
20. **Becker, Y., H. Dym, and I. Sarov.** 1968. Herpes simplex virus DNA. *Virology* **36**:184-92.
21. **Becker-Catania, S. G., and R. A. Gatti.** 2001. Ataxia-telangiectasia. *Adv Exp Med Biol* **495**:191-8.
22. **Beltinger, C., S. Fulda, T. Kammertoens, E. Meyer, W. Uckert, and K. M. Debatin.** 1999. Herpes simplex virus thymidine kinase/ganciclovir-induced apoptosis involves ligand-independent death receptor aggregation and activation of caspases. *Proc Natl Acad Sci U S A* **96**:8699-704.
23. **Ben-Porat, T., and S. A. Tokazewski.** 1977. Replication of herpesvirus DNA. II. Sedimentation characteristics of newly synthesized DNA. *Virology* **79**:292-301.

24. **Betz, A. L., P. Shakui, and B. L. Davidson.** 1998. Gene transfer to rodent brain with recombinant adenoviral vectors: effects of infusion parameters, infectious titer, and virus concentration on transduction volume. *Exp Neurol* **150**:136-42.
25. **Black, P. M.** 1991. Brain tumors. Part 1. *N Engl J Med* **324**:1471-6.
26. **Bobo, R. H., D. W. Laske, A. Akbasak, P. F. Morrison, R. L. Dedrick, and E. H. Oldfield.** 1994. Convection-enhanced delivery of macromolecules in the brain. *Proc Natl Acad Sci U S A* **91**:2076-80.
27. **Boris-Lawrie, K., and H. M. Temin.** 1994. The retroviral vector. Replication cycle and safety considerations for retrovirus-mediated gene therapy. *Ann N Y Acad Sci* **716**:59-70; discussion 71.
28. **Boutell, C., S. Sadis, and R. D. Everett.** 2002. Herpes simplex virus type 1 immediate-early protein ICP0 and its isolated RING finger domain act as ubiquitin E3 ligases in vitro. *J Virol* **76**:841-50.
29. **Brada, M., K. Hoang-Xuan, R. Rampling, P. Y. Dietrich, L. Y. Dirix, D. Macdonald, J. J. Heimans, B. A. Zonnenberg, J. M. Bravo-Marques, R. Henriksson, R. Stupp, N. Yue, J. Bruner, M. Dugan, S. Rao, and S. Zaknoen.** 2001. Multicenter phase II trial of temozolomide in patients with glioblastoma multiforme at first relapse. *Ann Oncol* **12**:259-66.
30. **Bradley, J. D., Y. Kataoka, S. Advani, S. M. Chung, R. B. Arani, G. Y. Gillespie, R. J. Whitley, J. M. Markert, B. Roizman, and R. R. Weichselbaum.** 1999. Ionizing radiation improves survival in mice bearing intracranial high-grade gliomas injected with genetically modified herpes simplex virus. *Clin Cancer Res* **5**:1517-22.
31. **Bredel, M., I. F. Pollack, R. L. Hamilton, and C. D. James.** 1999. Epidermal growth factor receptor expression and gene amplification in high-grade non-brainstem gliomas of childhood. *Clin Cancer Res* **5**:1786-92.
32. **Brehm, M., L. A. Samaniego, R. H. Bonneau, N. A. DeLuca, and S. S. Tevethia.** 1999. Immunogenicity of herpes simplex virus type 1 mutants containing deletions in one or more alpha-genes: ICP4, ICP27, ICP22, and ICP0. *Virology* **256**:258-69.
33. **Brehm, M. A., R. H. Bonneau, D. M. Knipe, and S. S. Tevethia.** 1997. Immunization with a replication-deficient mutant of herpes simplex virus type 1 (HSV-1) induces a CD8+ cytotoxic T-lymphocyte response and confers a level of protection comparable to that of wild-type HSV-1. *J Virol* **71**:3534-44.
34. **Brem, H., M. S. Mahaley, Jr., N. A. Vick, K. L. Black, S. C. Schold, Jr., P. C. Burger, A. H. Friedman, I. S. Ciric, T. W. Eller, J. W. Cozzens, and et al.** 1991. Interstitial chemotherapy with drug polymer implants for the treatment of recurrent gliomas. *J Neurosurg* **74**:441-6.

35. **Brem, H., S. Piantadosi, P. C. Burger, M. Walker, R. Selker, N. A. Vick, K. Black, M. Sisti, S. Brem, G. Mohr, and et al.** 1995. Placebo-controlled trial of safety and efficacy of intraoperative controlled delivery by biodegradable polymers of chemotherapy for recurrent gliomas. The Polymer-brain Tumor Treatment Group. *Lancet* **345**:1008-12.
36. **Burger, P. C., and S. B. Green.** 1987. Patient age, histologic features, and length of survival in patients with glioblastoma multiforme. *Cancer* **59**:1617-25.
37. **Burger, P. C., E. R. Heinz, T. Shibata, and P. Kleihues.** 1988. Topographic anatomy and CT correlations in the untreated glioblastoma multiforme. *J Neurosurg* **68**:698-704.
38. **Burma, S., B. P. Chen, M. Murphy, A. Kurimasa, and D. J. Chen.** 2001. ATM phosphorylates histone H2AX in response to DNA double-strand breaks. *J Biol Chem* **276**:42462-7.
39. **Burma, S., A. Kurimasa, G. Xie, Y. Taya, R. Araki, M. Abe, H. A. Crissman, H. Ouyang, G. C. Li, and D. J. Chen.** 1999. DNA-dependent protein kinase-independent activation of p53 in response to DNA damage. *J Biol Chem* **274**:17139-43.
40. **Cai, W., T. L. Astor, L. M. Liptak, C. Cho, D. M. Coen, and P. A. Schaffer.** 1993. The herpes simplex virus type 1 regulatory protein ICP0 enhances virus replication during acute infection and reactivation from latency. *J Virol* **67**:7501-12.
41. **Carbone, R., M. Pearson, S. Minucci, and P. G. Pelicci.** 2002. PML NBs associate with the hMre11 complex and p53 at sites of irradiation induced DNA damage. *Oncogene* **21**:1633-40.
42. **Carrozza, M. J., and N. A. DeLuca.** 1996. Interaction of the viral activator protein ICP4 with TFIID through TAF250. *Mol Cell Biol* **16**:3085-93.
43. **Carter, K. L., and B. Roizman.** 1996. Alternatively spliced mRNAs predicted to yield frame-shift proteins and stable intron 1 RNAs of the herpes simplex virus 1 regulatory gene alpha 0 accumulate in the cytoplasm of infected cells. *Proc Natl Acad Sci U S A* **93**:12535-40.
44. **Chan, D. W., B. P. Chen, S. Prithivirajsingh, A. Kurimasa, M. D. Story, J. Qin, and D. J. Chen.** 2002. Autophosphorylation of the DNA-dependent protein kinase catalytic subunit is required for rejoining of DNA double-strand breaks. *Genes Dev* **16**:2333-8.
45. **Chang, C., K. A. Biedermann, M. Mezzina, and J. M. Brown.** 1993. Characterization of the DNA double strand break repair defect in scid mice. *Cancer Res* **53**:1244-8.
46. **Chelbi-Alix, M. K., and H. de The.** 1999. Herpes virus induced proteasome-dependent degradation of the nuclear bodies-associated PML and Sp100 proteins. *Oncogene* **18**:935-41.

47. **Chen, J., and S. Silverstein.** 1992. Herpes simplex viruses with mutations in the gene encoding ICP0 are defective in gene expression. *J Virol* **66**:2916-27.
48. **Chiocca, E. A.** 2002. Oncolytic viruses. *Nat Rev Cancer* **2**:938-50.
49. **Chou, J., E. R. Kern, R. J. Whitley, and B. Roizman.** 1990. Mapping of herpes simplex virus-1 neurovirulence to gamma 134.5, a gene nonessential for growth in culture. *Science* **250**:1262-6.
50. **Chou, J., and B. Roizman.** 1994. Herpes simplex virus 1 gamma(1)34.5 gene function, which blocks the host response to infection, maps in the homologous domain of the genes expressed during growth arrest and DNA damage. *Proc Natl Acad Sci U S A* **91**:5247-51.
51. **Chou, J., and B. Roizman.** 1990. The herpes simplex virus 1 gene for ICP34.5, which maps in inverted repeats, is conserved in several limited-passage isolates but not in strain 17syn+. *J Virol* **64**:1014-20.
52. **Clements, G. B., and N. D. Stow.** 1989. A herpes simplex virus type 1 mutant containing a deletion within immediate early gene 1 is latency-competent in mice. *J Gen Virol* **70 (Pt 9)**:2501-6.
53. **Clements, J. B., R. J. Watson, and N. M. Wilkie.** 1977. Temporal regulation of herpes simplex virus type 1 transcription: location of transcripts on the viral genome. *Cell* **12**:275-85.
54. **Coen, D. M., M. Kosz-Vnenchak, J. G. Jacobson, D. A. Leib, C. L. Bogard, P. A. Schaffer, K. L. Tyler, and D. M. Knipe.** 1989. Thymidine kinase-negative herpes simplex virus mutants establish latency in mouse trigeminal ganglia but do not reactivate. *Proc Natl Acad Sci U S A* **86**:4736-40.
55. **Cook, M. L., and J. G. Stevens.** 1973. Pathogenesis of herpetic neuritis and ganglionitis in mice: evidence for intra-axonal transport of infection. *Infect Immun* **7**:272-88.
56. **Cook, W. J., B. Gu, N. A. DeLuca, E. B. Moynihan, and D. M. Coen.** 1995. Induction of transcription by a viral regulatory protein depends on the relative strengths of functional TATA boxes. *Mol Cell Biol* **15**:4998-5006.
57. **Costanzo, F., G. Campadelli-Fiume, L. Foa-Tomasi, and E. Cassai.** 1977. Evidence that herpes simplex virus DNA is transcribed by cellular RNA polymerase B. *J Virol* **21**:996-1001.
58. **Critchlow, S. E., and S. P. Jackson.** 1998. DNA end-joining: from yeast to man. *Trends Biochem Sci* **23**:394-8.
59. **Croen, K. D., J. M. Ostrove, L. J. Dragovic, J. E. Smialek, and S. E. Straus.** 1987. Latent herpes simplex virus in human trigeminal ganglia. Detection of an immediate early gene "anti-sense" transcript by in situ hybridization. *N Engl J Med* **317**:1427-32.

60. **Croteau, D., S. Walbridge, P. F. Morrison, j. a. Butman, a. o. Vortmeyer, d. Johnson, E. H. Oldfield, and R. R. Lonser.** 2005. Real-time in vivo imaging of the convective distribution of a low-molecular-weight tracer. *J neurosurg* **102**:90-97.
61. **Cunningham, J., Y. Oiwa, D. Nagy, G. Podsakoff, P. Colosi, and K. S. Bankiewicz.** 2000. Distribution of AAV-TK following intracranial convection-enhanced delivery into rats. *Cell Transplant* **9**:585-94.
62. **D'Amours, D., and S. P. Jackson.** 2002. The Mre11 complex: at the crossroads of dna repair and checkpoint signalling. *Nat Rev Mol Cell Biol* **3**:317-27.
63. **Dai, C., and E. Holland.** 2005. *Glioblastoma Multiforme*. Jones and Bartlett, Sudbury, MA.
64. **Davis, F. G., B. J. McCarthy, and M. S. Berger.** 1999. Centralized databases available for describing primary brain tumor incidence, survival, and treatment: Central Brain Tumor Registry of the United States; Surveillance, Epidemiology, and End Results; and National Cancer Data Base. *Neuro-oncol* **1**:205-11.
65. **Davis, L. W.** 1989. Malignant glioma--a nemesis which requires clinical and basic investigation in radiation oncology. *Int J Radiat Oncol Biol Phys* **16**:1355-65.
66. **de Bruyn Kops, A., and D. M. Knipe.** 1988. Formation of DNA replication structures in herpes virus-infected cells requires a viral DNA binding protein. *Cell* **55**:857-68.
67. **de Bruyn Kops, A., S. L. Uprichard, M. Chen, and D. M. Knipe.** 1998. Comparison of the intranuclear distributions of herpes simplex virus proteins involved in various viral functions. *Virology* **252**:162-78.
68. **DeLuca, N., D. J. Bzik, V. C. Bond, S. Person, and W. Snipes.** 1982. Nucleotide sequences of herpes simplex virus type 1 (HSV-1) affecting virus entry, cell fusion, and production of glycoprotein gb (VP7). *Virology* **122**:411-23.
69. **DeLuca, N. A., A. M. McCarthy, and P. A. Schaffer.** 1985. Isolation and characterization of deletion mutants of herpes simplex virus type 1 in the gene encoding immediate-early regulatory protein ICP4. *J Virol* **56**:558-70.
70. **DeLuca, N. A., and P. A. Schaffer.** 1985. Activation of immediate-early, early, and late promoters by temperature-sensitive and wild-type forms of herpes simplex virus type 1 protein ICP4. *Mol Cell Biol* **5**:1997-2008.
71. **DeLuca, N. A., and P. A. Schaffer.** 1988. Physical and functional domains of the herpes simplex virus transcriptional regulatory protein ICP4. *J Virol* **62**:732-43.
72. **Desai, P. J., P. A. Schaffer, and A. C. Minson.** 1988. Excretion of non-infectious virus particles lacking glycoprotein H by a temperature-sensitive mutant of herpes simplex virus type 1: evidence that gH is essential for virion infectivity. *J Gen Virol* **69 (Pt 6)**:1147-56.

73. **Deshmane, S. L., and N. W. Fraser.** 1989. During latency, herpes simplex virus type 1 DNA is associated with nucleosomes in a chromatin structure. *J Virol* **63**:943-7.
74. **Dikomey, E., J. Dahm-Daphi, I. Brammer, R. Martensen, and B. Kaina.** 1998. Correlation between cellular radiosensitivity and non-repaired double-strand breaks studied in nine mammalian cell lines. *Int J Radiat Biol* **73**:269-78.
75. **Ding, H., L. Roncari, P. Shannon, X. Wu, N. Lau, J. Karaskova, D. H. Gutmann, J. A. Squire, A. Nagy, and A. Guha.** 2001. Astrocyte-specific expression of activated p21-ras results in malignant astrocytoma formation in a transgenic mouse model of human gliomas. *Cancer Res* **61**:3826-36.
76. **Dixon, R. A., and P. A. Schaffer.** 1980. Fine-structure mapping and functional analysis of temperature-sensitive mutants in the gene encoding the herpes simplex virus type 1 immediate early protein VP175. *J Virol* **36**:189-203.
77. **Dropcho, E. J., S. S. Rosenfeld, J. Vitek, B. L. Guthrie, and R. B. Morawetz.** 1998. Phase II study of intracarotid or selective intracerebral infusion of cisplatin for treatment of recurrent anaplastic gliomas. *J Neurooncol* **36**:191-8.
78. **Dutch, R. E., V. Bianchi, and I. R. Lehman.** 1995. Herpes simplex virus type 1 DNA replication is specifically required for high-frequency homologous recombination between repeated sequences. *J Virol* **69**:3084-9.
79. **Dutch, R. E., R. C. Bruckner, E. S. Mocarski, and I. R. Lehman.** 1992. Herpes simplex virus type 1 recombination: role of DNA replication and viral α sequences. *J Virol* **66**:277-85.
80. **Dyer, A. P., B. W. Banfield, D. Martindale, D. M. Spanner, and F. Tufaro.** 1997. Dextran sulfate can act as an artificial receptor to mediate a type-specific herpes simplex virus infection via glycoprotein B. *J Virol* **71**:191-8.
81. **Eidson, K. M., W. E. Hobbs, B. J. Manning, P. Carlson, and N. A. DeLuca.** 2002. Expression of herpes simplex virus ICP0 inhibits the induction of interferon-stimulated genes by viral infection. *J Virol* **76**:2180-91.
82. **Elion, G. B.** 1993. Acyclovir: discovery, mechanism of action, and selectivity. *J Med Virol Suppl* **1**:2-6.
83. **Ellis, C. A., M. D. Vos, H. Howell, T. Vallecorsa, D. W. Fults, and G. J. Clark.** 2002. Rig is a novel Ras-related protein and potential neural tumor suppressor. *Proc Natl Acad Sci U S A* **99**:9876-81.
84. **Evans, S. M., K. D. Judy, I. Dunphy, W. T. Jenkins, P. T. Nelson, R. Collins, E. P. Wileyto, K. Jenkins, S. M. Hahn, C. W. Stevens, A. R. Judkins, P. Phillips, B. Geoerger, and C. J. Koch.** 2004. Comparative measurements of hypoxia in human brain tumors using needle electrodes and EF5 binding. *Cancer Res* **64**:1886-92.

85. **Everett, R., P. O'Hare, D. O'Rourke, P. Barlow, and A. Orr.** 1995. Point mutations in the herpes simplex virus type 1 Vmw110 RING finger helix affect activation of gene expression, viral growth, and interaction with PML-containing nuclear structures. *J Virol* **69**:7339-44.
86. **Everett, R. D.** 1984. A detailed analysis of an HSV-1 early promoter: sequences involved in trans-activation by viral immediate-early gene products are not early-gene specific. *Nucleic Acids Res* **12**:3037-56.
87. **Everett, R. D.** 2000. ICP0, a regulator of herpes simplex virus during lytic and latent infection. *Bioessays* **22**:761-70.
88. **Everett, R. D.** 1984. Trans activation of transcription by herpes virus products: requirement for two HSV-1 immediate-early polypeptides for maximum activity. *Embo J* **3**:3135-41.
89. **Everett, R. D., P. Barlow, A. Milner, B. Luisi, A. Orr, G. Hope, and D. Lyon.** 1993. A novel arrangement of zinc-binding residues and secondary structure in the C3HC4 motif of an alpha herpes virus protein family. *J Mol Biol* **234**:1038-47.
90. **Everett, R. D., A. Cross, and A. Orr.** 1993. A truncated form of herpes simplex virus type 1 immediate-early protein Vmw110 is expressed in a cell type dependent manner. *Virology* **197**:751-6.
91. **Everett, R. D., W. C. Earnshaw, J. Findlay, and P. Lomonte.** 1999. Specific destruction of kinetochore protein CENP-C and disruption of cell division by herpes simplex virus immediate-early protein Vmw110. *Embo J* **18**:1526-38.
92. **Everett, R. D., W. C. Earnshaw, A. F. Pluta, T. Sternsdorf, A. M. Ainsztein, M. Carmena, S. Ruchaud, W. L. Hsu, and A. Orr.** 1999. A dynamic connection between centromeres and ND10 proteins. *J Cell Sci* **112 (Pt 20)**:3443-54.
93. **Everett, R. D., P. Freemont, H. Saitoh, M. Dasso, A. Orr, M. Kathoria, and J. Parkinson.** 1998. The disruption of ND10 during herpes simplex virus infection correlates with the Vmw110- and proteasome-dependent loss of several PML isoforms. *J Virol* **72**:6581-91.
94. **Everett, R. D., and G. G. Maul.** 1994. HSV-1 IE protein Vmw110 causes redistribution of PML. *Embo J* **13**:5062-9.
95. **Everett, R. D., M. Meredith, and A. Orr.** 1999. The ability of herpes simplex virus type 1 immediate-early protein Vmw110 to bind to a ubiquitin-specific protease contributes to its roles in the activation of gene expression and stimulation of virus replication. *J Virol* **73**:417-26.
96. **Everett, R. D., A. Orr, and M. Elliott.** 1991. High level expression and purification of herpes simplex virus type 1 immediate early polypeptide Vmw110. *Nucleic Acids Res* **19**:6155-61.

97. **Ezzeddine, Z. D., R. L. Martuza, D. Platika, M. P. Short, A. Malick, B. Choi, and X. O. Breakefield.** 1991. Selective killing of glioma cells in culture and in vivo by retrovirus transfer of the herpes simplex virus thymidine kinase gene. *New Biol* **3**:608-14.
98. **Flanagan, W. M., A. G. Papavassiliou, M. Rice, L. B. Hecht, S. Silverstein, and E. K. Wagner.** 1991. Analysis of the herpes simplex virus type 1 promoter controlling the expression of UL38, a true late gene involved in capsid assembly. *J Virol* **65**:769-86.
99. **Flint, J., and T. Shenk.** 1997. Viral transactivating proteins. *Annu Rev Genet* **31**:177-212.
100. **Flint, S. J., L. W. Enquist, V. R. Racaniello, and A. M. Skalka.** 2004. Principles of Virology, Second ed. ASM Press, Washington D. C.
101. **Freeman, S. M., C. N. Abboud, K. A. Whartenby, C. H. Packman, D. S. Koeplin, F. L. Moolten, and G. N. Abraham.** 1993. The "bystander effect": tumor regression when a fraction of the tumor mass is genetically modified. *Cancer Res* **53**:5274-83.
102. **Freemont, P. S.** 1993. The RING finger. A novel protein sequence motif related to the zinc finger. *Ann N Y Acad Sci* **684**:174-92.
103. **Freemont, P. S., I. M. Hanson, and J. Trowsdale.** 1991. A novel cysteine-rich sequence motif. *Cell* **64**:483-4.
104. **Friedman, H. S., T. Kerby, and H. Calvert.** 2000. Temozolomide and treatment of malignant glioma. *Clin Cancer Res* **6**:2585-97.
105. **Friedman, H. S., R. E. McLendon, T. Kerby, M. Dugan, S. H. Bigner, A. J. Henry, D. M. Ashley, J. Krischer, S. Lovell, K. Rasheed, F. Marchev, A. J. Seman, I. Cokgor, J. Rich, E. Stewart, O. M. Colvin, J. M. Provenzale, D. D. Bigner, M. M. Haglund, A. H. Friedman, and P. L. Modrich.** 1998. DNA mismatch repair and O6-alkylguanine-DNA alkyltransferase analysis and response to Temodal in newly diagnosed malignant glioma. *J Clin Oncol* **16**:3851-7.
106. **Furlong, D., H. Swift, and B. Roizman.** 1972. Arrangement of herpesvirus deoxyribonucleic acid in the core. *J Virol* **10**:1071-4.
107. **Galanis, E., J. Buckner, D. Kimmel, R. Jenkins, B. Alderete, J. O'Fallon, C. H. Wang, B. W. Scheithauer, and C. D. James.** 1998. Gene amplification as a prognostic factor in primary and secondary high-grade malignant gliomas. *Int J Oncol* **13**:717-24.
108. **Garber, D. A., S. M. Beverley, and D. M. Coen.** 1993. Demonstration of circularization of herpes simplex virus DNA following infection using pulsed field gel electrophoresis. *Virology* **197**:459-62.

109. **Gatti, R. A., S. Becker-Catania, H. H. Chun, X. Sun, M. Mitui, C. H. Lai, N. Khanlou, M. Babaei, R. Cheng, C. Clark, Y. Huo, N. C. Udar, and R. K. Iyer.** 2001. The pathogenesis of ataxia-telangiectasia. Learning from a Rosetta Stone. *Clin Rev Allergy Immunol* **20**:87-108.
110. **Gehan, E. A., and M. D. Walker.** 1977. Prognostic factors for patients with brain tumors. *Natl Cancer Inst Monogr* **46**:189-95.
111. **Gelman, I. H., and S. Silverstein.** 1986. Co-ordinate regulation of herpes simplex virus gene expression is mediated by the functional interaction of two immediate early gene products. *J Mol Biol* **191**:395-409.
112. **Gelman, I. H., and S. Silverstein.** 1987. Dissection of immediate-early gene promoters from herpes simplex virus: sequences that respond to the virus transcriptional activators. *J Virol* **61**:3167-72.
113. **Gelman, I. H., and S. Silverstein.** 1985. Identification of immediate early genes from herpes simplex virus that transactivate the virus thymidine kinase gene. *Proc Natl Acad Sci U S A* **82**:5265-9.
114. **Geraghty, R. J., C. Krummenacher, G. H. Cohen, R. J. Eisenberg, and P. G. Spear.** 1998. Entry of alphaherpesviruses mediated by poliovirus receptor-related protein 1 and poliovirus receptor. *Science* **280**:1618-20.
115. **Gilbert, H., A. R. Kagan, F. Cassidy, J. Wagner, K. Fuchs, D. Fox, I. Macri, D. Gilbert, A. Rao, H. Nussbaum, A. Forsythe, J. Eder, F. Latino, L. Youleles, P. Chan, and B. L. Hintz.** 1981. Glioblastoma multiforme is not a uniform disease! *Cancer Clin Trials* **4**:87-9.
116. **Gomez-Manzano, C., J. Fueyo, A. P. Kyritsis, P. A. Steck, J. A. Roth, T. J. McDonnell, K. D. Steck, V. A. Levin, and W. K. Yung.** 1996. Adenovirus-mediated transfer of the p53 gene produces rapid and generalized death of human glioma cells via apoptosis. *Cancer Res* **56**:694-9.
117. **Gordon, Y. J., J. L. McKnight, J. M. Ostrove, E. Romanowski, and T. Araullo-Cruz.** 1990. Host species and strain differences affect the ability of an HSV-1 ICP0 deletion mutant to establish latency and spontaneously reactivate in vivo. *Virology* **178**:469-77.
118. **Gottlieb, T. M., and S. P. Jackson.** 1993. The DNA-dependent protein kinase: requirement for DNA ends and association with Ku antigen. *Cell* **72**:131-42.
119. **Gruenheid, S., L. Gatzke, H. Meadows, and F. Tufaro.** 1993. Herpes simplex virus infection and propagation in a mouse L cell mutant lacking heparan sulfate proteoglycans. *J Virol* **67**:93-100.
120. **Gu, B., and N. DeLuca.** 1994. Requirements for activation of the herpes simplex virus glycoprotein C promoter in vitro by the viral regulatory protein ICP4. *J Virol* **68**:7953-65.

121. **Guha, A., M. M. Feldkamp, N. Lau, G. Boss, and A. Pawson.** 1997. Proliferation of human malignant astrocytomas is dependent on Ras activation. *Oncogene* **15**:2755-65.
122. **Haarr, L., and S. Skulstad.** 1994. The herpes simplex virus type 1 particle: structure and molecular functions. Review article. *Apmis* **102**:321-46.
123. **Haas-Kogan, D., N. Shalev, M. Wong, G. Mills, G. Yount, and D. Stokoe.** 1998. Protein kinase B (PKB/Akt) activity is elevated in glioblastoma cells due to mutation of the tumor suppressor PTEN/MMAC. *Curr Biol* **8**:1195-8.
124. **Haas-Kogan, D. A., S. S. Kogan, G. Yount, J. Hsu, M. Haas, D. F. Deen, and M. A. Israel.** 1999. p53 function influences the effect of fractionated radiotherapy on glioblastoma tumors. *Int J Radiat Oncol Biol Phys* **43**:399-403.
125. **Haas-Kogan, D. A., G. Yount, M. Haas, D. Levi, S. S. Kogan, L. Hu, C. Vidair, D. F. Deen, W. C. Dewey, and M. A. Israel.** 1996. p53-dependent G1 arrest and p53-independent apoptosis influence the radiobiologic response of glioblastoma. *Int J Radiat Oncol Biol Phys* **36**:95-103.
126. **Hadjipanayis, C. G., and N. A. DeLuca.** 2005. Inhibition of DNA repair by a herpes simplex virus vector enhances the radiosensitivity of human glioblastoma cells. *Cancer Res* **65**:5310-5316.
127. **Hagglund, R., and B. Roizman.** 2004. Role of ICP0 in the strategy of conquest of the host cell by herpes simplex virus 1. *J Virol* **78**:2169-78.
128. **Halford, W. P., C. D. Kemp, J. A. Isler, D. J. Davido, and P. A. Schaffer.** 2001. ICP0, ICP4, or VP16 expressed from adenovirus vectors induces reactivation of latent herpes simplex virus type 1 in primary cultures of latently infected trigeminal ganglion cells. *J Virol* **75**:6143-53.
129. **Halford, W. P., and P. A. Schaffer.** 2001. ICP0 is required for efficient reactivation of herpes simplex virus type 1 from neuronal latency. *J Virol* **75**:3240-9.
130. **Hall, E. J.** 1988. *Radiobiology for the Radiologist*, Third ed. Lippincott Company, Philadelphia.
131. **Hardwicke, M. A., and R. M. Sandri-Goldin.** 1994. The herpes simplex virus regulatory protein ICP27 contributes to the decrease in cellular mRNA levels during infection. *J Virol* **68**:4797-810.
132. **Hardy, W. R., and R. M. Sandri-Goldin.** 1994. Herpes simplex virus inhibits host cell splicing, and regulatory protein ICP27 is required for this effect. *J Virol* **68**:7790-9.
133. **Harper, D. R.** 1994. *Molecular Virology*. Bios Scientific Publishers, Ltd., Oxford, United Kingdom.

134. **Harrow, S., V. Papanastassiou, J. Harland, R. Mabbs, R. Petty, M. Fraser, D. Hadley, J. Patterson, S. M. Brown, and R. Rampling.** 2004. HSV1716 injection into the brain adjacent to tumour following surgical resection of high-grade glioma: safety data and long-term survival. *Gene Ther* **11**:1648-58.
135. **Harsh, G. R. t., V. A. Levin, P. H. Gutin, M. Seager, P. Silver, and C. B. Wilson.** 1987. Reoperation for recurrent glioblastoma and anaplastic astrocytoma. *Neurosurgery* **21**:615-21.
136. **Hayward, G. S., R. J. Jacob, S. C. Wadsworth, and B. Roizman.** 1975. Anatomy of herpes simplex virus DNA: evidence for four populations of molecules that differ in the relative orientations of their long and short components. *Proc Natl Acad Sci U S A* **72**:4243-7.
137. **He, J., J. J. Olson, and C. D. James.** 1995. Lack of p16INK4 or retinoblastoma protein (pRb), or amplification-associated overexpression of cdk4 is observed in distinct subsets of malignant glial tumors and cell lines. *Cancer Res* **55**:4833-6.
138. **Hegi, M. E., A. C. Diserens, S. Godard, P. Y. Dietrich, L. Regli, S. Ostermann, P. Otten, G. Van Melle, N. de Tribolet, and R. Stupp.** 2004. Clinical trial substantiates the predictive value of O-6-methylguanine-DNA methyltransferase promoter methylation in glioblastoma patients treated with temozolomide. *Clin Cancer Res* **10**:1871-4.
139. **Hegi, M. E., A. C. Diserens, T. Gorlia, M. F. Hamou, N. de Tribolet, M. Weller, J. M. Kros, J. A. Hainfellner, W. Mason, L. Mariani, J. E. Bromberg, P. Hau, R. O. Mirimanoff, J. G. Cairncross, R. C. Janzer, and R. Stupp.** 2005. MGMT gene silencing and benefit from temozolomide in glioblastoma. *N Engl J Med* **352**:997-1003.
140. **Hentschel, S. J., and F. F. Lang.** 2003. Current surgical management of glioblastoma. *Cancer J* **9**:113-25.
141. **Hess, K. R.** 1999. Extent of resection as a prognostic variable in the treatment of gliomas. *J Neurooncol* **42**:227-31.
142. **Hirose, Y., M. S. Berger, and R. O. Pieper.** 2001. p53 effects both the duration of G2/M arrest and the fate of temozolomide-treated human glioblastoma cells. *Cancer Res* **61**:1957-63.
143. **Hobbs, W. E., 2nd, and N. A. DeLuca.** 1999. Perturbation of cell cycle progression and cellular gene expression as a function of herpes simplex virus ICP0. *J Virol* **73**:8245-55.
144. **Hobbs, W. E., D. E. Brough, I. Kovesdi, and N. A. DeLuca.** 2001. Efficient activation of viral genomes by levels of herpes simplex virus ICP0 insufficient to affect cellular gene expression or cell survival. *J Virol* **75**:3391-403.
145. **Hochberg, F. H., and A. Pruitt.** 1980. Assumptions in the radiotherapy of glioblastoma. *Neurology* **30**:907-11.

146. **Hoeijmakers, J. H.** 2001. Genome maintenance mechanisms for preventing cancer. *Nature* **411**:366-74.
147. **Holland, E. C., J. Celestino, C. Dai, L. Schaefer, R. E. Sawaya, and G. N. Fuller.** 2000. Combined activation of Ras and Akt in neural progenitors induces glioblastoma formation in mice. *Nat Genet* **25**:55-7.
148. **Holland, E. C., W. P. Hively, V. Gallo, and H. E. Varmus.** 1998. Modeling mutations in the G1 arrest pathway in human gliomas: overexpression of CDK4 but not loss of INK4a-ARF induces hyperploidy in cultured mouse astrocytes. *Genes Dev* **12**:3644-9.
149. **Homa, F. L., and J. C. Brown.** 1997. Capsid assembly and DNA packaging in herpes simplex virus. *Rev Med Virol* **7**:107-122.
150. **Honess, R. W., and B. Roizman.** 1974. Regulation of herpesvirus macromolecular synthesis. I. Cascade regulation of the synthesis of three groups of viral proteins. *J Virol* **14**:8-19.
151. **Honess, R. W., and B. Roizman.** 1975. Regulation of herpesvirus macromolecular synthesis: sequential transition of polypeptide synthesis requires functional viral polypeptides. *Proc Natl Acad Sci U S A* **72**:1276-80.
152. **Hunter, W. D., R. L. Martuza, F. Feigenbaum, T. Todo, T. Mineta, T. Yazaki, M. Toda, J. T. Newsome, R. C. Platenberg, H. J. Manz, and S. D. Rabkin.** 1999. Attenuated, replication-competent herpes simplex virus type 1 mutant G207: safety evaluation of intracerebral injection in nonhuman primates. *J Virol* **73**:6319-26.
153. **Ikeda, K., T. Ichikawa, H. Wakimoto, J. S. Silver, T. S. Deisboeck, D. Finkelstein, G. R. t. Harsh, D. N. Louis, R. T. Bartus, F. H. Hochberg, and E. A. Chiocca.** 1999. Oncolytic virus therapy of multiple tumors in the brain requires suppression of innate and elicited antiviral responses. *Nat Med* **5**:881-7.
154. **Ishov, A. M., A. G. Sotnikov, D. Negorev, O. V. Vladimirova, N. Neff, T. Kamitani, E. T. Yeh, J. F. Strauss, 3rd, and G. G. Maul.** 1999. PML is critical for ND10 formation and recruits the PML-interacting protein daxx to this nuclear structure when modified by SUMO-1. *J Cell Biol* **147**:221-34.
155. **Ivanchuk, S. M., S. Mondal, P. B. Dirks, and J. T. Rutka.** 2001. The INK4A/ARF locus: role in cell cycle control and apoptosis and implications for glioma growth. *J Neurooncol* **51**:219-29.
156. **Jackson, S. A., and N. A. DeLuca.** 2003. Relationship of herpes simplex virus genome configuration to productive and persistent infections. *Proc Natl Acad Sci U S A* **100**:7871-6.
157. **Jackson, S. P.** 2002. Sensing and repairing DNA double-strand breaks. *Carcinogenesis* **23**:687-96.

158. **Jacob, R. J., L. S. Morse, and B. Roizman.** 1979. Anatomy of herpes simplex virus DNA. XII. Accumulation of head-to-tail concatemers in nuclei of infected cells and their role in the generation of the four isomeric arrangements of viral DNA. *J Virol* **29**:448-57.
159. **Jean, J. H., M. L. Blankenship, and T. Ben-Porat.** 1977. Replication of herpesvirus DNA. I. Electron microscopic analysis of replicative structures. *Virology* **79**:281-91.
160. **Johnson, P. A., C. MacLean, H. S. Marsden, R. G. Dalziel, and R. D. Everett.** 1986. The product of gene US11 of herpes simplex virus type 1 is expressed as a true late gene. *J Gen Virol* **67 (Pt 5)**:871-83.
161. **Johnson, P. A., M. J. Wang, and T. Friedmann.** 1994. Improved cell survival by the reduction of immediate-early gene expression in replication-defective mutants of herpes simplex virus type 1 but not by mutation of the virion host shutoff function. *J Virol* **68**:6347-62.
162. **Jordan, R., and P. A. Schaffer.** 1997. Activation of gene expression by herpes simplex virus type 1 ICP0 occurs at the level of mRNA synthesis. *J Virol* **71**:6850-62.
163. **Kato, H., S. Kato, T. Kumabe, Y. Sonoda, T. Yoshimoto, S. Kato, S. Y. Han, T. Suzuki, H. Shibata, R. Kanamaru, and C. Ishioka.** 2000. Functional evaluation of p53 and PTEN gene mutations in gliomas. *Clin Cancer Res* **6**:3937-43.
164. **Kaufman, B., O. Scharf, J. Arbeit, M. Ashcroft, J. M. Brown, R. K. Bruick, J. D. Chapman, S. M. Evans, A. J. Giaccia, A. L. Harris, E. Huang, R. Johnson, W. Kaelin, Jr., C. J. Koch, P. Maxwell, J. Mitchell, L. Neckers, G. Powis, J. Rajendran, G. L. Semenza, J. Simons, E. Storkebaum, M. J. Welch, M. Whitelaw, G. Melillo, and S. P. Ivy.** 2004. Proceedings of the Oxygen Homeostasis/Hypoxia Meeting. *Cancer Res* **64**:3350-6.
165. **Kelly, P. J., C. Daumas-Duport, D. B. Kispert, B. A. Kall, B. W. Scheithauer, and J. J. Illig.** 1987. Imaging-based stereotaxic serial biopsies in untreated intracranial glial neoplasms. *J Neurosurg* **66**:865-74.
166. **Kelly, P. J., C. Daumas-Duport, B. W. Scheithauer, B. A. Kall, and D. B. Kispert.** 1987. Stereotactic histologic correlations of computed tomography- and magnetic resonance imaging-defined abnormalities in patients with glial neoplasms. *Mayo Clin Proc* **62**:450-9.
167. **Kerr, J. F., C. M. Winterford, and B. V. Harmon.** 1994. Apoptosis. Its significance in cancer and cancer therapy. *Cancer* **73**:2013-26.
168. **Khanna, K. K., and S. P. Jackson.** 2001. DNA double-strand breaks: signaling, repair and the cancer connection. *Nat Genet* **27**:247-54.
169. **Kieff, E. D., S. L. Bachenheimer, and B. Roizman.** 1971. Size, composition, and structure of the deoxyribonucleic acid of herpes simplex virus subtypes 1 and 2. *J Virol* **8**:125-32.

170. **Kitchens, D. L., E. Y. Snyder, and D. I. Gottlieb.** 1994. FGF and EGF are mitogens for immortalized neural progenitors. *J Neurobiol* **25**:797-807.
171. **Kleihues, P., P. C. Burger, V. P. Collins, E. W. Newcomb, H. Ohgaki, and W. Cavenee (ed.).** 2000. *Glioblastoma*, Second ed. International Agency for Research on Cancer, Lyon, France.
172. **Knipe, D. M., D. Senechek, S. A. Rice, and J. L. Smith.** 1987. Stages in the nuclear association of the herpes simplex virus transcriptional activator protein ICP4. *J Virol* **61**:276-84.
173. **Kobayashi, J., H. Tauchi, S. Sakamoto, A. Nakamura, K. Morishima, S. Matsuura, T. Kobayashi, K. Tamai, K. Tanimoto, and K. Komatsu.** 2002. NBS1 localizes to gamma-H2AX foci through interaction with the FHA/BRCT domain. *Curr Biol* **12**:1846-51.
174. **Kornblum, H. I., R. Hussain, J. Wiesen, P. Miettinen, S. D. Zurcher, K. Chow, R. Derynck, and Z. Werb.** 1998. Abnormal astrocyte development and neuronal death in mice lacking the epidermal growth factor receptor. *J Neurosci Res* **53**:697-717.
175. **Kramm, C. M., M. Chase, U. Herrlinger, A. Jacobs, P. A. Pechan, N. G. Rainov, M. Sena-Esteves, M. Aghi, F. H. Barnett, E. A. Chiocca, and X. O. Breakefield.** 1997. Therapeutic efficiency and safety of a second-generation replication-conditional HSV1 vector for brain tumor gene therapy. *Hum Gene Ther* **8**:2057-68.
176. **Kraus, A., M. W. Gross, R. Knuechel, K. Munkel, F. Neff, and J. Schlegel.** 2000. Aberrant p21 regulation in radioresistant primary glioblastoma multiforme cells bearing wild-type p53. *J Neurosurg* **93**:863-72.
177. **Kraus, J. A., J. Felsberg, J. C. Tonn, G. Reifenberger, and T. Pietsch.** 2002. Molecular genetic analysis of the TP53, PTEN, CDKN2A, EGFR, CDK4 and MDM2 tumour-associated genes in supratentorial primitive neuroectodermal tumours and glioblastomas of childhood. *Neuropathol Appl Neurobiol* **28**:325-33.
178. **Krisky, D. M., P. C. Marconi, T. J. Oligino, R. J. Rouse, D. J. Fink, J. B. Cohen, S. C. Watkins, and J. C. Glorioso.** 1998. Development of herpes simplex virus replication-defective multigene vectors for combination gene therapy applications. *Gene Ther* **5**:1517-30.
179. **Kristie, T. M., J. H. LeBowitz, and P. A. Sharp.** 1989. The octamer-binding proteins form multi-protein--DNA complexes with the HSV alpha TIF regulatory protein. *Embo J* **8**:4229-38.
180. **Kristie, T. M., and B. Roizman.** 1987. Host cell proteins bind to the cis-acting site required for virion-mediated induction of herpes simplex virus 1 alpha genes. *Proc Natl Acad Sci U S A* **84**:71-5.

181. **Kroin, J. S.** 1992. Intrathecal drug administration. Present use and future trends. *Clin Pharmacokinet* **22**:319-26.
182. **Kunwar, S., M. D. Prados, and F. F. Lang.** 2003. Pre and post-operative infusion of IL13-pE38QQR cytotoxin by convection-enhanced delivery (CED) in recurrent malignant glioma: a phase I study. *Proc Am Soc Clin Oncol* **22**:119 (Abstract).
183. **Kurimasa, A., S. Kumano, N. V. Boubnov, M. D. Story, C. S. Tung, S. R. Peterson, and D. J. Chen.** 1999. Requirement for the kinase activity of human DNA-dependent protein kinase catalytic subunit in DNA strand break rejoining. *Mol Cell Biol* **19**:3877-84.
184. **Lacroix, M., D. Abi-Said, D. R. Fourney, Z. L. Gokaslan, W. Shi, F. DeMonte, F. F. Lang, I. E. McCutcheon, S. J. Hassenbusch, E. Holland, K. Hess, C. Michael, D. Miller, and R. Sawaya.** 2001. A multivariate analysis of 416 patients with glioblastoma multiforme: prognosis, extent of resection, and survival. *J Neurosurg* **95**:190-8.
185. **Lang, F. F., D. C. Miller, M. Koslow, and E. W. Newcomb.** 1994. Pathways leading to glioblastoma multiforme: a molecular analysis of genetic alterations in 65 astrocytic tumors. *J Neurosurg* **81**:427-36.
186. **Lang, F. F., W. K. Yung, U. Raju, F. Libunao, N. H. Terry, and P. J. Tofilon.** 1998. Enhancement of radiosensitivity of wild-type p53 human glioma cells by adenovirus-mediated delivery of the p53 gene. *J Neurosurg* **89**:125-32.
187. **Laquerre, S., R. Argnani, D. B. Anderson, S. Zucchini, R. Manservigi, and J. C. Glorioso.** 1998. Heparan sulfate proteoglycan binding by herpes simplex virus type 1 glycoproteins B and C, which differ in their contributions to virus attachment, penetration, and cell-to-cell spread. *J Virol* **72**:6119-30.
188. **Lees-Miller, S. P., R. Godbout, D. W. Chan, M. Weinfeld, R. S. Day, 3rd, G. M. Barron, and J. Allalunis-Turner.** 1995. Absence of p350 subunit of DNA-activated protein kinase from a radiosensitive human cell line. *Science* **267**:1183-5.
189. **Lees-Miller, S. P., M. C. Long, M. A. Kilvert, V. Lam, S. A. Rice, and C. A. Spencer.** 1996. Attenuation of DNA-dependent protein kinase activity and its catalytic subunit by the herpes simplex virus type 1 transactivator ICP0. *J Virol* **70**:7471-7.
190. **Leib, D. A., D. M. Coen, C. L. Bogard, K. A. Hicks, D. R. Yager, D. M. Knipe, K. L. Tyler, and P. A. Schaffer.** 1989. Immediate-early regulatory gene mutants define different stages in the establishment and reactivation of herpes simplex virus latency. *J Virol* **63**:759-68.
191. **Leibel, S. A., and G. E. Sheline.** 1987. Radiation therapy for neoplasms of the brain. *J Neurosurg* **66**:1-22.

192. **Lieber, M. R., Y. Ma, U. Pannicke, and K. Schwarz.** 2004. The mechanism of vertebrate nonhomologous DNA end joining and its role in V(D)J recombination. *DNA Repair (Amst)* **3**:817-26.
193. **Lilley, C. E., C. T. Carson, A. R. Muotri, F. H. Gage, and M. D. Weitzman.** 2005. DNA repair proteins affect the lifecycle of herpes simplex virus 1. *Proc Natl Acad Sci U S A* **102**:5844-9.
194. **Lin, E., and J. Nemunaitis.** 2004. Oncolytic viral therapies. *Cancer Gene Ther* **11**:643-64.
195. **Liptak, L. M., S. L. Uprichard, and D. M. Knipe.** 1996. Functional order of assembly of herpes simplex virus DNA replication proteins into prereplicative site structures. *J Virol* **70**:1759-67.
196. **Lomonte, P., and R. D. Everett.** 1999. Herpes simplex virus type 1 immediate-early protein Vmw110 inhibits progression of cells through mitosis and from G(1) into S phase of the cell cycle. *J Virol* **73**:9456-67.
197. **Lomonte, P., K. F. Sullivan, and R. D. Everett.** 2001. Degradation of nucleosome-associated centromeric histone H3-like protein CENP-A induced by herpes simplex virus type 1 protein ICP0. *J Biol Chem* **276**:5829-35.
198. **Lopez, P., C. Van Sant, and B. Roizman.** 2001. Requirements for the nuclear-cytoplasmic translocation of infected-cell protein 0 of herpes simplex virus 1. *J Virol* **75**:3832-40.
199. **Louis, D. N.** 1997. A molecular genetic model of astrocytoma histopathology. *Brain Pathol* **7**:755-64.
200. **Lowe, S. W., H. E. Ruley, T. Jacks, and D. E. Housman.** 1993. p53-dependent apoptosis modulates the cytotoxicity of anticancer agents. *Cell* **74**:957-67.
201. **Lum, J. T., T. Nguyen, and L. P. Felpel.** 1984. Drug distribution in solid tissue of the brain following chronic local perfusion utilizing implanted osmotic minipumps. *J Pharmacol Methods* **12**:141-7.
202. **Marconi, P., M. Tamura, S. Moriuchi, D. M. Krisky, A. Niranjana, W. F. Goins, J. B. Cohen, and J. C. Glorioso.** 2000. Connexin 43-enhanced suicide gene therapy using herpesviral vectors. *Mol Ther* **1**:71-81.
203. **Marintcheva, B., and S. K. Weller.** 2001. A tale of two HSV-1 helicases: roles of phage and animal virus helicases in DNA replication and recombination. *Prog Nucleic Acid Res Mol Biol* **70**:77-118.
204. **Markert, J. M.** 2004. Biologic warfare for a good cause: HSV-1 anti-tumor therapy. *Clin Neurosurg* **51**:73-80.

205. **Markert, J. M., G. Y. Gillespie, R. R. Weichselbaum, B. Roizman, and R. J. Whitley.** 2000. Genetically engineered HSV in the treatment of glioma: a review. *Rev Med Virol* **10**:17-30.
206. **Markert, J. M., M. D. Medlock, S. D. Rabkin, G. Y. Gillespie, T. Todo, W. D. Hunter, C. A. Palmer, F. Feigenbaum, C. Tornatore, F. Tufaro, and R. L. Martuza.** 2000. Conditionally replicating herpes simplex virus mutant, G207 for the treatment of malignant glioma: results of a phase I trial. *Gene Ther* **7**:867-74.
207. **Marshall, C. J.** 1995. Specificity of receptor tyrosine kinase signaling: transient versus sustained extracellular signal-regulated kinase activation. *Cell* **80**:179-85.
208. **Martuza, R. L., A. Malick, J. M. Markert, K. L. Ruffner, and D. M. Coen.** 1991. Experimental therapy of human glioma by means of a genetically engineered virus mutant. *Science* **252**:854-6.
209. **Maul, G. G., and R. D. Everett.** 1994. The nuclear location of PML, a cellular member of the C3HC4 zinc-binding domain protein family, is rearranged during herpes simplex virus infection by the C3HC4 viral protein ICP0. *J Gen Virol* **75 (Pt 6)**:1223-33.
210. **Maul, G. G., A. M. Ishov, and R. D. Everett.** 1996. Nuclear domain 10 as preexisting potential replication start sites of herpes simplex virus type-1. *Virology* **217**:67-75.
211. **Maysinger, D., and A. Morinville.** 1997. Drug delivery to the nervous system. *Trends Biotechnol* **15**:410-8.
212. **McCarthy, A. M., L. McMahan, and P. A. Schaffer.** 1989. Herpes simplex virus type 1 ICP27 deletion mutants exhibit altered patterns of transcription and are DNA deficient. *J Virol* **63**:18-27.
213. **McGeoch, D. J., B. C. Barnett, and C. A. MacLean.** 1993. Emerging functions of alphaherpesvirus genes. *Semin Virol* **4**:125-134.
214. **McGeoch, D. J., M. A. Dalrymple, A. J. Davison, A. Dolan, M. C. Frame, D. McNab, L. J. Perry, J. E. Scott, and P. Taylor.** 1988. The complete DNA sequence of the long unique region in the genome of herpes simplex virus type 1. *J Gen Virol* **69 (Pt 7)**:1531-74.
215. **McGeoch, D. J., A. Dolan, S. Donald, and D. H. Brauer.** 1986. Complete DNA sequence of the short repeat region in the genome of herpes simplex virus type 1. *Nucleic Acids Res* **14**:1727-45.
216. **McGregor, F., A. Phelan, J. Dunlop, and J. B. Clements.** 1996. Regulation of herpes simplex virus poly (A) site usage and the action of immediate-early protein IE63 in the early-late switch. *J Virol* **70**:1931-40.

217. **McLauchlan, J., A. Phelan, C. Loney, R. M. Sandri-Goldin, and J. B. Clements.** 1992. Herpes simplex virus IE63 acts at the posttranscriptional level to stimulate viral mRNA 3' processing. *J Virol* **66**:6939-45.
218. **McMahan, L., and P. A. Schaffer.** 1990. The repressing and enhancing functions of the herpes simplex virus regulatory protein ICP27 map to C-terminal regions and are required to modulate viral gene expression very early in infection. *J Virol* **64**:3471-85.
219. **Mellerick, D. M., and N. W. Fraser.** 1987. Physical state of the latent herpes simplex virus genome in a mouse model system: evidence suggesting an episomal state. *Virology* **158**:265-75.
220. **Mettenleiter, T. C.** 2002. Herpesvirus assembly and egress. *J Virol* **76**:1537-47.
221. **Michael, N., and B. Roizman.** 1993. Repression of the herpes simplex virus 1 alpha 4 gene by its gene product occurs within the context of the viral genome and is associated with all three identified cognate sites. *Proc Natl Acad Sci U S A* **90**:2286-90.
222. **Mineta, T., S. D. Rabkin, T. Yazaki, W. D. Hunter, and R. L. Martuza.** 1995. Attenuated multi-mutated herpes simplex virus-1 for the treatment of malignant gliomas. *Nat Med* **1**:938-43.
223. **Mirzoeva, O. K., and J. H. Petrini.** 2001. DNA damage-dependent nuclear dynamics of the Mre11 complex. *Mol Cell Biol* **21**:281-8.
224. **Mitchell, C., J. A. Blaho, A. L. McCormick, and B. Roizman.** 1997. The nucleotidylation of herpes simplex virus 1 regulatory protein alpha22 by human casein kinase II. *J Biol Chem* **272**:25394-400.
225. **Montgomery, R. I., M. S. Warner, B. J. Lum, and P. G. Spear.** 1996. Herpes simplex virus-1 entry into cells mediated by a novel member of the TNF/NGF receptor family. *Cell* **87**:427-36.
226. **Moolten, F. L.** 1986. Tumor chemosensitivity conferred by inserted herpes thymidine kinase genes: paradigm for a prospective cancer control strategy. *Cancer Res* **46**:5276-81.
227. **Moolten, F. L., and J. M. Wells.** 1990. Curability of tumors bearing herpes thymidine kinase genes transferred by retroviral vectors. *J Natl Cancer Inst* **82**:297-300.
228. **Morgan, C., H. M. Rose, and B. Mednis.** 1968. Electron microscopy of herpes simplex virus. I. Entry. *J Virol* **2**:507-16.
229. **Moriuchi, S., T. Oligino, D. Krisky, P. Marconi, D. Fink, J. Cohen, and J. C. Glorioso.** 1998. Enhanced tumor cell killing in the presence of ganciclovir by herpes simplex virus type 1 vector-directed coexpression of human tumor necrosis factor-alpha and herpes simplex virus thymidine kinase. *Cancer Res* **58**:5731-7.

230. **Morrison, P. F., D. W. Laske, H. Bobo, E. H. Oldfield, and R. L. Dedrick.** 1994. High-flow microinfusion: tissue penetration and pharmacodynamics. *Am J Physiol* **266**:R292-305.
231. **Mosmann, T.** 1983. Rapid colorimetric assay for cellular growth and survival: application to proliferation and cytotoxicity assays. *J Immunol Methods* **65**:55-63.
232. **Myers, R. D., and L. Gurley-Orkin.** 1985. New "micro push-pull" catheter system for localized perfusion of diminutive structures in brain. *Brain Res Bull* **14**:477-83.
233. **Nazarov, I. B., Smirnova, A.N., Krutilina, R.I., Svetlova, M.P., Solovjeva, L.V., Nikiforov, A.A., Zalenskaya, I.A., Yau, P.M., Bradbury, E.M., Tomilin, N.V.** 2003. Dephosphorylation of histone gamma-H2AX during repair of DNA double-strand breaks in mammalian cells and its inhibition by calyculin A. *Radiation res* **160**:309-317.
234. **Nazzaro, J. M., and E. A. Neuwelt.** 1990. The role of surgery in the management of supratentorial intermediate and high-grade astrocytomas in adults. *J Neurosurg* **73**:331-44.
235. **Negorev, D., and G. G. Maul.** 2001. Cellular proteins localized at and interacting within ND10/PML nuclear bodies/PODs suggest functions of a nuclear depot. *Oncogene* **20**:7234-42.
236. **Neils, E. W., R. Lukin, T. A. Tomsick, and J. M. Tew.** 1987. Magnetic resonance imaging and computerized tomography scanning of herpes simplex encephalitis. Report of two cases. *J Neurosurg* **67**:592-4.
237. **Nelson, S. J., and S. Cha.** 2003. Imaging glioblastoma multiforme. *Cancer J* **9**:134-45.
238. **Newlands, E. S., G. R. Blackledge, J. A. Slack, G. J. Rustin, D. B. Smith, N. S. Stuart, C. P. Quarterman, R. Hoffman, M. F. Stevens, M. H. Brampton, and et al.** 1992. Phase I trial of temozolomide (CCRG 81045: M&B 39831: NSC 362856). *Br J Cancer* **65**:287-91.
239. **Newton, H. B., M. A. Slivka, C. L. Stevens, E. C. Bourekas, G. A. Christoforidis, M. A. Baujan, and D. W. Chakeres.** 2002. Intra-arterial carboplatin and intravenous etoposide for the treatment of recurrent and progressive non-GBM gliomas. *J Neurooncol* **56**:79-86.
240. **Nguyen, J. B., R. Sanchez-Pernaute, J. Cunningham, and K. S. Bankiewicz.** 2001. Convection-enhanced delivery of AAV-2 combined with heparin increases TK gene transfer in the rat brain. *Neuroreport* **12**:1961-4.
241. **Nicholson, D. W., A. Ali, N. A. Thornberry, J. P. Vaillancourt, C. K. Ding, M. Gallant, Y. Gareau, P. R. Griffin, M. Labelle, Y. A. Lazebnik, and et al.** 1995. Identification and inhibition of the ICE/CED-3 protease necessary for mammalian apoptosis. *Nature* **376**:37-43.

242. **Nicola, A. V., A. M. McEvoy, and S. E. Straus.** 2003. Roles for endocytosis and low pH in herpes simplex virus entry into HeLa and Chinese hamster ovary cells. *J Virol* **77**:5324-32.
243. **Nimonkar, A. V., and P. E. Boehmer.** 2003. The herpes simplex virus type-1 single-strand DNA-binding protein (ICP8) promotes strand invasion. *J Biol Chem* **278**:9678-82.
244. **Niranjan, A., S. Moriuchi, L. D. Lunsford, D. Kondziolka, J. C. Flickinger, W. Fellows, S. Rajendiran, M. Tamura, J. B. Cohen, and J. C. Glorioso.** 2000. Effective treatment of experimental glioblastoma by HSV vector-mediated TNF alpha and HSV-tk gene transfer in combination with radiosurgery and ganciclovir administration. *Mol Ther* **2**:114-20.
245. **Niranjan, A., D. Wolfe, M. Tamura, M. K. Soares, D. M. Krisky, L. D. Lunsford, S. Li, W. Fellows-Mayle, N. A. DeLuca, J. B. Cohen, and J. C. Glorioso.** 2003. Treatment of rat gliosarcoma brain tumors by HSV-based multigene therapy combined with radiosurgery. *Mol Ther* **8**:530-42.
246. **Nouspikel, T., and P. C. Hanawalt.** 2000. Terminally differentiated human neurons repair transcribed genes but display attenuated global DNA repair and modulation of repair gene expression. *Mol Cell Biol* **20**:1562-70.
247. **Nozaki, M., M. Tada, H. Kobayashi, C. L. Zhang, Y. Sawamura, H. Abe, N. Ishii, and E. G. Van Meir.** 1999. Roles of the functional loss of p53 and other genes in astrocytoma tumorigenesis and progression. *Neuro-oncol* **1**:124-37.
248. **O'Hare, P., C. R. Goding, and A. Haigh.** 1988. Direct combinatorial interaction between a herpes simplex virus regulatory protein and a cellular octamer-binding factor mediates specific induction of virus immediate-early gene expression. *Embo J* **7**:4231-8.
249. **Ogle, W. O., T. I. Ng, K. L. Carter, and B. Roizman.** 1997. The UL13 protein kinase and the infected cell type are determinants of posttranslational modification of ICP0. *Virology* **235**:406-13.
250. **Ohgaki, H., B. Schauble, A. zur Hausen, K. von Ammon, and P. Kleihues.** 1995. Genetic alterations associated with the evolution and progression of astrocytic brain tumours. *Virchows Arch* **427**:113-8.
251. **Oldfield, E. H., Z. Ram, K. W. Culver, R. M. Blaese, H. L. DeVroom, and W. F. Anderson.** 1993. Gene therapy for the treatment of brain tumors using intra-tumoral transduction with the thymidine kinase gene and intravenous ganciclovir. *Hum Gene Ther* **4**:39-69.
252. **Papanastassiou, V., R. Rampling, M. Fraser, R. Petty, D. Hadley, J. Nicoll, J. Harland, R. Mabbs, and M. Brown.** 2002. The potential for efficacy of the modified (ICP 34.5(-)) herpes simplex virus HSV1716 following intratumoural injection into human malignant glioma: a proof of principle study. *Gene Ther* **9**:398-406.

253. **Pardridge, W. M.** 1997. Drug delivery to the brain. *J Cereb Blood Flow Metab* **17**:713-31.
254. **Parker, J. N., G. Y. Gillespie, C. E. Love, S. Randall, R. J. Whitley, and J. M. Markert.** 2000. Engineered herpes simplex virus expressing IL-12 in the treatment of experimental murine brain tumors. *Proc Natl Acad Sci U S A* **97**:2208-13.
255. **Parkinson, J., S. P. Lees-Miller, and R. D. Everett.** 1999. Herpes simplex virus type 1 immediate-early protein vmw110 induces the proteasome-dependent degradation of the catalytic subunit of DNA-dependent protein kinase. *J Virol* **73**:650-7.
256. **Party, M. R. C. B. T. W.** 2001. Randomized trial of procarbazine, CCNU, and vincristine in the adjuvant treatment of high grade astrocytoma. A Medical Research Council trial. *J Clin Oncol* **19**:509-518.
257. **Paull, T. T., E. P. Rogakou, V. Yamazaki, C. U. Kirchgessner, M. Gellert, and W. M. Bonner.** 2000. A critical role for histone H2AX in recruitment of repair factors to nuclear foci after DNA damage. *Curr Biol* **10**:886-95.
258. **Pereira, L., M. H. Wolff, M. Fenwick, and B. Roizman.** 1977. Regulation of herpesvirus macromolecular synthesis. V. Properties of alpha polypeptides made in HSV-1 and HSV-2 infected cells. *Virology* **77**:733-49.
259. **Pfeiffer, P., W. Goedecke, and G. Obe.** 2000. Mechanisms of DNA double-strand break repair and their potential to induce chromosomal aberrations. *Mutagenesis* **15**:289-302.
260. **Phelan, A., M. Carmo-Fonseca, J. McLaughlan, A. I. Lamond, and J. B. Clements.** 1993. A herpes simplex virus type 1 immediate-early gene product, IE63, regulates small nuclear ribonucleoprotein distribution. *Proc Natl Acad Sci U S A* **90**:9056-60.
261. **Phelan, A., J. Dunlop, A. H. Patel, N. D. Stow, and J. B. Clements.** 1997. Nuclear sites of herpes simplex virus type 1 DNA replication and transcription colocalize at early times postinfection and are largely distinct from RNA processing factors. *J Virol* **71**:1124-32.
262. **Poffenberger, K. L., E. Tabares, and B. Roizman.** 1983. Characterization of a viable, noninverting herpes simplex virus 1 genome derived by insertion and deletion of sequences at the junction of components L and S. *Proc Natl Acad Sci U S A* **80**:2690-4.
263. **Pollack, I. F., S. D. Finkelstein, J. Woods, J. Burnham, E. J. Holmes, R. L. Hamilton, A. J. Yates, J. M. Boyett, J. L. Finlay, and R. Sposto.** 2002. Expression of p53 and prognosis in children with malignant gliomas. *N Engl J Med* **346**:420-7.
264. **Prados, M. D., R. E. Warnick, E. E. Mack, K. L. Chandler, J. Rabbitt, M. Page, and M. Malec.** 1996. Intravenous carboplatin for recurrent gliomas. A dose-escalating phase II trial. *Am J Clin Oncol* **19**:609-12.

265. **Preston, C. M.** 1979. Control of herpes simplex virus type 1 mRNA synthesis in cells infected with wild-type virus or the temperature-sensitive mutant tsK. *J Virol* **29**:275-84.
266. **Preston, C. M.** 2000. Repression of viral transcription during herpes simplex virus latency. *J Gen Virol* **81**:1-19.
267. **Pyles, R. B., R. E. Warnick, C. L. Chalk, B. E. Szanti, and L. M. Parysek.** 1997. A novel multiply-mutated HSV-1 strain for the treatment of human brain tumors. *Hum Gene Ther* **8**:533-44.
268. **Quigley, M. R., and J. C. Maroon.** 1991. The relationship between survival and the extent of the resection in patients with supratentorial malignant gliomas. *Neurosurgery* **29**:385-8; discussion 388-9.
269. **Quinlan, M. P., L. B. Chen, and D. M. Knipe.** 1984. The intranuclear location of a herpes simplex virus DNA-binding protein is determined by the status of viral DNA replication. *Cell* **36**:857-68.
270. **Rainov, N. G., and C. M. Kramm.** 2001. Vector delivery methods and targeting strategies for gene therapy of brain tumors. *Curr Gene Ther* **1**:367-83.
271. **Rampling, R., G. Cruickshank, V. Papanastassiou, J. Nicoll, D. Hadley, D. Brennan, R. Petty, A. MacLean, J. Harland, E. McKie, R. Mabbs, and M. Brown.** 2000. Toxicity evaluation of replication-competent herpes simplex virus (ICP 34.5 null mutant 1716) in patients with recurrent malignant glioma. *Gene Ther* **7**:859-66.
272. **Rasheed, B. K., R. E. McLendon, J. E. Herndon, H. S. Friedman, A. H. Friedman, D. D. Bigner, and S. H. Bigner.** 1994. Alterations of the TP53 gene in human gliomas. *Cancer Res* **54**:1324-30.
273. **Rice, S. A., and D. M. Knipe.** 1988. Gene-specific transactivation by herpes simplex virus type 1 alpha protein ICP27. *J Virol* **62**:3814-23.
274. **Rich, T., R. L. Allen, and A. H. Wyllie.** 2000. Defying death after DNA damage. *Nature* **407**:777-83.
275. **Rijkers, T., J. Van Den Ouweland, B. Morolli, A. G. Rolink, W. M. Baarends, P. P. Van Sloun, P. H. Lohman, and A. Pastink.** 1998. Targeted inactivation of mouse RAD52 reduces homologous recombination but not resistance to ionizing radiation. *Mol Cell Biol* **18**:6423-9.
276. **Rogakou, E. P., C. Boon, C. Redon, and W. M. Bonner.** 1999. Megabase chromatin domains involved in DNA double-strand breaks in vivo. *J Cell Biol* **146**:905-16.
277. **Rogakou, E. P., D. R. Pilch, A. H. Orr, V. S. Ivanova, and W. M. Bonner.** 1998. DNA double-stranded breaks induce histone H2AX phosphorylation on serine 139. *J Biol Chem* **273**:5858-68.

278. **Rogers-Bald, M., R. G. Sargent, and P. E. Bryant.** 2000. Production of chromatid breaks by single dsb: evidence supporting the signal model. *Int J Radiat Biol* **76**:23-9.
279. **Roizman, B.** 1979. The structure and isomerization of herpes simplex virus genomes. *Cell* **16**:481-94.
280. **Roizman, B., and A. E. Sears (ed.).** 1996. Herpes simplex viruses and their replication. Lippincott-Raven Publishers, Philadelphia, PA.
281. **Roop, C., L. Hutchinson, and D. C. Johnson.** 1993. A mutant herpes simplex virus type 1 unable to express glycoprotein L cannot enter cells, and its particles lack glycoprotein H. *J Virol* **67**:2285-97.
282. **Russell, J., N. D. Stow, E. C. Stow, and C. M. Preston.** 1987. Herpes simplex virus genes involved in latency in vitro. *J Gen Virol* **68 (Pt 12)**:3009-18.
283. **Sacks, W. R., and P. A. Schaffer.** 1987. Deletion mutants in the gene encoding the herpes simplex virus type 1 immediate-early protein ICP0 exhibit impaired growth in cell culture. *J Virol* **61**:829-39.
284. **Samaniego, L. A., L. Neiderhiser, and N. A. DeLuca.** 1998. Persistence and expression of the herpes simplex virus genome in the absence of immediate-early proteins. *J Virol* **72**:3307-20.
285. **Samaniego, L. A., A. L. Webb, and N. A. DeLuca.** 1995. Functional interactions between herpes simplex virus immediate-early proteins during infection: gene expression as a consequence of ICP27 and different domains of ICP4. *J Virol* **69**:5705-15.
286. **Samaniego, L. A., N. Wu, and N. A. DeLuca.** 1997. The herpes simplex virus immediate-early protein ICP0 affects transcription from the viral genome and infected-cell survival in the absence of ICP4 and ICP27. *J Virol* **71**:4614-25.
287. **Sandri-Goldin, R. M.** 2001. Nuclear export of herpes virus RNA. *Curr Top Microbiol Immunol* **259**:2-23.
288. **Sandri-Goldin, R. M.** 2003. Replication of the herpes simplex virus genome: does it really go around in circles? *Proc Natl Acad Sci U S A* **100**:7428-9.
289. **Sandri-Goldin, R. M., M. K. Hibbard, and M. A. Hardwicke.** 1995. The C-terminal repressor region of herpes simplex virus type 1 ICP27 is required for the redistribution of small nuclear ribonucleoprotein particles and splicing factor SC35; however, these alterations are not sufficient to inhibit host cell splicing. *J Virol* **69**:6063-76.
290. **Sears, A. E., I. W. Halliburton, B. Meignier, S. Silver, and B. Roizman.** 1985. Herpes simplex virus 1 mutant deleted in the alpha 22 gene: growth and gene expression in permissive and restrictive cells and establishment of latency in mice. *J Virol* **55**:338-46.

291. **Sekulovich, R. E., K. Leary, and R. M. Sandri-Goldin.** 1988. The herpes simplex virus type 1 alpha protein ICP27 can act as a trans-repressor or a trans-activator in combination with ICP4 and ICP0. *J Virol* **62**:4510-22.
292. **Selker, R. G., W. R. Shapiro, P. Burger, M. S. Blackwood, V. C. Arena, J. C. Gilder, M. G. Malkin, J. J. Mealey, Jr., J. H. Neal, J. Olson, J. T. Robertson, G. H. Barnett, S. Bloomfield, R. Albright, F. H. Hochberg, E. Hiesiger, and S. Green.** 2002. The Brain Tumor Cooperative Group NIH Trial 87-01: a randomized comparison of surgery, external radiotherapy, and carmustine versus surgery, interstitial radiotherapy boost, external radiation therapy, and carmustine. *Neurosurgery* **51**:343-55; discussion 355-7.
293. **Shand, N., F. Weber, L. Mariani, M. Bernstein, A. Gianella-Borradori, Z. Long, A. G. Sorensen, and N. Barbier.** 1999. A phase 1-2 clinical trial of gene therapy for recurrent glioblastoma multiforme by tumor transduction with the herpes simplex thymidine kinase gene followed by ganciclovir. GLI328 European-Canadian Study Group. *Hum Gene Ther* **10**:2325-35.
294. **Shapiro, W. R., S. B. Green, P. C. Burger, R. G. Selker, J. C. VanGilder, J. T. Robertson, J. Mealey, Jr., J. Ransohff, and M. S. Mahaley, Jr.** 1992. A randomized comparison of intra-arterial versus intravenous BCNU, with or without intravenous 5-fluorouracil, for newly diagnosed patients with malignant glioma. *J Neurosurg* **76**:772-81.
295. **Shieh, M. T., D. WuDunn, R. I. Montgomery, J. D. Esko, and P. G. Spear.** 1992. Cell surface receptors for herpes simplex virus are heparan sulfate proteoglycans. *J Cell Biol* **116**:1273-81.
296. **Shiloh, Y.** 2003. ATM and related protein kinases: safeguarding genome integrity. *Nat Rev Cancer* **3**:155-68.
297. **Shinoura, N., S. Sakurai, A. Asai, T. Kirino, and H. Hamada.** 2001. Over-expression of APAF-1 and caspase-9 augments radiation-induced apoptosis in U-373MG glioma cells. *Int J Cancer* **93**:252-61.
298. **Shu, H. K., M. M. Kim, P. Chen, F. Furman, C. M. Julin, and M. A. Israel.** 1998. The intrinsic radioresistance of glioblastoma-derived cell lines is associated with a failure of p53 to induce p21(BAX) expression. *Proc Natl Acad Sci U S A* **95**:14453-8.
299. **Skaliter, R., A. M. Makhov, J. D. Griffith, and I. R. Lehman.** 1996. Rolling circle DNA replication by extracts of herpes simplex virus type 1-infected human cells. *J Virol* **70**:1132-6.
300. **Smith, C. A., P. Bates, R. Rivera-Gonzalez, B. Gu, and N. A. DeLuca.** 1993. ICP4, the major transcriptional regulatory protein of herpes simplex virus type 1, forms a tripartite complex with TATA-binding protein and TFIIB. *J Virol* **67**:4676-87.
301. **Smith, G. C., and S. P. Jackson.** 1999. The DNA-dependent protein kinase. *Genes Dev* **13**:916-34.

302. **Smolewski, P., E. Bedner, L. Du, T. C. Hsieh, J. M. Wu, D. J. Phelps, and Z. Darzynkiewicz.** 2001. Detection of caspases activation by fluorochrome-labeled inhibitors: Multiparameter analysis by laser scanning cytometry. *Cytometry* **44**:73-82.
303. **Soliman, T. M., R. M. Sandri-Goldin, and S. J. Silverstein.** 1997. Shuttling of the herpes simplex virus type 1 regulatory protein ICP27 between the nucleus and cytoplasm mediates the expression of late proteins. *J Virol* **71**:9188-97.
304. **Spear, P. G.** 1993. Entry of alphaherpesviruses into cells. *Semin. Virol.* **4**:167-180.
305. **Spivack, J. G., and N. W. Fraser.** 1987. Detection of herpes simplex virus type 1 transcripts during latent infection in mice. *J Virol* **61**:3841-7.
306. **Stambolic, V., A. Suzuki, J. L. de la Pompa, G. M. Brothers, C. Mirtsos, T. Sasaki, J. Ruland, J. M. Penninger, D. P. Siderovski, and T. W. Mak.** 1998. Negative regulation of PKB/Akt-dependent cell survival by the tumor suppressor PTEN. *Cell* **95**:29-39.
307. **Steffy, K. R., and J. P. Weir.** 1991. Mutational analysis of two herpes simplex virus type 1 late promoters. *J Virol* **65**:6454-60.
308. **Stevens, J. G., E. K. Wagner, G. B. Devi-Rao, M. L. Cook, and L. T. Feldman.** 1987. RNA complementary to a herpesvirus alpha gene mRNA is prominent in latently infected neurons. *Science* **235**:1056-9.
309. **Stow, N. D., and E. C. Stow.** 1986. Isolation and characterization of a herpes simplex virus type 1 mutant containing a deletion within the gene encoding the immediate early polypeptide Vmw110. *J Gen Virol* **67 (Pt 12)**:2571-85.
310. **Strasser, J. F., L. K. Fung, S. Eller, S. A. Grossman, and W. M. Saltzman.** 1995. Distribution of 1,3-bis(2-chloroethyl)-1-nitrosourea and tracers in the rabbit brain after interstitial delivery by biodegradable polymer implants. *J Pharmacol Exp Ther* **275**:1647-55.
311. **Stupp, R., M. Gander, S. Leyvraz, and E. Newlands.** 2001. Current and future developments in the use of temozolomide for the treatment of brain tumours. *Lancet Oncol* **2**:552-60.
312. **Stupp, R., W. Mason, M. Van Den Bent, M. Weller, B. Fisher, M. Taphoorn, A. Brandes, J. Cairncross, D. Lacombe, and R. Mirimanoff.** 2004. Concomitant and adjuvant temozolomide (TMZ) and radiotherapy (RT) for newly diagnosed glioblastoma multiforme (GBM). Conclusive result of a randomized phase III trial by the EORTC Brain and RT Groups and NCIC Clinical Trials Group. *J Clin Oncol* **22**:1S.
313. **Stupp, R., W. P. Mason, M. J. van den Bent, M. Weller, B. Fisher, M. J. Taphoorn, K. Belanger, A. A. Brandes, C. Marosi, U. Bogdahn, J. Curschmann, R. C. Janzer, S. K. Ludwin, T. Gorlia, A. Allgeier, D. Lacombe, J. G. Cairncross, E. Eisenhauer,**

- and R. O. Mirimanoff.** 2005. Radiotherapy plus concomitant and adjuvant temozolomide for glioblastoma. *N Engl J Med* **352**:987-96.
314. **Sung, T., D. C. Miller, R. L. Hayes, M. Alonso, H. Yee, and E. W. Newcomb.** 2000. Preferential inactivation of the p53 tumor suppressor pathway and lack of EGFR amplification distinguish de novo high grade pediatric astrocytomas from de novo adult astrocytomas. *Brain Pathol* **10**:249-59.
 315. **Surawicz, T. S., B. J. McCarthy, V. Kupelian, P. J. Jukich, J. M. Bruner, and F. G. Davis.** 1999. Descriptive epidemiology of primary brain and CNS tumors: results from the Central Brain Tumor Registry of the United States, 1990-1994. *Neuro-oncol* **1**:14-25.
 316. **Tanaka, T., T. Yamagami, Y. Oka, T. Nomura, and H. Sugiyama.** 1993. The scid mutation in mice causes defects in the repair system for both double-strand DNA breaks and DNA cross-links. *Mutat Res* **288**:277-80.
 317. **Taylor, T. J., and D. M. Knipe.** 2004. Proteomics of herpes simplex virus replication compartments: association of cellular DNA replication, repair, recombination, and chromatin remodeling proteins with ICP8. *J Virol* **78**:5856-66.
 318. **Triezenberg, S. J., R. C. Kingsbury, and S. L. McKnight.** 1988. Functional dissection of VP16, the trans-activator of herpes simplex virus immediate early gene expression. *Genes Dev* **2**:718-29.
 319. **Triezenberg, S. J., K. L. LaMarco, and S. L. McKnight.** 1988. Evidence of DNA: protein interactions that mediate HSV-1 immediate early gene activation by VP16. *Genes Dev* **2**:730-42.
 320. **Tyler, K. L.** 2004. Herpes simplex virus infections of the central nervous system: encephalitis and meningitis, including Mollaret's. *Herpes* **11 Suppl 2**:57A-64A.
 321. **Uziel, T., Y. Lerenthal, L. Moyal, Y. Andegeko, L. Mittelman, and Y. Shiloh.** 2003. Requirement of the MRN complex for ATM activation by DNA damage. *Embo J* **22**:5612-21.
 322. **Valtonen, S., U. Timonen, P. Toivanen, H. Kalimo, L. Kivipelto, O. Heiskanen, G. Unsgaard, and T. Kuurne.** 1997. Interstitial chemotherapy with carmustine-loaded polymers for high-grade gliomas: a randomized double-blind study. *Neurosurgery* **41**:44-8; discussion 48-9.
 323. **van Heyningen, P., A. R. Calver, and W. D. Richardson.** 2001. Control of progenitor cell number by mitogen supply and demand. *Curr Biol* **11**:232-41.
 324. **van Rijn, J., J. J. Heimans, J. van den Berg, P. van der Valk, and B. J. Slotman.** 2000. Survival of human glioma cells treated with various combination of temozolomide and X-rays. *Int J Radiat Oncol Biol Phys* **47**:779-84.

325. **Veuger, S. J., N. J. Curtin, C. J. Richardson, G. C. Smith, and B. W. Durkacz.** 2003. Radiosensitization and DNA repair inhibition by the combined use of novel inhibitors of DNA-dependent protein kinase and poly(ADP-ribose) polymerase-1. *Cancer Res* **63**:6008-15.
326. **Voges, J., R. Reszka, A. Gossmann, C. Dittmar, R. Richter, G. Garlip, L. Kracht, H. H. Coenen, V. Sturm, K. Wienhard, W. D. Heiss, and A. H. Jacobs.** 2003. Imaging-guided convection-enhanced delivery and gene therapy of glioblastoma. *Ann Neurol* **54**:479-87.
327. **von Deimling, A., D. N. Louis, K. von Ammon, I. Petersen, T. Hoell, R. Y. Chung, R. L. Martuza, D. A. Schoenfeld, M. G. Yasargil, O. D. Wiestler, and et al.** 1992. Association of epidermal growth factor receptor gene amplification with loss of chromosome 10 in human glioblastoma multiforme. *J Neurosurg* **77**:295-301.
328. **Wagner, E. K., M. D. Petroski, N. T. Pande, P. T. Lieu, and M. Rice.** 1998. Analysis of factors influencing kinetics of herpes simplex virus transcription utilizing recombinant virus. *Methods* **16**:105-16.
329. **Walker, M., and T. A. Strike.** 1976. Presented at the Proc Am Assoc Cancer Res.
330. **Walker, M. D., E. Alexander, Jr., W. E. Hunt, C. S. MacCarty, M. S. Mahaley, Jr., J. Mealey, Jr., H. A. Norrell, G. Owens, J. Ransohoff, C. B. Wilson, E. A. Gehan, and T. A. Strike.** 1978. Evaluation of BCNU and/or radiotherapy in the treatment of anaplastic gliomas. A cooperative clinical trial. *J Neurosurg* **49**:333-43.
331. **Walker, M. D., S. B. Green, D. P. Byar, E. Alexander, Jr., U. Batzdorf, W. H. Brooks, W. E. Hunt, C. S. MacCarty, M. S. Mahaley, Jr., J. Mealey, Jr., G. Owens, J. Ransohoff, 2nd, J. T. Robertson, W. R. Shapiro, K. R. Smith, Jr., C. B. Wilson, and T. A. Strike.** 1980. Randomized comparisons of radiotherapy and nitrosoureas for the treatment of malignant glioma after surgery. *N Engl J Med* **303**:1323-9.
332. **Wang, S., M. Guo, H. Ouyang, X. Li, C. Cordon-Cardo, A. Kurimasa, D. J. Chen, Z. Fuks, C. C. Ling, and G. C. Li.** 2000. The catalytic subunit of DNA-dependent protein kinase selectively regulates p53-dependent apoptosis but not cell-cycle arrest. *Proc Natl Acad Sci U S A* **97**:1584-8.
333. **Warnick, R. E., M. D. Prados, E. E. Mack, K. L. Chandler, F. Doz, J. E. Rabbitt, and M. K. Malec.** 1994. A phase II study of intravenous carboplatin for the treatment of recurrent gliomas. *J Neurooncol* **19**:69-74.
334. **Watanabe, K., O. Tachibana, K. Sata, Y. Yonekawa, P. Kleihues, and H. Ohgaki.** 1996. Overexpression of the EGF receptor and p53 mutations are mutually exclusive in the evolution of primary and secondary glioblastomas. *Brain Pathol* **6**:217-23; discussion 23-4.
335. **Watson, R. J., and J. B. Clements.** 1978. Characterization of transcription-deficient temperature-sensitive mutants of herpes simplex virus type 1. *Virology* **91**:364-79.

336. **Weaver, M., and D. W. Laske.** 2003. Transferrin receptor ligand-targeted toxin conjugate (Tf-CRM107) for therapy of malignant gliomas. *J Neurooncol* **65**:3-13.
337. **Wedge, S. R., J. K. Porteous, M. G. Glaser, K. Marcus, and E. S. Newlands.** 1997. In vitro evaluation of temozolomide combined with X-irradiation. *Anticancer Drugs* **8**:92-7.
338. **Weingart, J., L. C. Strauss, and S. A. Grossman.** 2002. Phase I/II study: intra-tumoral infusion of IL13-pE38QQR cytotoxin for recurrent supratentorial malignant glioma. *Neuro-oncol* **4**:379 (Abstract).
339. **Weir, J. P.** 2001. Regulation of herpes simplex virus gene expression. *Gene* **271**:117-30.
340. **Weissenberger, J., S. Loeffler, A. Kappeler, M. Kopf, A. Lukes, T. A. Afanasieva, A. Aguzzi, and J. Weis.** 2004. IL-6 is required for glioma development in a mouse model. *Oncogene* **23**:3308-16.
341. **Weissenberger, J., J. P. Steinbach, G. Malin, S. Spada, T. Rulicke, and A. Aguzzi.** 1997. Development and malignant progression of astrocytomas in GFAP-v-src transgenic mice. *Oncogene* **14**:2005-13.
342. **Weller, S. K. e.** 1995. Herpes simplex virus DNA replication and genome maturation. ASM Press, Washington, D.C.
343. **Weyerbrock, A., S. Walbridge, R. M. Pluta, J. E. Saavedra, L. K. Keefer, and E. H. Oldfield.** 2003. Selective opening of the blood-tumor barrier by a nitric oxide donor and long-term survival in rats with C6 gliomas. *J Neurosurg* **99**:728-37.
344. **Whitley, R. J., and B. Roizman.** 2001. Herpes simplex virus infections. *Lancet* **357**:1513-8.
345. **Wilcock, D., and D. P. Lane.** 1991. Localization of p53, retinoblastoma and host replication proteins at sites of viral replication in herpes-infected cells. *Nature* **349**:429-31.
346. **Wilkinson, D. E., and S. K. Weller.** 2004. Recruitment of cellular recombination and repair proteins to sites of herpes simplex virus type 1 DNA replication is dependent on the composition of viral proteins within prereplicative sites and correlates with the induction of the DNA damage response. *J Virol* **78**:4783-96.
347. **Willers, H., J. Dahm-Daphi, and S. N. Powell.** 2004. Repair of radiation damage to DNA. *Br J Cancer* **90**:1297-301.
348. **Wu, J. K., W. G. Cano, S. A. Meylaerts, P. Qi, F. Vrionis, and V. Cherington.** 1994. Bystander tumoricidal effect in the treatment of experimental brain tumors. *Neurosurgery* **35**:1094-102; discussion 1102-3.

349. **Wu, N., S. C. Watkins, P. A. Schaffer, and N. A. DeLuca.** 1996. Prolonged gene expression and cell survival after infection by a herpes simplex virus mutant defective in the immediate-early genes encoding ICP4, ICP27, and ICP22. *J Virol* **70**:6358-69.
350. **WuDunn, D., and P. G. Spear.** 1989. Initial interaction of herpes simplex virus with cells is binding to heparan sulfate. *J Virol* **63**:52-8.
351. **Xu, Z. X., A. Timanova-Atanasova, R. X. Zhao, and K. S. Chang.** 2003. PML colocalizes with and stabilizes the DNA damage response protein TopBP1. *Mol Cell Biol* **23**:4247-56.
352. **Yao, F., and P. A. Schaffer.** 1994. Physical interaction between the herpes simplex virus type 1 immediate-early regulatory proteins ICP0 and ICP4. *J Virol* **68**:8158-68.
353. **Yao, K. C., T. Komata, Y. Kondo, T. Kanzawa, S. Kondo, and I. M. Germano.** 2003. Molecular response of human glioblastoma multiforme cells to ionizing radiation: cell cycle arrest, modulation of the expression of cyclin-dependent kinase inhibitors, and autophagy. *J Neurosurg* **98**:378-84.
354. **Yao, X. D., and P. Elias.** 2001. Recombination during early herpes simplex virus type 1 infection is mediated by cellular proteins. *J Biol Chem* **276**:2905-13.
355. **York, I. A., C. Roop, D. W. Andrews, S. R. Riddell, F. L. Graham, and D. C. Johnson.** 1994. A cytosolic herpes simplex virus protein inhibits antigen presentation to CD8⁺ T lymphocytes. *Cell* **77**:525-35.
356. **Yount, G. L., D. A. Haas-Kogan, C. A. Vidair, M. Haas, W. C. Dewey, and M. A. Israel.** 1996. Cell cycle synchrony unmasks the influence of p53 function on radiosensitivity of human glioblastoma cells. *Cancer Res* **56**:500-6.
357. **Yung, W. K., M. D. Prados, R. Yaya-Tur, S. S. Rosenfeld, M. Brada, H. S. Friedman, R. Albright, J. Olson, S. M. Chang, A. M. O'Neill, A. H. Friedman, J. Bruner, N. Yue, M. Dugan, S. Zaknoen, and V. A. Levin.** 1999. Multicenter phase II trial of temozolomide in patients with anaplastic astrocytoma or anaplastic oligoastrocytoma at first relapse. Temodal Brain Tumor Group. *J Clin Oncol* **17**:2762-71.
358. **Zabierowski, S., and N. A. DeLuca.** 2004. Differential cellular requirements for activation of herpes simplex virus type 1 early (tk) and late (gC) promoters by ICP4. *J Virol* **78**:6162-70.
359. **Zhang, Y. F., and E. K. Wagner.** 1987. The kinetics of expression of individual herpes simplex virus type 1 transcripts. *Virus Genes* **1**:49-60.